Nucleic acid reactions investigated by cantilever-based sensors

Marie, Rodolphe

Publication date:
2004

Document Version
Publisher's PDF, also known as Version of record

Nucleic acids reactions investigated by cantilever-based sensor

Rodolphe Marie

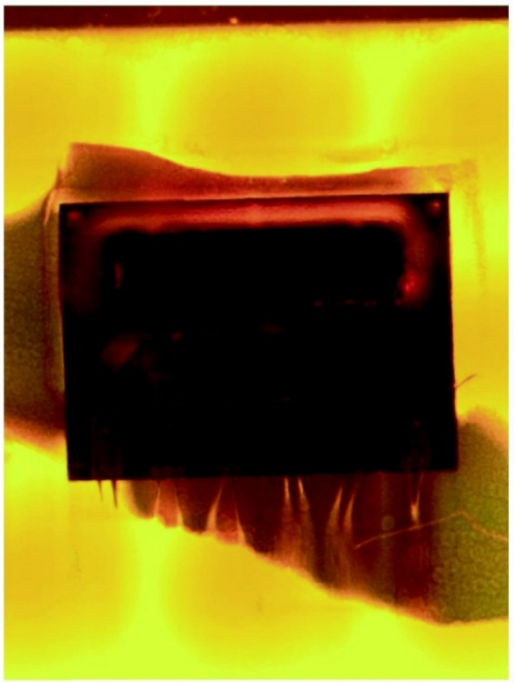

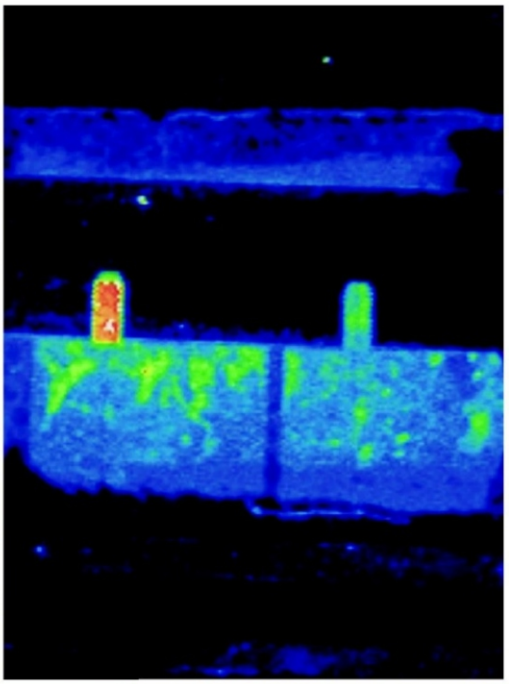

Ph.D. Thesis, December 2003

MIC, Department of Micro and Nanotechnology
DTU, Technical University of Denmark

Nucleic acids reactions investigated by cantilever-based sensor

Ph. D. Thesis

Rodolphe Marie[1]

3rd June 2004

[1]MIC - Department of Micro and Nanotechnology, Technical University of Denmark
DTU - Building 345east, DK-2800 Kongens Lyngby, Denmark

Preface

This thesis has been written as a part of the requirements for obtaining the Ph.D. degree at the Technical University of Denmark (DTU). The Ph.D. project has been carried out at the Department of Micro and Nanotechnology (MIC) at DTU in the period from the 1st of January 2001 to the 31st of December 2003.

This Ph.D. project has been a part of the Bioprobe project, Nanotechnology division, at MIC and was financed by a DTU Ph.D. grant. This project was realized under the supervision of:

Dr Anja Boisen
Main supervisor

Dr. Claus Bo Vöge Christensen
Co-supervisor

This project continued a period of almost two years spent in Denmark which would never have happen without the help of Anja Boisen, François Grey and the Freja grant. This Ph.D. project started by an original idea born at MIC to combine the activities of the Bioprobe project and the micro-array project, the biochemistry machinery and the micromechanical sensing, an idea that was and still is very new and challenging. MIC has been a special place to work at and because as a young researcher I don't know any other, I might not measure how easy and valuable it has been for a PhD student and foreigner to work at this place, among these people. At MIC, I have always felt as a member of the Bioprobe project, a team of cosmopolite, competent and enthusiastic people lead by Anja Boisen.

Thanks to Claus Christensen for supervising the micro-array part of my project. Martin Dufva has always had precious advices about the biochemistry. Thanks to Jens Ulstrup and his team for a very fruitful collaboration. I'd like to thank Helle Vendelbo Jensen, Yvonne Gyrsting and Dorthe Ganzhorn for helping me in and outside the cleanroom and to Stig Ahrent Petersen for his diligence to help me with my "bricolage". Thanks to the people at Cantion that provided me with

good chips, good advices and a competing spirit that is rather motivating.

During this period I managed to forget, sometimes, the ups and downs of research; for that, thanks to Seb for his twenty years friendship. Thanks to the people at Jomsborg kollegiet, who I lived with and who rarely asked me about my project. Thanks to Lotte. Thanks to my parents, Monique and Jean, because I contributed to this project with the best of my education and personality, which they are highly responsible for.

Rodolphe MARIE
Bioprobe project
MIC - Department of Micro and Nanotechnology
Technical University of Denmark DTU - Building 345east
DK-2800 Kongens Lyngby
Denmark

Abstract

Cantilever-based surface stress sensing has been shown sensitive enough to detect interactions of monolayers of biomolecules. This has a direct application for making a new generation of mechanical biosensors for label-free detection of Deoxyribose Nucleic Acids (DNA) and antigens/antibody recognition. The goal of this project has been to detect the melting of DNA as a first step toward the *in-situ* monitoring of Polymerase Chain Reaction (PCR).

All works published about the detection of biomolecular recognition use the optical leverage read-out technique for detecting the bending of the cantilever. In this project, cantilever based sensors with integrated piezoresistive read-out were used. A sensor sustaining the conditions of salt concentration and temperature required for *in situ* PCR monitoring was build by packaging a silicon cantilever chip into polymer. The sensor was characterized by recording the output voltage during PCR-like heat cycles and during repeated two-temperatures heat cycles.

In parallel, the immobilization of thiol-modified DNA on gold surfaces for PCR conditions was developed and characterized. First, the thermal stability of DNA immobilized on gold in a micro-array format was characterized during PCR heat-cycling by fluorescence scanning and radio-labeling. Thereafter, the method was successfully used to locally immobilize DNA on one side of a cantilever inside a fully packaged cantilever-based sensor.

Moreover, measurements of DNA hybridization in a flow were performed. Those measurements are a pre-requisite to detecting non-isothermal hybridization or melting of DNA. They were realized using two different set-ups, one at Cantion A/S and one at MIC. The results of the measurements are discussed. The measurements using one gold coated cantilever as reference yield a tensile surface stress signal of about 16 mN/m but non-specific signals in the same order of magnitude were also obtained. Further control experiments are being pursued.

Attempts of detecting the melting of DNA by monitoring the output signal of the sensor while successively heating and cooling the sensor in presence of the complementary DNA was performed. The results of those attempt are presented

and discussed.

Contents

List of Figures

List of Tables

Glossary

AFM : Atomic Force Microscopy.

Cantilever : a suspended beam clamped at one end.

Cation/Anion : cations are ions that carry a negative charge. Anions carry a positive charge.

DMT : Dimethoxytrityl.

DNA : Deoxyribose Nucleic Acid.

DTT : 1,4-dithio-DL-threitol .

EDTA : ethylene diamine tetraacetic acid.

Functionalization : in the biosensor community, it is the step where biomolecules are attached to the sensor surface in order to make it sensitive to the analyte.

GPIB : General Purpose Interface Bus.

Hybridization : pairing reaction of complementary nucleic acids. Is also called annealing when talking of PCR primers hybridizing on the template.

MCH : 6-mercapto-1-hexanol.

Melting : separation of hybridized nucleic acids under heating. Also called Helix-coil transition when refereing to the conformation change of the DNA.

PCR : Polymerase Chain Reaction. Amplification method for nucleic acids.

PDMS : Poly (dimethyl siloxane).

Piezo-resisitive : said of a material which resistance changes when it is deformed.

PMMA : Poly(methyl methacrylate).

PMT : Photo-Multiplicator Tube.

PSD : Position Sensitive Diode.

RNA : Ribose Nucleic Acid. mRNA refers to the mesenger RNA, principal vector of the gene expression in eukaryotic cells.

SAM : Self Assembled Monolayer. Said of a monolayer of molecules that adsorb spontaneously at an interface.

SDS : Sodium Dodecyl Sulfate.

SNP : Single Nucleotide Polymorphism. Said of the variations of gene coding involving only one nucleotide. A map of those single point mutations for an individual is like a genetic fingerprint.

Spiked : said of a solution of molecules that contain a small fraction of the radiolabeled form of this molecule.

SSC : sodium chloride/sodium citrate.

XPS : stands for X-ray induced Photoemission Spectroscopy. XPS is based on the detection of photons emitted by a material under exposure to X-rays. By XPS, one gathers information about the chemical state of the material.

5'end/3'end : this denotes the two extremities of a ssDNA. The 5'end is terminated by a phosphate group and the 3'end by a hydroxyl group. DNA polymerase extends the 3'end of a ssDNA.

Chapter 1

Introduction

A micro-cantilever is a suspended beam clamped at one end which has at least one of its dimensions in the micrometer range. Micro-cantilevers were originally made for carrying a tip and are used in Atomic Force Microscopy (AFM) to scan surfaces. Because the micro-cantilevers used in AFM are so thin, the interactions between the tip and the sample make the cantilever bend. The bending of the cantilever is traditionally detected via an optical read-out and registered as the topology of the surface. Cantilevers have interesting mechanical properties (figure 1.1), some of which were already used for making sensors before the era of micro-technology. The bimetallic, also called bimorph, effect is well known since the nineteenth century. As shown in figure 1.1A, a beam made of at least two different materials bends under temperature changes due to the different thermal expansion coefficients of the materials. A second property of interest is the mass dependency of the resonant frequency of a cantilever (figure 1.1B). Finally, a cantilever bends under surface stress difference between its opposite sides (figure 1.1C). As the cantilevers dimensions shrink down to micrometer or nanometer dimensions, the sensitivity reaches the range of temperature, mass or surface-stress changes of reactions involving monolayers of molecules and are potentially sensitive enough for single-molecule approach. Here the sensitivity to surface stress changes is of special interest. As it is made thinner, a cantilever bends under smaller surface-stress differences between its two sides perpendicular to its thickness. The adsorption of molecular layers on solid surfaces from gas or liquid phase is known for producing surface stress changes. This is the basic idea for developing mechanical sensors for bio-chemical sensors in gas and liquids. The detection of bio-molecules in liquid in particular finds its applications in research and diagnostics for genomics and proteomics. Indeed, cantilever-based sensing relies on the biomolecular recognition and is thus applicable to any nucleic acids or protein system as long as the adsorption of the analyte onto the surface of the cantilever can be made specific. By using the interaction between complementary biomolecules, the surface stress sensing benefits from the high specificity of those interactions. There is thus an opportunity for making highly sensitive biosensors

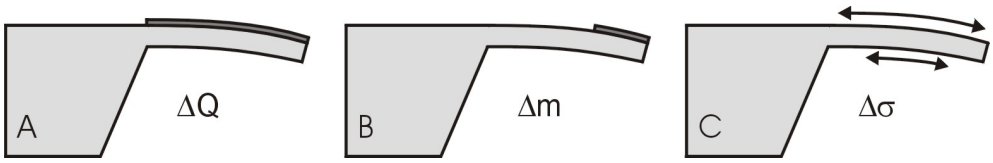

Figure 1.1: Three main properties of cantilevers. (**A**) When adsorbing heat, a composite cantilever bends toward the material with the lowest thermal expansion coefficient. (**B**) Under an increase of its mass, the resonant frequency of a cantilever decreases. (**C**) A difference in surface stress of the two opposite sides makes the cantilever bend away from the side subjected to compressive stress.

based on micro- and nano-cantilevers.

1.1 Read-out techniques

In AFM the bending of the cantilever is traditionally detected optically. A laser beam is shone onto the cantilever and reflected toward a position sensitive diode (PSD). The PSD is divided into four quadrants which enable to read-out the deflection of the laser beam in two dimensions, corresponding to the bending and the torsion of the cantilever. The optical read-out is successfully implemented for cantilever-based bio-sensors. There are some alternatives to passive probes notably active probes with integrated read-out. Proven read-out concepts are so far, capacitive [1, 2], piezoelectric [3] and piezo-resistive read-out [4]. In those approach the basic concept is to embed in the cantilever a layer of material which properties change under the bending of the cantilever. In the capacitive read-out a dielectric layer (*e.g.* air, vacuum) is placed between an electrode and the cantilever which is itself the second electrode. The capacitance value of the system changes under the deformation of the cantilever. In the piezoelectric read-out a layer of piezoelectric material (Zinc Oxide in [3]) is embedded and the electric field across the material changes when the cantilever bends. Finally, in the piezo-resistive read-out, the resistance of a piezo-resistive layer changes when the material is deformed. The piezo-resistive read-out is developed in the BioProbe project at MIC.

Integrated piezo-resistive read-out
The basic principle of an integrated piezo-resistive read-out is depicted in figure 1.2. The piezo-resistor is one U shaped resistor (or several in series) oriented with the two long branches along the length of the cantilever. In the most simple approach, the piezo-resistive material could simply be deposited on one side of the cantilever but in order to be operated in liquid, it is instead embedded in the cantilever made of a dielectric material. Several combination of a piezo-resistive and dielectric materials were tried such as silicon/silicon nitride or oxide [5, 6, 7]

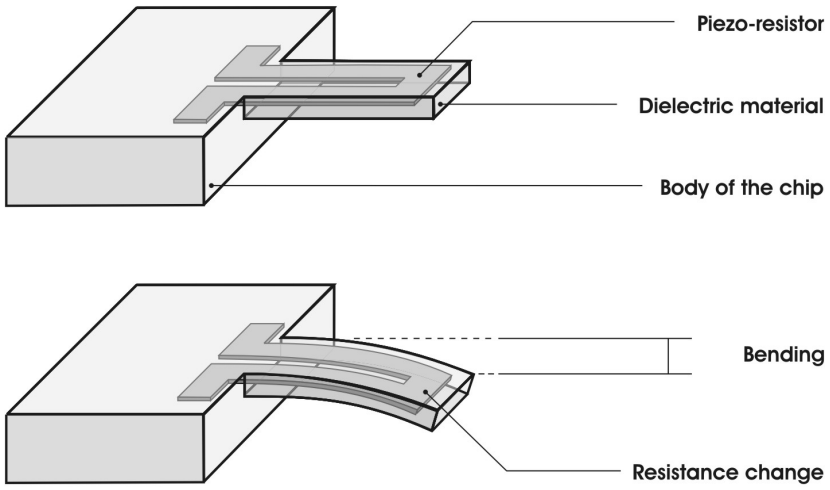

Figure 1.2: A piezo-resistive material is embedded in the cantilever. The bending of the cantilever yields a change of resistance of the material. For clarity, the contacts to the resistor are not shown.

and gold/polymer [8, 9].

The sensitivity of the cantilever is proportional to the gauge factor of the piezo-resistive material and inversely proportional to the Young's modulus of the cantilever. It is also dependent on the position of the piezo-resistive layer compared to the neutral axis of the cantilever where the strain is zero. Generally the piezo-resistive layer should be placed as far as possible from the neutral axis. The sensitivity of the piezo-resistive read-out is described elsewhere [5, 6, 7]. Briefly, for a piezo-resistor embedded in a cantilever (figure 1.3A) and placed in a wheatstone bridge configuration together with three other almost identical piezo-resistors (figure 1.3B), one placed on a reference cantilever and two placed on the body of the chip (figure 1.3C), the sensitivity of the read-out can be written as:

$$\Delta V_{out} = -\frac{1}{4}\,\frac{\Delta R}{R}\,V_{in} \tag{1.1-1}$$

By calculating the changes of resistance induced by a surface stress difference between both sides of the cantilever 1, the change of surface stress can be expressed as proportional to the output voltage of the wheatstone bridge:

$$\Delta\sigma = A\,\frac{\Delta V_{out}}{V_{in}} \tag{1.1-2}$$

where A is the factor that is derived from the geometry of the cantilever and of the piezo-resistor, the gauge factor of the piezo-resistive material and the Young's modulus and Poisson ratio of the multi-layered structure. This factor is constant

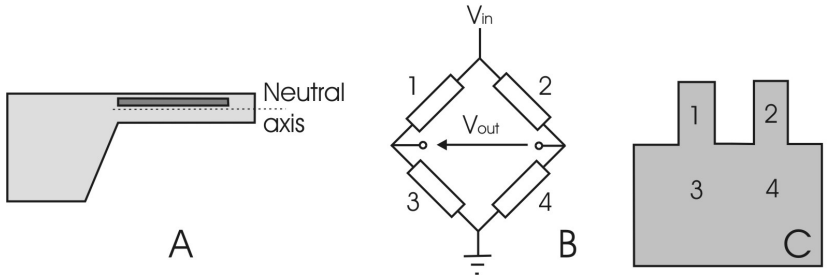

Figure 1.3: (**A**) The piezo-resistor is embedded at a distance from the neutral axis of the cantilever. (**B**) Wheatstone bridge configuration with four piezo-resistors, (**C**) two are placed on cantilevers and two on the body of the chip.

for a given cantilever sensor and V_{in} is the only parameter needed for converting the change of output voltage Δ V_{out} into a surface stress value in N/m. In this report the n-doped single crystalline cantilever chips from the company Cantion (Cantion 3 in table 4.1) were modelled and the sensitivity was calculated as +3252 $N.m^{-1}.V^{-1}$ for V_{in} = 1 V [1]. A is positive because in this thesis:

- The piezoresistor is placed above the neutral axis
- The piezoresistor is made of n-doped silicon which gauge factor is negative
- V_{in} and V_{out} are oriented as in figure 1.3B
- The cantilever 2 is always the reference cantilever
- $\Delta\sigma$ is assumed positive if there is a compressive stress on the top side of the cantilever 1

Therefore we can write that in the following, measuring a compressive surface stress yields an increase of the output voltage.

Integrated read-out vs. optical read-out

From the point of view of detecting the bending of a micro-cantilever, the optical read-out is the most sensitive technique and has the benefit of several decades of development for AFM. Making a sensor for monitoring bio-recognition requires that the sensor is operated in liquid as biochemical reactions occur in aqueous solutions. The optical read-out was successfully implemented in systems that combine all the elements for making a cantilever-based biosensor *i.e.* a reaction chamber comprising a cantilever sensor coupled to a micro-fluidic system. In those systems the optical read-out that requires a laser or a laser photodiode

[1] The value was communicated by Cantion A/S. Peter A. Rasmussen calculated +3780 $N.m^{-1}.V^{-1}$ assuming ν=0.25, K=50. Details about the calculation can be found in [7].

array and a PSD was necessarily placed outside of the reaction chamber. This makes it difficult to implement the optical read-out for large arrays of cantilevers in a portable device format. Furthermore, optical read-outs can only be operated in solutions that are transparent to the laser beam and require that the refractive index of the solution remains constant during the measurements as a change of refractive index might be interpreted as a false bending of the cantilever unless such effects are cancelled by using a reference cantilever. Working with transparent solutions might be a requirement difficult to meet when working with biological samples. This major drawback is the basis for the investigation of non-optical integrated read-out as the piezo-resistive read-out.
There are also challenges to overcome for operating a piezo-resistive read-out in liquid. First of all, the piezo-resistive read-out is a rather new technique for cantilever sensors. The read-out system needs to be integrated on the cantilever and encapsulated in order to be used in liquid. Both are major challenges for the cost and fabrication of the cantilever sensor. On the other hand the measurement system is rather inexpensive as it consists of a voltage measurement system. Mass producing of the cantilever sensor might reduce the cost of fabrication of the system. Apart from that the sensitivity of such a read-out is an issue. Polycrystalline silicon piezo-resistors are still less sensitive than the optical read-out but the implementation of single-crystalline piezo-resistors makes the technique reach the sensitivity range necessary for detecting DNA hybridization signals (in the mN/m range). The combination of low Young's modulus materials such as polymers with a low-noise piezo-resistive material in the gold/SU8 technology might be a cheap alternative for larger surface stress change applications.

1.2 Principle

Cantilever-based biochemical sensing is based on the detection of the surface stress developed under the adsorption of a molecular layer on a solid-liquid interface. As depicted in figure 1.4, the adsorption of molecules on one side of the cantilever causes the cantilever to bend. The direction of bending depends on the nature of the surface stress and thus on the interactions of the molecules inside the molecular layer. The surface stress can either be compressive which causes the cantilever to bend away from the adsorbed layer (case in figure 1.4) or tensile causing the cantilever to bend toward the adsorbed layer. The origin of the surface stress is a matter of debate and two models were studied until now, both trying to interpret DNA immobilization and hybridization data. In one model, the surface stress results from the molecular interactions within the molecular layer. It is thus resulting from the electrostatic interactions, the Van der Waals interactions (also called steric hindrance) and the entropy changes of the layer [10]. In a second approach, the curvature of the cantilever counterbalances the gradient of electrostatic field across the adsorbed layer and is called

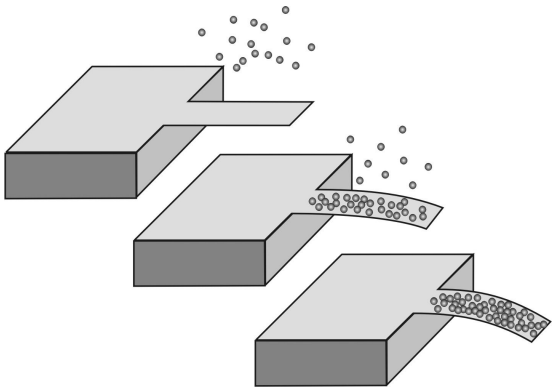

Figure 1.4: Principle of cantilever-based biochemical sensing.

the flexoelectric effect [11]. Most probably, both effects are involved and one or the other is predominant depending on the properties of the molecular layer: coverage, thickness, size and charges of the molecules.
More specifically, cantilever-based detection of biomolecules is based on the detection of the surface stress developed in a layer of receptor molecules under the specific adsorption of the analyte molecule. The receptor molecule and the analyte work as a key-lock system. The lock molecule is first immobilized on one side of the cantilever and the key molecule is then introduced in solution. The key molecules adsorb on the cantilever which causes it to bend. In case of DNA detection the receptor molecule is a single stranded DNA molecule (probe DNA) and the analyte molecule is the complementary single stranded DNA (target DNA). In case of protein based detection, the receptor/analyte couple can be antibody/antigen or antibody/antibody. Other protein systems (*e.g.* avidin/biotin) than antibodies are also very specific and can thus be used in a cantilever-based detection. Mixed systems can involve nucleic acids and an enzymes specific to the base sequence of the DNA (*e.g.* restriction enzymes, zinc fingers, nucleases).

1.3 State of the art

Both nucleic acids hybridization and protein recognition have been demonstrated, in static and flowing solution [12, 13, 10].

The hybridization of DNA was the first obvious choice for such a system because of its commercial relevancy and accessibility and because of its high and predictable affinity. DNA hybridization was first detected in static solution [12] and later in a flow [13, 10]. The effort was pushed toward the sequence discrimination [12], then the sensitivity of the system was investigated and brought to the nanomolar range together with single nucleotide discrimination which are rele-

vant for Single Nucleotide Polymorphism (SNP) studies [13]. The state of the art is the detection of 75 nM of 12'mer complementary oligos in a custom hybridization buffer with a reference cantilever coated with a non complementary 12'mer sequence producing a surface stress change of 1.4 mN/m [13]. Wu *et al.* have published results of hybridization at higher concentrations without a reference cantilever and the extrapolation of their data for a 12'mer sequence yields a surface stress of 3.7 mN/m. In both articles the surface stress is evaluated from the deflection using the Stoney's formula for a beam coated with gold. The detection of large genomic DNA from real sample or obtained by PCR amplification has not yet been reported.
Protein interaction was also detected and notably the recognition of prostate specific antibodies (PSA) [14]. The detection of pesticides by antibody detection is also reported [15]. Soon the RNA detection will probably be published because of the high commercial and diagnostic relevance of gene expression profiling based on mRNA. Though, this applications require very high sensitivity due to the very low concentrations.
Surprisingly, the biotin-avidin has not been used yet as model system for the protein recognition proof of concept. This is though an obvious choice as the specificity of the biotin-avidin interaction is the largest for proteins with an equilibrium constant of 10^{15}. This is to be compared with the equilibrium constant of a short DNA strand in the 10^{29} range [2]. The biotin-Avidin binding is also well characterized and the change of the avidin tertiary structure that occurs under the binding of biotin could induce a large surface stress change and thus be valuable as a model system.

Reference cantilever vs. no reference cantilever
As mentioned above similar experimental works were published on short sequence DNA hybridization. Though the surface-stress change published are in the same order of magnitude (1.4 and 3.7 mN/m) those experiments are radically different in the sense that one uses a reference cantilever (differential measurement) and the other does not. Including an internal reference cantilever appears to me as the best way of performing detection based on bio-interaction in which unspecific binding of the bio-molecules is expected.

Applications of DNA mixed layers
DNA mixed layers are self assembled layers of DNA where a spacer molecule, also self assembled, is used to fill in the holes between the DNA. On gold, thiol-based DNA mixed layers were shown to improve the hybridization coverage and is therefore very attractive. However, no results have been published from the surface-stress sensing community concerning the implementation of DNA mixed

[2]This value is calculated on the basis of a free energy of hybridization of 40 kcal/mole for the BRCA1 probe sequence in 0.1 M salt at 25 °C.

layers even though some groups have tried. As the origin of the surface-stress in hybridization experiment is a matter of discussion, it is unclear why using a spacer molecule can inhibit the surface-stress as observed in other groups (personal communication from R. McKendry). Though, one can imagine that the morphology of the DNA layer is modified by the spacer molecule in such a way that the interactions between molecules is not transferred to the cantilever surface.

1.4 Motivation

There is little literature available on enzymatic reactions involving nucleic acids detected by surface stress sensing. This is probably due to the difficulty to combine enzymatic activity, nucleic acids and solid phase reactions of those. Monitoring those reactions is of real interest as it may enable to detect smaller concentrations of the nucleic acid and with a higher specificity. Stevenson *et al.* published their work on the detection of the digestion of nucleic acids immobilized on a cantilever sensor [16]. The digestion of a nucleic acid sequence is a sequence specific reaction that can thus enable SNP detection. This technique can be used to overcome the difficulty of detecting small amounts of nucleic acids by hybridization as the hybridization might be very slow, limited by the diffusion. However, once the nucleic acid is hybridized, the kinetics of the restriction reaction can be controlled and the detection made easier. One can imagine that even the restriction of few nucleic acid strands can produce high enough surface-stress to be detected due to the size of the restriction enzyme (in the 100 nm range). On the other hand the restriction enzymes (more generally proteins) are expected to adsorb unspecifically to surfaces, which can produce unspecific surface stress. Finding a reliable reference system that includes the unspecific binding of proteins is thus necessary.
Polymerase Chain Reaction (PCR) is another enzymatic reaction of interest. PCR is an amplification reaction routinely used for increasing the amount of a given nucleic acid sequence. Monitoring the PCR could enable the determination of the concentration of the nucleic acid sequence at the very beginning of the reaction when only a few copies of the nucleic acids are present. This thesis is about setting the first milestones toward on-line monitoring of PCR by surface-stress sensing.

In chapter 2 the essential properties of on one hand the DNA and on the other hand the polymerase chain reaction are described, as well as the challenges of surface stress sensing of biomolecular interactions. This shows how those three things can be combined. Then the measurement of the melting temperature of DNA is presented and discussed. These measurements are a pre-requisite to the understanding of the same measurements attempted by surface stress sensing.

In chapter 3, the optimization of an immobilization method for DNA is made. The investigation, made mainly by fluorescence detection is aiming at producing an immobilization protocol that fulfills the requirements to cantilever-based sensing under PCR conditions. Chapter 4 describes with the packaging of the cantilever chip and the experimental set-up is presented. The results of melting temperature measurement attempts are presented in chapter 6 together with the measurement of DNA hybridization in a flow made by cantilever-based surface stress sensing. Chapters 2,3 and 6 describe mainly the biochemistry and surface science aspects of the project while chapter 4 describes the hardware part.

The goal of this project has been to

- **Functionalize the cantilever-based sensor** in order to optimize it for surface stress sensing of hybridization/melting of DNA.
- **Make a surface stress sensor** out of cantilever-based silicon devices, together with building and characterizing an experimental set-up.
- Detect **DNA hybridization** in a flow.
- **Investigate the feasibility of surface stress sensing of the melting of DNA** in static solution.

Chapter 2

Theory and principle

The idea of making a cantilever-based sensor for monitoring polymerase chain reaction (PCR) relies strongly on the process known as melting of the DNA, the transition between the double stranded and the single stranded state of the DNA, also called helix-coil transition. This transition occurs at the melting temperature which depends on the intrinsic properties of the DNA. Those properties are first described and their influence on the melting temperature is then described. The mechanism of the PCR which is a DNA amplification process is also described in order to show how a cantilever-sensor can be implemented for monitoring *in situ* the concentration of the DNA amplified by PCR. Finally results of melting temperature measurements are presented and modelled.

2.1 DNA

The Deoxyribose Nucleic Acid (DNA) is the molecule that carries in its structure the genetic information kept within all living cells. The DNA is constituted of two chains of "letters" (called strands) linked by covalent bonds. This constitutes the configuration of the DNA. Those two strands are associated by weak bonding in a three-dimensional structures called the double-helix and was first described in 1953 by Watson and Cricks [17]. In the following a strand of DNA that is not associated to its complementary strand is referred as a polynucleotide or a single-stranded DNA (ssDNA) while two strands associated together are referred as one double-stranded DNA (dsDNA). In the following the configuration and the conformation of DNA is described in more details before the helix-coil transition and the melting temperature is examined.

2.1.1 Configuration

The configuration of a DNA molecule is the covalent structure linking the nucleotides together into a ssDNA. Adenine, guanine, thymine and cytosine are the

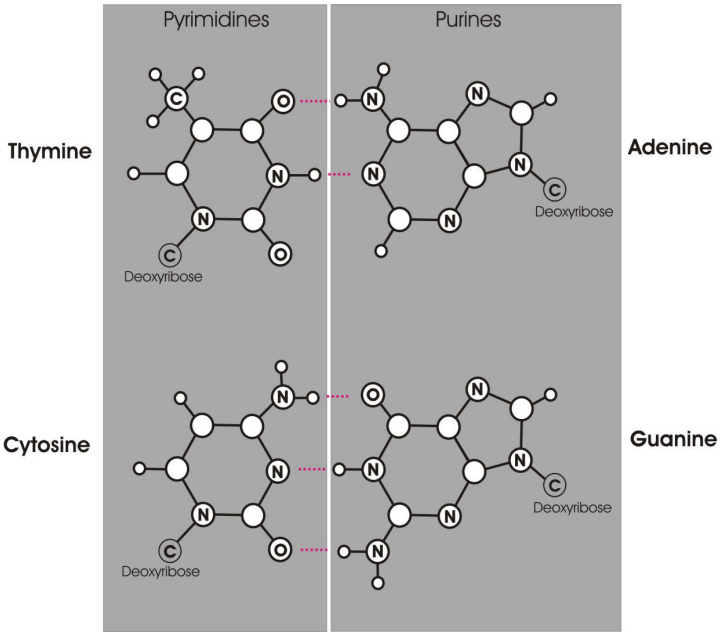

Figure 2.1: Structure of the four DNA-bases associated in Watson-Cricks pairs.

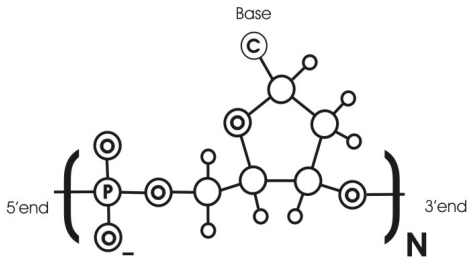

Figure 2.2: The polymeric scheme of Deoxyribose Nucleic Acid.

bases or "letters", with which the genetic code is written. Adenine and guanine are purines, formed of two rings containing carbon and nitrogen atoms. Thymine and cytosine are pyrimidines composed of only one ring (figure 2.1). Adenine is also a key molecule of the cellular metabolism as it is the basis for the adenosine triphosphate (ATP), the cellular chemical energy.

DNA belongs to the nucleic acids family that also contains the Ribo Nucleic Acid (RNA). DNA is a biopolymer and consists of DNA bases connected to a backbone of sugar rings (deoxyribose) attached to one another by phosphodiester bonds. Each sugar ring in the backbone caries one of the four possible bases thus forming a nucleotide (figure 2.2). The chain of nucleotides is oriented and has a 5'end and a 3'end . Those notations are later used to locate the modifications of single

stranded DNA.

The structure of the DNA has three physical properties that are relevant for the later discussion of its secondary structure (also called conformation).

- Each **interatomic bond can rotate** thus enabling the structure to adopt a three-dimensional structure.

- The bases can form **hydrogen bonds** with other molecules, principally water, other bases and proteins. Oxygen and nitrogen atoms of the cycles are hydrogen-bond acceptors and hydrogen atoms of amino and imino groups are hydrogen-bond donors. The distance of typical hydrogen bond length is 2.8 to 3.0 Å. In aqueous solution, the bases make hydrogen bonds mainly with water molecules and with other bases of DNA.

- Phosphate groups of the backbone of the DNA can carry one negative charge each when they are deprotonated, which is the case for pH values greater than 1. DNA is thus a **negatively charge polyelectrolite** with one elementary charge per base. This is the basis for the later discussion of the influence of ionic compound on the DNA secondary structure in solution.

In addition, each of the bases can be potentially protonated or ionised at the imino groups but at pH 7 (from 4.2 to 9.2 [18, 19]) the bases are neutral. One can note that the protonation or ionisation of the bases can strongly influence the number of hydrogen bonds that bases can form and thus pH variations influences the stability of the DNA secondary structure in solution as will be discussed later.

2.1.2 Comformation

The secondary structure or conformation of polynucleotides is a product of the primary structure (base sequence) and the environment. The secondary structure of dsDNA is the double helix formed by the two complementary strands of DNA and described as "two helical chains each coiled round the same axis" when proposed for the interpretation of X-ray diffraction patterns by Watson and Cricks [17]. The transition between the ssDNA state (unpaired) and the dsDNA state (paired) is called hybridization and is the corner stone of modern genomics. The reverse transition is called the helix-coil transition (or melting). Both transitions involve major changes of the conformation of DNA and large energy changes that need to be understood before discussing the detection of DNA hybridization/melting by surface-stress sensing. In the following we will focus on the melting of DNA and describe it through the melting temperature.

2.1.3 The helix-coil transition

The helix-coil transition is the reaction by which the double-stranded DNA is split in its two single-strands components. The reverse reaction is the hybridization of the complementary strands. The helix-coil transition can be induced by a change in the environment thus making the dsDNA energetically less favorable than the single strands. The helix-coil transition is also called melting of the DNA when it occurs upon heating and denaturation when it occurs upon other environmental variations (for example addition of agents destabilizing the helix as urea). The number of dsDNA as a function of the temperature is called melting curve and is, through the melting temperature T_m, a characteristic of a given DNA molecule. T_m is defined as the temperature at which half of the DNA molecules are hybridized. For large DNA molecules the fine structure of the profile of the melting curve is revealing the different domains of the sequence unwinding at different temperatures (figure 2.3). Theoretically, efforts are put into finding models to the helix coil transition in order to predict the melting curve [20] and thus the T_m from the base sequence only. In a first step empirical models for determining T_m were developed. The most simple one is

$$T_m = 2\ (A+T) + 4\ (G+C) \tag{2.1-1}$$

A+T is the number of adenine and thymine in the sequence and G+C is for guanine and cytosine. This model is valid only for short DNA strands (14-20 bases) for a given salt concentration (0.9 M monovalent cations) and is thus of limited use. The most commonly used model is [21]:

$$T_m = 81.5{+}16.6\ Log_{10}([Na^+]){+}0.41\ (GC\%){-}\frac{500}{N}{-}0.65\ (formamide\%) \tag{2.1-2}$$

where GC% is the guanine and cytosine content of the sequence in percent, N is the length of the sequence (number of bases), $[Na^+]$ is the concentration of

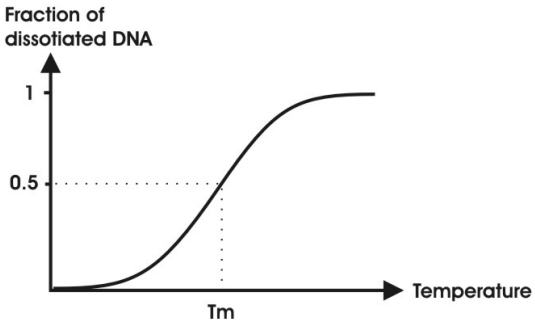

Figure 2.3: The melting curve of DNA is the number of discociated DNA vs. the temperature. At T_m half of the DNA is in the dsDNA state.

monovalent cations (sodium) and $formamide\%$ is the percentage of formamide in the solution. This model is valid for oligos longer than 50 bases and does not take into account the effect of the base stacking, meaning that T_m is then independent of the base sequence. The factor 500/N is also changed to 675/N for sequences down to 20 bases [22]. A model taking into account the base stacking was developed for short sequences and involves the *ab initio* calculations of the enthalpy and entropy term of the helix-coil transition [23]:

$$T_m = \frac{\Delta H^\circ}{\Delta S^\circ + R\ Ln[c]} - 273.15 + 12.0\ Log_{10}[Na^+] \qquad (2.1\text{-}3)$$

Where ΔH° and ΔS° are the enthalpy and entropy of the helix-coil transition at 298 K, [c] is the concentration of DNA. The calculation of ΔH° and ΔS° is based on nearest neighbor interactions of the bases. Briefly, the enthalpy and the entropy of hybridization of a whole sequence is calculated as a linear combination of the enthalpy and entropy values of the couples of bases that are nearest neighbors. For a given experimental set of oligos, ΔH° and ΔS° were expressed as a function of the enthalpy and entropy of each of the ten possible combinations of nearest neighbors. Then the melting temperature was expressed as a function of the set of parameters and compared to experimental values, thus yielding a set of enthalpy and entropy values for each nearest neighbor combination [23]. Note that the T_m is then dependent on the base sequence. Tools for computing the free energy of transitions and thus the melting temperature based on the nearest neighbor model are available on the internet [1].This model applies to oligos with length in the range of 8 to 40 bases and in solution containing 10 mM to 1.2 M of monovalent cations at pH 7-8.

Additives and energetic considerations

The enthalpy and entropy change of the melting reaction, and their respective amplitudes determines the melting temperature and need to be mentioned here. Moreover, they are expected to influence the amplitude of surface stress change that occur during the melting (or the hybridization) of DNA that is the quantity we want to detect with a cantilever-based sensor. In the following the enthalpy and entropy changes and thus the environment changes that influence them are briefly described.

The single-stranded DNA state is not a linear molecule and has also a three dimensional structure with a short persistence length (*i.e.* the molecule is very flexible). The three dimensional structure of ssDNA is due to the formation of **hydrogen bonds** with the water (polar solvent) and to the interaction of bases with each other called **the base stacking** which is the main driving mechanism of the conformation change. From the energy point of view, the binding of the

[1]Integrated DNA Technology at http://biotools.idtdna.com/gateway/

water molecules to the bases is an ordering process thus yielding a negative entropy change (unfavorable). Base stacking is the process by which the adjacent bases of a polynucleotide align along the direction normal to their ring plane. The stacking of the bases is allowed by the rotation freedom of covalent bonds in the phosphate backbone and between the sugar and the bases. Base stacking yields a strongly unfavorable entropy change because it is an ordering of the covalent structure of the molecule that reduces the rotation freedom of those bonds to the configuration that minimize the free energy of the system (ssDNA and solvent). The main term counteracting this unfavorable entropy term is a favorable enthalpy change due to the interaction of the adjacent bases. The interaction is of electronic nature and is also called the π stacking of the bases because due to the interaction of the π orbital of the rings. π stacking is found to be responsible for charge transfer in DNA [24, 25]. In addition, we can notice that the hydrophobic effect or in other words the displacement of water molecules hydrogen-bonded to the bases is also a positive favorable entropy change of the solvent but it is too small in order to account alone for the base stacking.

The double-stranded DNA forms by association of the complementary ssDNA. This process involves at the same time:

1. A change in the conformation of the backbone of each polynucleotide. dsDNA formation further increases the order of the ssDNA structure by restricting their conformation thus yielding a negative (unfavorable) entropy term accounting for most of the entropy change during dsDNA formation. This also accounts for the higher stiffness of the dsDNA compared to ssDNA and yields a longer persistence length.

2. A change in the base stacking of each polynucleotide. The change in base stacking occurring during the transition from ssDNA (where the bases are stacked) to dsDNA (where the bases are also stacked but in a different way) yields a change of enthalpy. This mainly account for the dependence of the melting temperature on the base sequence of the oligos.

3. The replacement of the water molecules that were hydrogen bonded to the unpaired bases by hydrogen bonds between complementary bases. Base pairing mechanism is the driving mechanism of the dsDNA formation. The formation of hydrogen bonds between the bases of the two complementary strands is energetically favorable and the change of free energy due only to the hydrogen bond formation is estimated in the range of - 2 to - 8.4 kJ/mol of hydrogen bonds while the favorable energy change due to the stacking is up to - 15 kJ/mol of bases [26].

4. The electrostatic repulsion of the two negatively charged phosphate backbone is counteracting the formation of the helix and contributes to a large positive (unfavorable) enthalpy term.

From the point of view of the solvent, the formation of the duplex decreases the order of the water by displacing some of the water involved in the hydrogen bonded network around the bases thus yielding a positive (favorable) entropy term.

In the general case, dsDNA of random sequence in aqueous solution and at a salt concentration below 3 M adopt the B form, a right-handed helix with 10 bases and 33.8 Å of axial rise per turn (p226 in [27]).

Environment changes
From the interactions involved in the formation of dsDNA described above, one can deduce the environment changes that can destabilize the ssDNA compared to the dsDNA in solution. First of all, increasing the **temperature** destabilize the dsDNA. At higher temperatures the entropy term of the free energy prevail over the enthalpy. Those DNA entropy terms are, as mentioned above, mainly unfavorable. Secondly, the **solvent** plays a major role on the formation of ordered structures of the ssDNA. The solvation and conformational change of the ssDNA are always submitted to mainly energetically costly entropy term from the water. The addition of cosolvent (*e.g.* alcohols, detergents, urea and formamide [28]) can ease the solvation of the bases and thus destabilize the dsDNA. Finally, the presence of **cations** in the solution stabilizes the dsDNA by enabling the electrostatic screening of the negative charges of the complementary strands thus reducing the unfavorable enthalpy due to electrostatic repulsion.

There are a number of ions/additives that are commonly used in nucleic acid solutions but these are not considered in this model including divalent cations and EDTA (ethylene diamine tetraacetic acid). Briefly, cations that carry multiple positive elementary charges are expected to create a higher density of countercharges thus yielding a better electrostatic screening than monovalent cations would do at equivalent concentration thus stabilizing dsDNA and raises the T_m. But the effect of cations depends not only on their charge but also on how they interact with the nucleic acid molecules. This accounts for the fact that some divalent cations stabilize the helix while other destabilize it at high concentration. Magnesium (Mg^{2+}) is extensively used for raising the melting temperature of nucleic acid in solution and Cu^{2+} reduces the T_m at low concentrations. Multivalent cations such as hexamine ($[Co(NH_3)_6]^{3+}$) and polyamines (spermidine^{3+}, spermine^{4+}) are also molecules carrying multiple positive charges and, because they form complexes with DNA, they cause the DNA to aggregate and precipitate in solution. Finally, the model doesn't consider the effect of EDTA which prevents Mg^{2+} to interact with the nucleic acid and thus disables most of its stabilizing effect. In Equation 2.1-3 the concentration of Magnesium ions can be

converted to an equivalent concentration of monovalent cations as follows [29]:

$$[Na^+]_{eq} = 4\ \sqrt{[Mg^{2+}]} \tag{2.1-4}$$

Measurement techniques

Melting curves can be measured by differential calorimetry or spectrophotometry. Calorimetry relies on the measurement of the heat needed to increase the temperature of a DNA sample. When the temperature increases above its T_m, the specific heat of a DNA sample varies because of the change of enthalpy during the helix-coil transition of the DNA sample. The measurement by spectrophotometry relies on the fact that the adsorbance at 260 nm of the DNA bases increases when the base pairs are separated *i.e.* during the helix-coil transition. This is called the *hyperchromicity* of the DNA [30]. By measuring the adsorbance at 260 nm of a DNA sample while increasing the temperature one obtain the melting curve of the sample and thus its T_m as shown in figure 2.3. This technique is used in section 2.4.

The case of surface bound DNA

Surface bound DNA molecules exhibit specific properties compared to DNA free in solution. Those properties are increasingly relevant for the development of biosensors and DNA "chips" involving usually DNA-capture probes (or analogues) bound onto the solid surface of the device and target DNA free in solution. The immobilization of DNA molecules on a surface strongly influences both the kinetics and yield of the hybridization, mainly because of steric hindrance, electrostatic effects and two-dimensional confinement with regards to the molecule diffusion. Generally, the melting temperature of a DNA sequence is reduced by at the most 5°C when the duplex is bound to a solid surface [31].

2.2 Polymerase Chain Reaction (PCR)

2.2.1 Principle

Polymerase chain reaction is the standard way of making *in vitro* DNA amplification. First described by Mullis *et al.* [32], the amplification method is based on the activity of the DNA polymerase, the enzyme that is responsible for the reproduction of the DNA in the cell. *In vivo*, DNA polymerase is a part of a larger enzymatic machinery (the enzyme complex for DNA replication) that aims at reproducing the genetic information by duplicating each chromosome inside a cell before its mitosis. The polymerase has the ability to "walk" along a single strand of DNA (the template) in its 3' to 5' end direction extending the complementary strand by assembling it nucleotide by nucleotide. The polymerase copies a single

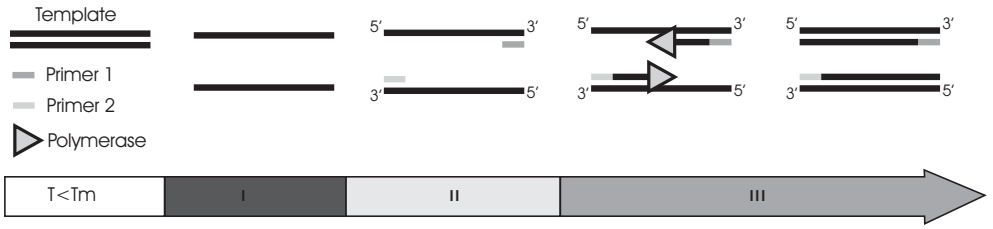

Figure 2.4: In a PCR process, (I) the DNA sample is denatured at ~ 95 °C (II) The primers are annealed to the template at ~ 55 °C and (III) the polymerase replicates the DNA strands at ~ 72 °C.

strand of DNA from where the complementary strand stops and until it meets the end of the strand, eventually displacing ssDNA fragments hybridized to it. *In vitro*, the PCR process consists of controlling the temperature to start and stop the activity of the polymerase in order to make copies of a predefined portion of a DNA sample (the template). The main steps of a PCR process are:

1. **Melting**: The DNA sample is melted at ~ 95 °C.
2. **Hybridization**: Primers are annealed to the sample at ~ 55 °C. Primers are shorter than the DNA sample and hybridize on their complementary sites on the DNA strands. The pair of primer defines the replication frame.
3. **Extension**: The polymerase replicate the DNA at ~ 72 °C. Polymerase finds the primers hybridized on the strands and replicate the strands until their 5'end.

PCR is performed in a solution containing the reagents necessary to the activity of the polymerase that are listed below:

DNA sample
The DNA sample is for example a collection of DNA fragments obtained by restriction enzyme digestion where only one copy of the template sequence is present among a large amount of background DNA (genomic DNA).

Primers
The pair of short DNA single strands (primers) defines the replication frame because they define where, on each DNA strand, the polymerase starts the replication. The polymerase can replicate the DNA only in the direction 3' to 5'end and each primer defines the 5'end of the template strand produced. At the end of the heat cycle, the amount of templates is doubled and if the heat cycling is repeated n times, the amount of template varies roughly as 2^n. In figure 2.4 the primer sites are placed at the extremities of the DNA template but longer DNA fragments are also produced during a typical PCR process. The replication

frame is typically a small region of a longer piece of the sample DNA. In that case, during the first heat cycle of a PCR process the primers hybridize on their sites in the middle of long single strands of DNA. As the polymerase replicates a DNA strands until it meets its 5'end, the PCR process also copies fragments that carries the part of the sequence that is outside of the replication frame. Those sequence are called "5'-dangling end" in the following. The first DNA fragment having the length of the template appears first at the third cycle. While the amount of templates increases exponentially, the amount of the templates with 5'-dangling ends is increasing linearly and becomes a minority of the DNA in the solution.

Polymerase
The PCR method involves the melting of often large DNA fragments (genomic DNA) at temperatures where polypeptides are also denatured. Initially the Klenow fragment of *E. coli* polymerase I was used for the PCR and needed to be added to the PCR mix at each cycle because it was denatured at the first step of each cycle. Later thermal resistant DNA polymerases isolated from bacteria including *Thermus acquaticus, Thermus flavus* and *Thermus thermophilus* were used. Those polymerases are resistant to temperature. The extension is performed at higher temperature (72°C) enabling higher temperatures for the annealing of the primers and thus longer primers with better sequence specificity. Taq polymerases have been further engineered to carry a protection enabling its polymerase activity when first heat cycled (partially denatured).

Salt
PCR solution contains typically sodium chloride and magnesium chloride. The concentration of cations determine the stability of dsDNA and therefore adjusts the temperature at which primers hybridize to the template DNA and template DNA is denatured.

Reagents
The solution contains the four deoxynucleoside triphosphates (adenosine, guanine, cytosine and thymine triphosphates). Those are precursors for nucleotides carrying additional phosphate groups. The removal of those phosphate groups releases the energy necessary to form covalent bonds with the polynucleotide chain by the polymerase during the extension.

Other amplification methods
PCR is the most obvious choice for a DNA amplification method to monitor. This is first due to the predominant place of PCR as amplification method among all others. Never the less other methods are available. Schweitzer *et al.* has published a review of amplification methods for microarrays [33] as the Ligase Chain Reaction (LCR), the Strand Displacement Amplification (SDA) which is an isothermal

amplification that "employs a continuous amplification scheme compared with the stepwise nature of PCR" [34].

2.2.2 Quantitative PCR

Though the formulation is convenient, saying that the amount of template varies exponentially with the number of heat cycles is only partly true. There are three phases in a typical PCR process, as depicted in figure 2.5. First there is a lack phase where the number of templates increases only weakly. Then during a short exponential phase the number of templates varies as 2^n before reaching a saturation phase. This is the core of the amplification where the amount of templates increases steadily until the reaction reaches the saturation phase because of a lack of reagents (deoxynucleoside triphosphates) that causes the diffusion to slow down and an excess of product compared with the number of primers causing the templates to hybridize instead of hybridizing to primers and being extended. Therefore the number of templates stabilizes. Because the exponential phase is short and the concentration of products needs to reach the detection level, the concentration of PCR products is first detected in the saturation phase typically by fluorescence detection after separation of the products by gel electrophoresis. Therefore, the quantification of a DNA sequence by PCR is not simply the quantification of templates after n heat cycles and the extrapolation of the number of copies that were present at cycle 1 because the duration of the different phases are unknown. Ultimately, it is necessary to detect the end of the lack phase, meaning being able to measure the amount of template in the concentration range close to the initial concentration of the sample which makes the amplification of the DNA by PCR then irrelevant for detection purposes.

Therefore so-called quantitative PCR relies on comparing the yield of a given PCR process performed on the DNA sample with the yield of the same PCR process performed either on the same sequence at different initial concentrations (calibration) or on an internal standard [35]. The modern way of performing quantitative PCR is Taqman PCR. In this method, a short ssDNA (probe) with at one end a fluorescent dye and at the other end a quentcher for this dye is introduced. The probe is complementary to the template inside the replication frame. When hybridized to the template, the fluorescent dye fluoresces. At each PCR cycle, the polymerase displaces the probe when copying the template. The probe is thus released in the solution and self-hybridizes which causes the quentching of the fluorescent dye. The amount of fluorescence is an indication of how many templates are in solution.

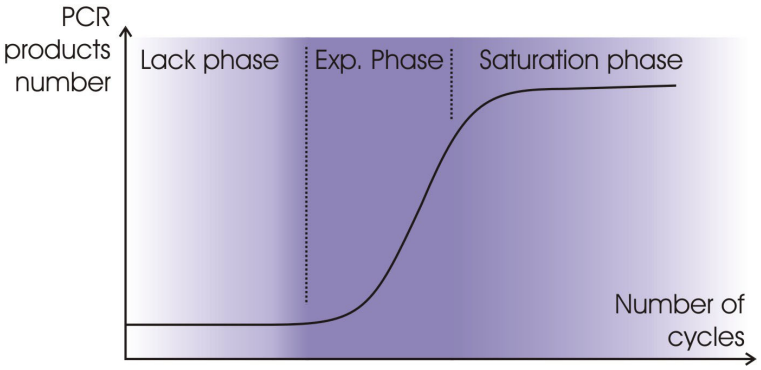

Figure 2.5: In a PCR process, the number of PCR products is stable during the lack phase, is doubled at each PCR cycle during the exponential phase and increases very slowly during the saturation phase.

2.2.3 Detection methods coupled to PCR, *ex* and *in situ*

In order to quantify *ex situ* the PCR product after a PCR amplification, the PCR products need to be separated from each other and from the rest of the PCR mix. Typically separation and detection are combined in an experimental protocol named gel electrophoresis (figure 2.6). Briefly, in a gel electrophoresis experiment the DNA contained in a solution can be separated by an electrostatic field inside a gel. The electrostatic field causes the DNA to migrate toward the positive electrode inside the gel. Because the migration speed depends solely on the length of the DNA, DNA molecules gather in bands of molecules having the same length. The gel can then be stained with an intercalating fluorescent dye (*e.g.* ethidium bromide) that makes the DNA fluorescence and can be identified as bands inside the gel. The bands corresponding to the PCR products are identified by length discrimination via comparison to length markers and their fluorescence intensity is quantified. The concentration of products is then derived from the fluorescence intensities. This approach has been integrated in a commercially microsystem-based device [36].

Other *ex situ* approaches include the detection by UV adsorption measurement that can also involve the separation by electrophoresis in microsystems [37], hybridization of the PCR products to DNA-captures probes micro-arrays with subsequent fluorescence detection [38], hybridization to quartz crystal microbalances [39, 40] and to surface plasmon resonance sensors [41, 42].

In situ, the concentration of PCR products is detected by fluorescence detection [43]. Briefly, intercalating dyes or oligonucleotides modified with fluorescent dyes are introduced in the PCR mix. In the first case, the intercalating dyes fluoresce when they intercalate to double stranded PCR products. One can thus

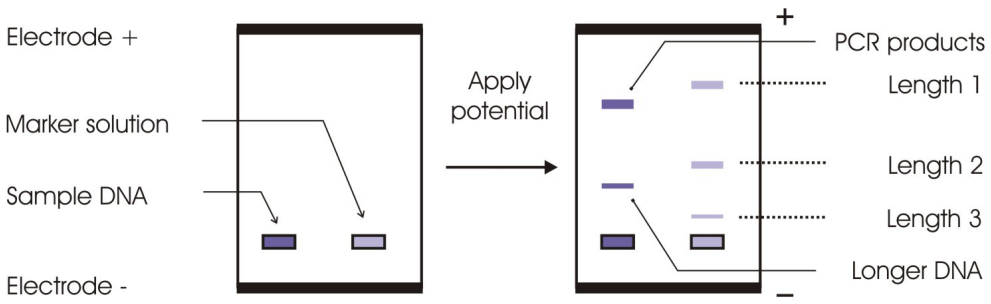

Figure 2.6: In gelelectrophoresis, the sample DNA molecules of increasing length diffuse slower toward the positive electrode. By comparing the bands position of DNA in the sample to the position of DNA markers of increasing length (1, 2 and 3), the band corresponding to the PCR fragments can be identified and quantified by fluorescence after staining of the gel.

measure the fluorescence during the melting of the templates yielding the melting curves of the PCR products which is used to quantify and discriminate the PCR products. In the second case, the labelled oligonucleotides are used as primers that hybridize to the PCR products thus yielding either the release of a fluorescent dye in solution, the quenching of the fluorescence or the change of color of the fluorescence during either the annealing of the primers or the extension phase (Taqman PCR).

2.3 Cantilever-based *in situ* monitoring of PCR: principle

The goal of the project is to monitor the evolution of a PCR process *in situ* by surface stress sensing. In order to do so, the detection principle should provide a way of measuring a quantity that relates to the progress or yield of the extension reaction. There are three quantities that do so: the amount of reagents, the amount of products and the change in free energy of the system. Considering the PCR, measuring the amount of nucleotides (reagents) in the solution would provide a measure of the yield of the reaction but nucleotides are molecules with low mass compared to polynucleotides which render them more difficult to detect than the polynucleotides (products). Conventionally, it is the amount of products of the PCR that is measured in a PCR monitoring systems (section 2.2.3). Alternatively, measuring the enthalpy of the extension or the melting/renaturation of the template DNA at each heat cycle provides a quantification of the yield of the reaction. Such measurement may be performed by conventional differential scanning calorimetry for example. However, differential calorimetry relies on comparing the sample with a reference sample and is a slow method that may be

in practice difficult to implement on complex biological samples.

Measuring the amount of PCR products by hybridization is the most obvious choice for surface stress sensing. The detection made by hybridization with DNA-capture probes immobilized on the sensor surface is the approach described here.

2.3.1 Challenges of surface-stress sensing for PCR monitoring

The surface stress sensing of a biomolecular interaction by cantilever-based sensor has been demonstrated for flow controlled and isothermal detection as described in chapter 1. The basic principle of the surface stress sensing is to immobilize DNA-capture probes onto one side of a cantilever and detect the surface stress induced by the interaction of the DNA-capture probes with the target DNA, in the case of PCR, the PCR products. There are though several issues to implementing this detection to *in situ* PCR monitoring:

Not only **hybridization but also melting** of the PCR products with the DNA-capture probes would take place on the cantilever surface at each PCR heat cycle. Both should yield a change of surface stress, of the same amplitude and opposite sign and are therefore potential detection point of the amount of PCR products.

Hybridization/melting occurs during cooling/heating phases respectively, and are thus **non-isothermal**. For most cantilever sensors reported in the literature, cantilevers are multi-layered structures because (1) they carry an integrated read-out, (2) they are coated with a metal in order to increase the reflectivity of the surface for optical read-out (3) they are coated with a gold layer used for the immobilization of a sensitive molecular layers or (4) a combination thereof. Such cantilevers are sensitive to temperature changes via the bimorph effect. In the case of monitoring hybridization/melting in PCR conditions, both the biomolecular interactions and the bimorph effect yield a bending of the cantilever.

The sensor is regenerated at each cycle because of the melting of the DNA: the PCR products desorb from the cantilever leaving the DNA-capture probes on the surface that can then re-hybridize at the next PCR cycle. This provides a way of performing the detection at each PCR cycle.

The PCR products are involved in the amplification reaction while the detection takes place. In other words, the PCR products that are detected by hybridization to the DNA-capture probes immobilized on the sensor surface are **also the template for the PCR reaction**. In the figure 2.7 it is obvious that DNA-capture probes hybridized to the PCR products act as primers and will be

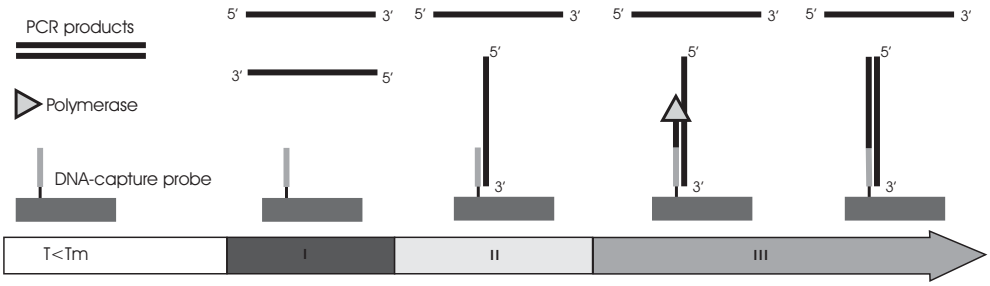

Figure 2.7: The DNA-capture probes are involved in the detection and amplification reaction. After the melting of the PCR products (**I**), the DNA-capture probes immobilized on the sensor surface are hybridizing to the PCR products (**II**). In the case where it produces a 5'end dangling end, the DNA-capture probe is elongated by the Polymerase (**III**)

elongated by the polymerase. After the elongation, the duplex is melted and the PCR products are released in the solution. In this case the surface of the sensor has been modified, in other words its sensitivity changed during the PCR cycle. Section 2.3.3 describes how it is possible to design the experimental protocol in order to overcome or take advantage of the participation of the DNA-capture probes in the amplification process.

2.3.2 DNA melting/re-hybridization detection by surface stress sensing

From the discussion above it appears that we need to design a detection protocol where it is possible to discriminate within the output signal the signal induced by the temperature change and the signal induced by the hybridization or melting. In the following, the principle of detecting the melting and the hybridization of DNA targets to DNA-capture probes immobilized on a cantilever is described in detail. It is assumed that the target DNA and the DNA-capture probes are fully complementary having the same length. Also assumed, the hybridization of target DNA to the DNA-capture probes on the test cantilever produces a tensile stress induced by the adsorption of a molecular layer on the test cantilever is visualized as a positive change of the output signal, the output signal of the sensor being the differential signal corresponding to the difference in bending of the test and reference cantilevers.

Melting

At a temperature below the melting temperature of the oligos, the target DNA is hybridized to the DNA-capture probes on the test cantilever surface. If raising the temperature above the T_m, the dsDNA is denatured and the target DNA is released in the solution, yielding a compressive stress change $\Delta\sigma_d$. In case the

surface stress change is proportional to the density of hybridized target oligos on the cantilever surface, the surface stress change as a function of temperature should be proportional to the melting curve of the DNA (figure 2.3), which is very specific to the target DNA through its T_m. At the melting temperature of the target DNA, the first derivative of the melting curve (or the output signal) is maximum. The detection of a peak of the surface stress derivative during the melting of the DNA target yields the melting temperature of the target: this is a very powerful tool for discriminating the PCR products during the PCR process. As mentioned before, the output signal includes the bimorph effect of the cantilevers. Assuming that the bimorph effect is linear within the PCR temperature range, it is possible to eliminate the bimorph component when calculating the derivative against temperature of the output signal. Practically, the output signal is recorded against time and it is also possible to eliminate the bimorph component by raising the temperature linearly with time and calculating the derivative against time of the output signal. Figure 2.8 shows how the output voltage of a cantilever-based sensor would look like during a heat cycle where (1) the heating/cooling rate is constant, (2) the bimorph effect is linear with temperature and (3) the surface stress change is proportional to the number of hybridized targets.

Hybridization versus melting

It is interesting to compare *a priori*, the output signal induced by hybridization and melting. First, from the point of view of the surface stress amplitude, the hybridization reaction should yield the same surface stress change as the melting. The amplitude of the signal is proportional to the density of targets hybridized to the cantilever surface and has been shown to be dependent on the concentration of the target [13]. At high concentrations, because of the high equilibrium constant of the DNA hybridization, the hybridization sites on the cantilever are saturated and the output signal is thus independent on the concentration. At low concentrations, in the diffusion-limited regime of the hybridization the density of hybridization is dependent on the target concentration. The limit of the two regimes was shown to be 250 nM (but might be dependent on the DNA-capture probe density).

Second, the kinetics of the hybridization reaction is dependent on the concentration as well. At constant temperature, the time dependence of the surface stress change due to hybridization is a Langmuir isotherm where the rate constant is a linear function of the target concentration. In the case of the re-hybridization at decreasing temperature, it is expected that the surface stress signal is a convolution of the reverse melting curve (re-naturation curve) and a Langmuir adsorption thus depending on the target concentration. This is in contrast with the case of the melting because the melting kinetics is not expected to be limited by diffusion [2]. The hybridization signal is not the reverse of the melting signal and in other

[2] even though the concentration of the oligos is included in the calculation of T_m in calcula-

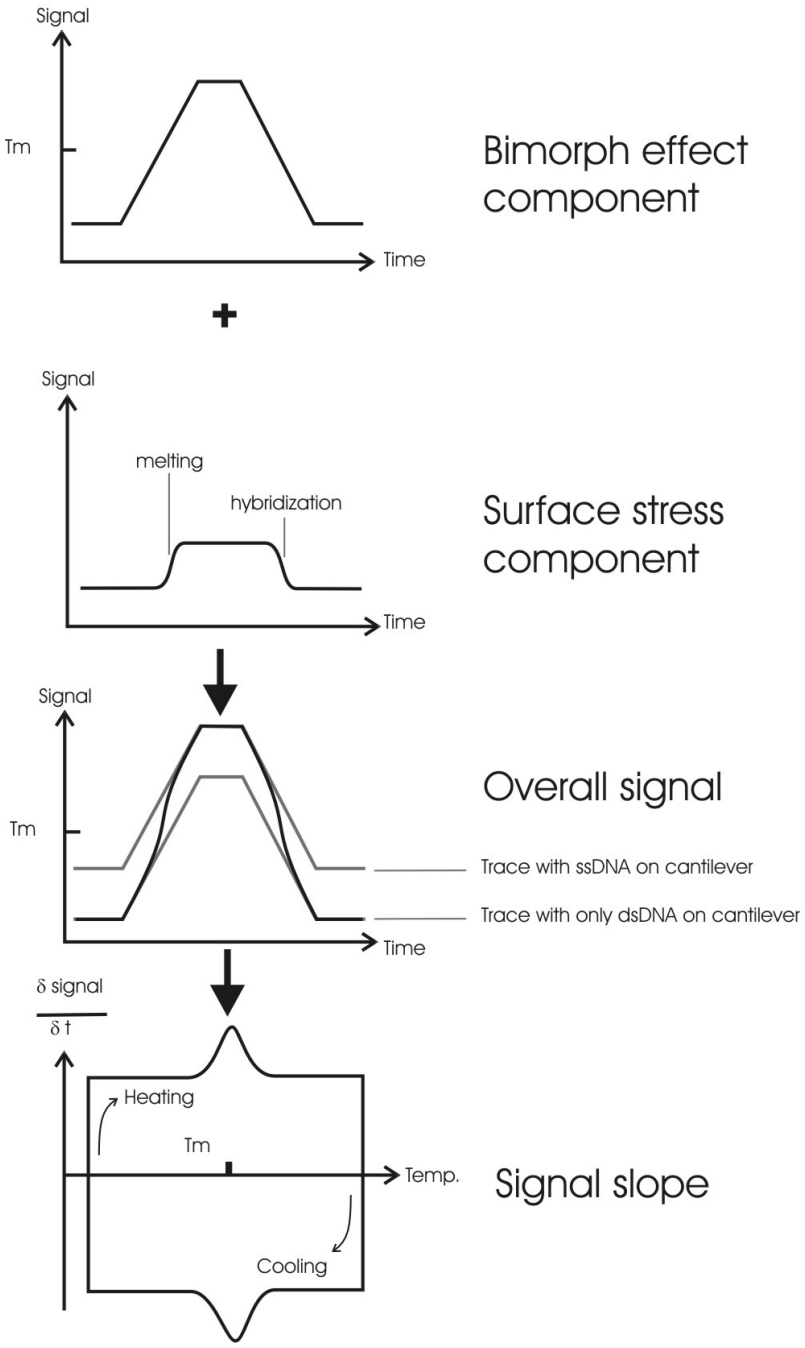

Figure 2.8: During the heating/cooling of the system, the output voltage of the cantilever-based is the convolution of the signal components due to the bimorph effect and to the change of surface stress occurring at the melting and hybridization of the DNA on one of the cantilevers. When the slope of the signal is calculated, the melting and hybridization of the DNA yield a peak (valley) at the temperature T_m.

tions based on equation 2.1-3

words, at low concentration the hybridization signal is expected to be slower than the melting signal.

2.3.3 Possible experimental protocol for PCR monitoring

A first solution for designing the experimental protocol and the most obvious is to immobilize on the cantilever surface one of the pair of primers. In this case the situation is as described in figure 2.7. As the template hybridize to the primers immobilized on the cantilever, it produces a 5'end overhang that is elongated by the polymerase. At each new PCR cycle, more primers hybridize to a template and are elongated. The primers that are elongated then serve as templates as the second primers hybridize to them. In this case, the sensitivity of the sensor might be increased because the DNA-capture probes are longer which is expected to produce higher surface stress during hybridization and elongation. This also means that the melting temperature of the DNA-capture probe increases because it is elongated. On the other hand, previous studies have shown that real solid-phase PCR may be a minority because of the desorption of the immobilized DNA; most of the enzymatic reaction would occur in liquid phase and only a few of the DNA capture probes on the surface would be elongated [44]. Another drawback is that early in the process, some of the primers will be elongated with the 5'-dangling end of the sequence as this occur is normal liquid phase PCR but those "wrong" copies are a minority. One can also immobilize both primers on the cantilever. In this case most of the amplification process is forced to happen on the cantilever surface as none of the primers are present initially in the solution.

Alternatively the DNA-capture probes on the cantilever can have a different sequence than the priming sequence (see figure 2.9). In particular, the sequence can be chosen to be at the 5'end of the template sequence (the primers are at the 3'end). In this case most of the amplification takes place in the liquid phase because the primers are in solution. When templates then hybridize to the capture probes on the cantilever, they do not produce a 5'end overhang so that they are not elongated. In that sense the surface of the cantilever is not modified and the melting temperature of the capture probes remain constant during the amplification. Of course at the beginning of the amplification, the capture probe could hybridize with some of the copies with 5'-dangling ends and then they would be elongated but those copies with 5'-dangling ends are minority.

Finally, using the PCR primers as capture probes with-out elongating them is possible by immobilizing them at their 3'end. Indeed they would be able to hybridize to the template but, as the thiol-modification is at their 3'end, the primers/capture probes are not elongated by the polymerase. Furthermore, those of the capture probes that desorb from the surface due to heat cycling cannot serve as primers for the elongation. One can thus separate detection and am-

plification by having one primer sequence immobilized on the cantilever and the other free in solution. As depicted in figure 2.10, the primer 1 are not elongated and the corresponding template are amplified in solution by the elongation of the primer 2. In this case the melting temperature of the DNA hybridized on the cantilever remains the same. On the other hand the amplification of the template is slower because only one template is amplified.

In conclusion, The main step toward the online monitoring of PCR by surface-stress sensing is to demonstrate that it is possible to detect non-isothermal melting or/and hybridization by this technique. The detection through non-isothermal hybridization or melting is a powerful tool to discriminate DNA molecules by their melting temperature. Once this is demonstrated several strategies can be chosen to immobilize DNA sequence specific to the PCR products that should be detected.

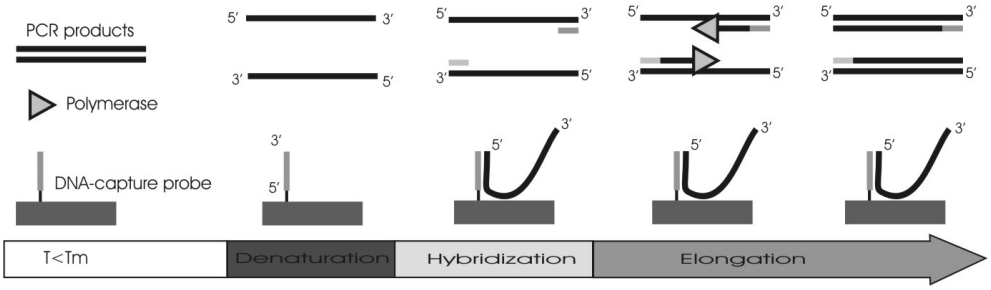

Figure 2.9: In case DNA-capture probes have a sequence different from the PCR primer sequence that matches the 5'end of the template, they are not elongated during the PCR/detection and their melting temperature remains constant. The elongation takes place in solution only.

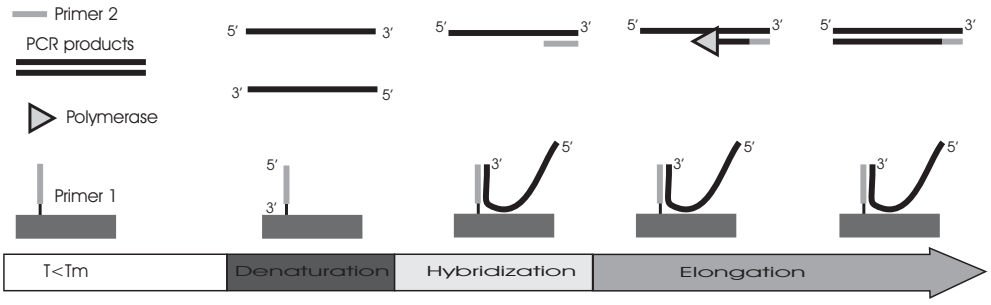

Figure 2.10: In case only the primer 2 is in solution, the DNA-capture probes on the cantilever are not elongated while the corresponding templates are copied in solution. Again the melting temperature of the DNA on the cantilever remains constant.

2.4 Denaturation of DNA measured by spectrophotometry

As an introduction to the measurement of DNA denaturation by cantilever-based sensor, the melting temperature of the BRCA1 probe DNA sequence was investigated by spectrophotometry.

2.4.1 Introduction to the method

Spectrophotometry is, together with calorimetry, the established method for investigating nucleic acids melting and hybridization reactions. It is relying on the change of adsorbance at 260 nm of the nucleic acid during melting (*hyperchromicity*).
The adsorbance is measured using a Hewlet-Packard 8453 diode array spectrophotometer. A quartz cell containing one mL of the DNA solution is placed on the path of the 260 nm light beam. The path length into the solution is one centimeter. The cell is thermostated by the circulation of water from a water bath and the temperature of the solution is measured with a digital thermometer. The probe of the thermometer is placed inside the solution and is removed during each adsorbance measurement. One adsorbance measurement is performed on a wide wavelength range for the buffer solution at room temperature. The solution containing the DNA is loaded and the water bath is heated continuously. The temperature rises from room temperature to 80 °C at a rate of about 1 °C/min. The temperature is measured before each adsorbance measurement performed from 240 to 280 nm. The software subtracts the reference adsorbance spectrum from the spectrum measured on the DNA solution and provides the direct peak adsorbance value (usually at 260 nm) in arbitrary units. The sequence of the BRCA1 probe used is 5'-ATT AAT GCT ATG CAG AAA ATC TTA G-3' and the target-DNA has the complementary sequence. In all measurements the concentration of the DNA capture probes and target is adjusted to 2.5 μM which yields an adsorbance in the middle of the adsorbance range of the apparatus (about 0.7) at room temperature. During heating the nucleic acids melt and the adsorbance increases before stabilizing at higher temperatures. The temperature of the middle point of the curve is the melting temperature of the DNA-oligos in the experimental conditions of pH, concentration and salts. At decreasing temperatures, the adsorbance decreases yielding the rehybridization curve. The melting and rehybridization curves were recorded in three different buffers. The 1xPCR buffer because that is the buffer for performing PCR, 1xTE buffer without additional salts and 1xTE with 0.1 M NaCl because that is the buffer solution used for the denaturation measurements with the cantilever-based sensor.

2.4.2 Melting temperature in 1xPCR buffer

The 1xPCR buffer (PCR buffer II, Perkin-Elmer) contains 10 mM tris·HCl and 50 mM of potassium chloride at pH 8.3. Two samples were tested. Figure 2.11 shows the melting curve for both samples. For each branch of the curve (heating and cooling) the adsorbance was normalized to the adsorbance values at the highest and the lowest temperature.

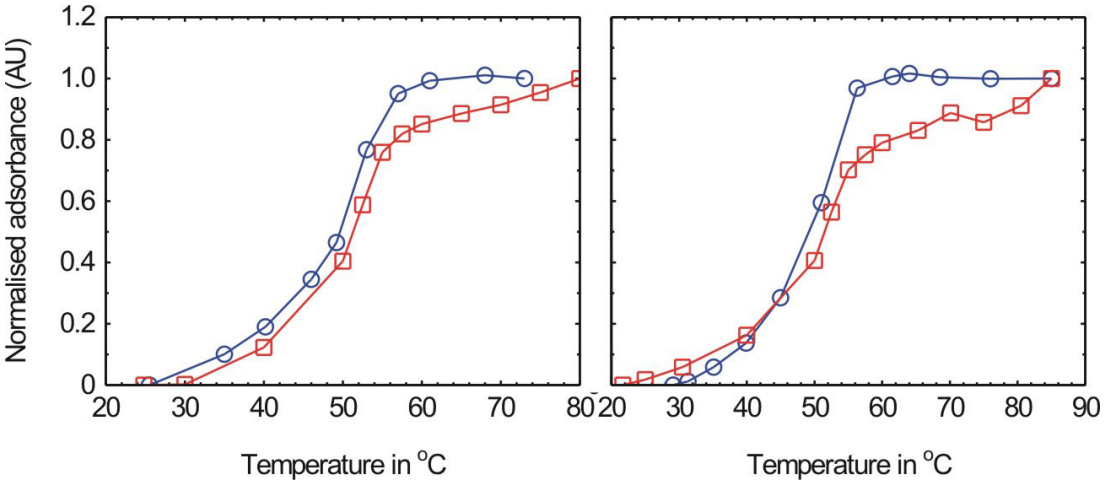

Figure 2.11: Melting curve in 1xPCR for two equivalent samples. Oligos are 25'mer long, diluted at 2.5 μM in 1xPCR buffer.

The temperature at the middle point of the curves is obtained at the adsorbance 0.5, both for the heating curve (squares) and cooling curve (circles) of each sample. The melting temperature for the oligos are obtained as the average of the temperatures determined for the heating and cooling curves:
Sample 1: $T_m = 50.5$ °C $\pm$ 1 °C
Sample 2: $T_m = 50.2$ °C $\pm$ 1 °C.
The theoretical T_m obtained for an oligo concentration of 2.5 μM and a salt concentration of 0.05 M from equation 2.1-3 is 54.3 $\pm$ 1.4 °C [3]. The difference can be explained by the pH value being slightly out of range of validity indicated for the equation.

2.4.3 Melting temperature in 1xTE buffer

The 1xTE buffer contains 10 mM of Tris·HCl (Trizma hypochloride, Sigma) and 1 mM of EDTA·Na_2 salt at pH 7.0. The EDTA·Na_2 salt contributes to the sodium ion concentration by 2 mM. The pH of the solution was adjusted by titration of

[3]The calculation was performed on the website of Integrated DNA Technology at http://biotools.idtdna.com/analyzer/

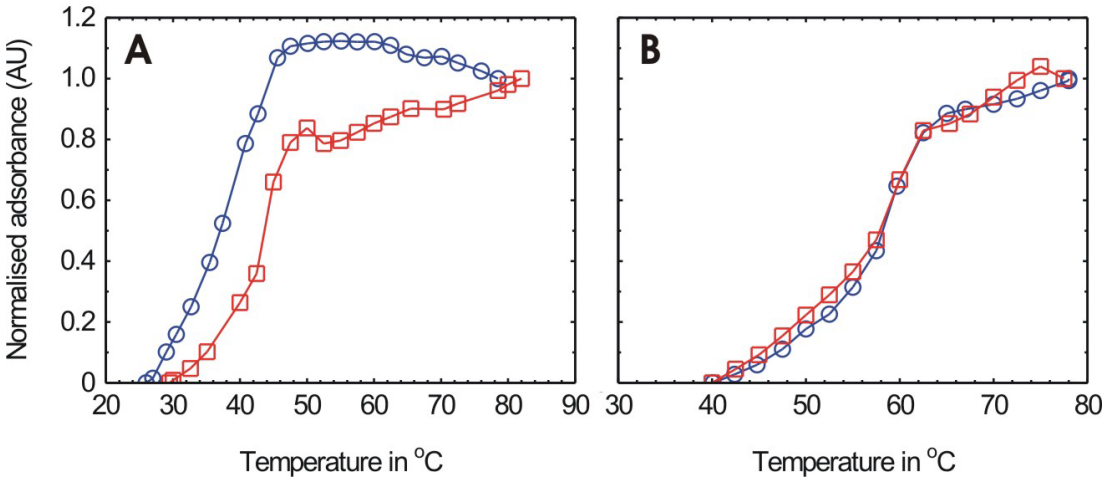

Figure 2.12: **A** Melting curve in 1xTE. **B** Melting curve in 1xTE + 0.1M NaCl. Oligos are 25'mer long diluted at 2.5 μM.

the HCl by NaOH which increases the concentration of sodium ions. Therefore, the concentration of sodium ions is not precisely known. Nevertheless, it is out of the range of applicability of the equation 2.1-3 in section 2.1.3. The melting curve is shown in figure 2.12 A.
The adsorbance values have been normalised at the highest and lowest temperature. For a normalized adsorbance of 0.5, the temperature is $T_m = 40 \pm 3$ °C.

2.4.4 Melting temperature in 1xTE + 0.1 M NaCl

The buffer contains 10 mM of Tris·HCl (Trizma hypochloride, Sigma), 1 mM of EDTA·Na_2 salt and 0.1 M of NaCl at pH 7.0. Again EDTA·Na_2 and NaOH used for adjusting the pH contributes to the sodium concentration but variations are minimal compared to the total concentration of Sodium. The melting curve is shown in figure 2.12 B.
Here the melting temperature is $T_m = 58 \pm 1$ °C. This is in very good agreement with the value of 57.9 ± 1.4 °C obtained for an oligo concentration of 2.5 μM and a salt concentration of 0.1 M from equation 2.1-3 [4].

2.4.5 About the shape of the melting curves

The shape of the melting/rehybridization curves suggests either a gaussian or a lorentzian rate of denaturation/hybridization. Both models were applied to the

[4]The calculation was performed on the website of Integrated DNA Technology at http://biotools.idtdna.com/analyzer/

melting curve in 1xTE + 0.1 M NaCl (figure 2.12 B). Assuming a lorentzian rate, the rate and the melting curve have the following forms:

$$\frac{dAdsorbance}{dT} = \frac{\alpha}{\pi}\frac{b}{(T-T_m)^2+b^2} \tag{2.4-1}$$

$$Adsorbance = \frac{\alpha}{\pi}\left[\arctan\left(\frac{T-T_m}{b}\right)+\frac{\pi}{2}\right]+cT+d \tag{2.4-2}$$

where T_m, b, c, d and α are parameters to be adjusted. T_m is the melting temperature of the oligos because is is the middle point of the melting curve where the rate of melting is the highest.

Assuming a gaussian rate, the rate and the melting curve have the forms:

$$\frac{dAdsorbance}{dT} = \alpha\ \exp\left[-\frac{(T-T_m)^2}{b}\right] \tag{2.4-3}$$

$$Adsorbance = \frac{\alpha\sqrt{\pi b}}{2}\left[1+erf\left(\frac{T-T_m}{\sqrt{b}}\right)\right]+cT+d \tag{2.4-4}$$

The linear function is used to model the drift of the measurement. The melting and rehybridization curves where modelled and the melting temperatures where extracted from the lorentzian and the gaussian profiles shown in figure 2.13 and 2.14.

The Lorentzian profiles yield $T_m = 57.875 \pm 0.025$ °C with a sum of squared residuals χ^2 of 0.010 and 0.008 for the heating and cooling data. The gaussian profiles yield $T_m = 57.875 \pm 0.001$ °C with the same fitting accuracy. This is in good agreement with the T_m determined graphically. In both cases the melting rate is lower than the rehybridization rate and the difference in peak area suggests that less oligos melt than rehybridize.

2.4.6 Conclusion

The spectrophotometry technique is adequate to measure the melting curve of the oligos and results are in agreement with the theoretical determination of T_m. In the following, T_m will be calculated using equation 2.1-3 to predict the results of the measurements by cantilever-based sensor. Moreover, the slope of the cantilever-based sensor output voltage obtained upon denaturation and rehybridization is expected to be proportional to the rate of melting/hybridization assuming that other contributions (bimorph and TCR) are proportional to the temperature. Therefore the output voltage slope should like the melting rate be well modelled by either a Lorentzian or Gaussian function.

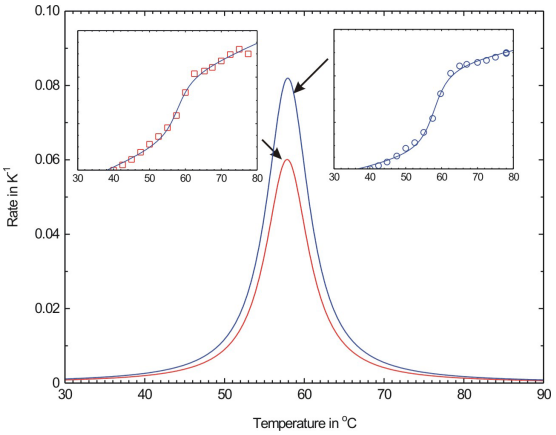

Figure 2.13: The Lorentzian rate of melting and rehybridization in 1xTE + 0.1 M NaCl. The linear component of the fit was removed before calculating the rate. Shown in inset, the heating (left) and cooling (right) data and Lorentzian fits.

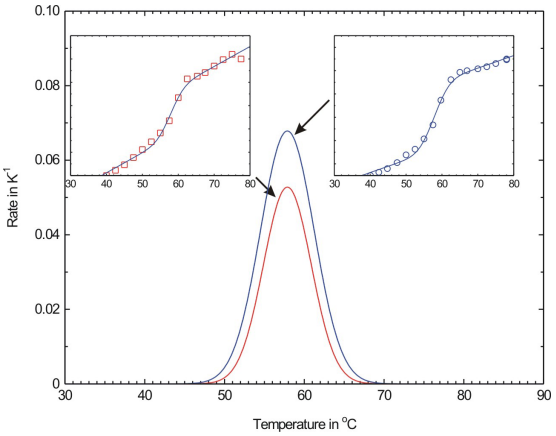

Figure 2.14: The Gaussian rate of melting and rehybridization in 1xTE + 0.1 M NaCl. The linear component of the fit was removed before calculating the rate. Shown in inset, the heating (left) and cooling (right) data and Gaussian fits.

Chapter 3

Immobilization of DNA-capture probes for cantilever-based sensor

3.1 DNA immobilization methods

DNA and protein immobilization onto solid surfaces is a key issue of the development of biosensors and, to some extend, of micro total analysis systems (μTAS). Cantilever-based sensors belong to a group of biosensors that rely on the interaction of the analyte with the surface of the sensor. This group includes micro-arrays, quartz crystal micro-balances (QCM), surface plasmon resonance (SPR) sensors and surface acoustic waves (SAW) devices. This is in contrast with biosensors/tests such as colorimetric sensors and optical sensors based on adsorption/fluorescence measurements where the analyte stays in the solution phase. Immobilizing receptor molecules on the sensor surface is called the *functionalization* of the sensor because attaching receptor molecules onto the surface of a biosensor makes it sensitive to the analyte molecules to be detected. Attaching biomolecules on the surface of a biosensor enables to localize and concentrate the signal for a better read out. In the case of micro arrays of DNA, patterning the surface enables to localize in one spot the DNA of same sequences and place many spots on one device. The different sequences are then optically identified by there locations on the surface. In the case of micro-cantilever sensors, attaching receptor molecules on the cantilever is the *sine qua non* condition for obtaining a surface stress change as described in section 1. In the case of a resonant sensor such as QCM or resonant micro-cantilevers, attaching the molecules onto the sensor surface increases its mass which yields a frequency change.
On the other hand, the localization of biomolecules to solid/liquid interfaces modifies their intrinsic properties as described for DNA in section 2.1.3. Therefore the immobilization technique shall also preserve the recognition ability of the receptor molecule. Several techniques exist for attaching DNA onto solid substrates. Here are described two major methods, the organosilicon-based and the

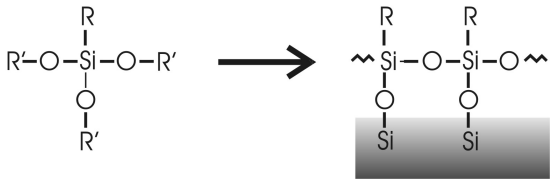

Figure 3.1: The silanes used for the derivatization of glass carry three identical alkyl R' and one group R. R is the group that points away from the surface when the silane has reacted with the glass surface.

organosulfur-based techniques with focus on their applicability to functionalize a cantilever-based biosensor.

3.1.1 Silanization

The development of micro-technology has provided an efficient way of coupling biomolecules to glass by silanization. Indeed micro-technology is largely based on silicon processing including controlled modifications of the physical, optical, electrical properties of the surface of silicon and its derivative, notably silicon oxide. The formation of self-assembled monolayers (SAM) of molecules on solid surfaces provides an efficient way of modifying the surface properties such as hydrophobicity, stiction properties or charges. Silanes form SAM on several surfaces including silicon oxide/glass and has therefore been extensively studied (for review see Ulman [45]). Silanization is a suitable chemistry for the modification of glass in order to attach DNA on glass substrate thus providing the basic coupling chemistry for making nucleic acids micro-arrays. Various coupling chemistries are available for immobilizing DNA on silicon-based support via silanization. Typically the silane used is as depicted in figure 3.1. The three radicals R' are typically methyl or ethyl groups [46]. The adsorption of silanes on silicon oxide/glass results in the elimination of the R' radicals yielding Si-O-Si bonds to the surface and requires hydroxyl groups on the surface. The radical R can be chosen in order to modify the surface with more or less any chemical group. As examples, un-modified alkyl typically make the surface hydrophobic and fluorinated alkyl make teflon-like surfaces. In order to attach DNA on the silanized surface, R is typically a hydrocarbon chain carrying a single reactive moiety at its end pointing away from the glass. Typically the silane caries an amino group (APTES [1] [46], EDA [2] and HDA [3] [47, 48]), an aldehyde group [49, 50], a thiol group [51] or an epoxy group (GOPS [4] [46]). The chemical function is used for

[1] γ aminopropyl-triethoxysilane
[2] N-(2-aminoethyl)-3-aminopropylmethyl dimethoxysilane
[3] N-(6-aminohexyl)-aminopropyl trimethoxysilane
[4] 3 glycidoxypropyl-trimethoxysilane

reacting either directly with naturally occurring chemical functions of DNA, with a modification of the DNA strand (at its 5' or 3'end) or with an intermediate molecule (called spacer or hetero- and homo-difunctional linker) that reacts with DNA. More direct approaches that also rely on silanization consist of modifying DNA strands with a silyl group which react with the unmodified glass substrate [52] or to modify glass by silanization with an aminosilane and make it react directly with the thymine bases of DNA under UV exposure [53].
Some of those methods were compared by Zammatteo *et al.* [49]. The maximum hybridization efficiency is obtained on on aldehyde-coated glass but is still only 10 %. The authors conclude also that higher coverage of capture probes doesn't necessarily mean higher hybridization coverage.

On gold, the physisorption of trichlorosilane has been reported but the study does not conclude to a strong binding of the silane to the gold as the gold is inert and cannot covalently bind silanes [54].

3.1.2 Thiol-Gold chemistry

There is a growing interest for using gold as an immobilization surface for biomolecules both within the micro-array and the micromechanical sensor communities [55, 10]. The reason being the strong binding between gold and free thiol groups which takes place in a short time by passive adsorption. This makes it possible to achieve high coverage of any type of molecule that naturally include thiol groups in their structure or carry a thiol modification. Examples of such molecules are proteins naturally containing thiol *e.g.* cysteine amino acids or DNA-oligos modified with a thiol group. The adsorption of alkanethiols, thiol-modified DNA-oligos and proteins have been extensively studied by various techniques including Atomic Force Microscopy (AFM) [56], X-ray induced Photoemission spectroscopy (XPS) [57], *in situ* Scanning Tunnelling Microscopy (STM) [58], neutron reflectivity [59], radioactive tagging [60] and a combinaison of those techniques on antibodies [61], metalloprotein [62] and oligonucleotides [63, 60].
The adsorption of alkanethiols on single crystalline gold (111) constitutes the model system for the SAM formation of thiols on gold (see figure 3.2). The focus of alkanethiol studies is to understand the mechanism of formation of the SAM and conclusions are:

- **Alkanethiols form ordered films on Au(111)**. The alkane chains form a close packed hexagonal structure with a tilt angle of 30 ° to the surface and an inter-chain distance of 5 Å. It was shown that the sulfur atoms are paired in dimers and that the two atoms of the dimer may have different binding states with the surface [64, 65, 66].

- **The S-Au bond strength** is estimated to 167 kJ/mole [45]. This is to be compared with the typical C-C bond strength of $\sim$ 376 kJ/mole.

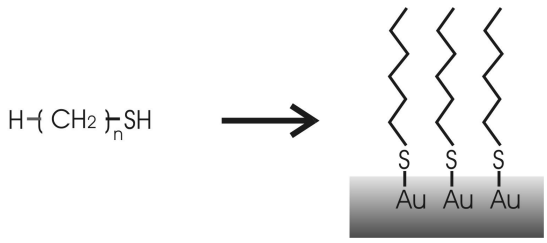

Figure 3.2: (**Left**) Alkanethiols are saturated hydrocarbon chains (with n being the number of carbon atoms) which carry a thiol function.(**right**) Thiols adsorb on gold by forming an almost covalent bond between the sulfur and the gold surface. Mercapto-hexane (n=6) is shown as an example.

- **The kinetics** of adsorption is a two step kinetics where the first step is a diffusion limited Langmuir adsorption dependent on the concentration and the second step corresponds to the ordering of the layer which is dependent on intermolecular interactions, mainly Van der Waals and dipole interactions for charged molecules [45]. Complete ordering can be observed for alkanethiols longer than 16 carbons and no ordering is observed for shorter than 8 carbons [67].

- **The stability** of adsorbed alkanethiols depends on temperature and length of the alkanethiol. For short alkanethiols, annealing can improve the order, while it is the opposite for long alkanethiols [68]. The desorption or decomposition of alkanethiols starts at 100 °C. Garg *et al.* reported the desorption in a hydrocarbon solvent of alkanethiols adsorbed on polycrystalline gold with length of 15 and 19 carbons for temperatures between 60 and 110 °C [69]. The results show that the fraction of SAM remaining is below 10 % after 1 hour at 100 °C and after only 5 minutes at 110 °C. Shorter alkanethiols tend to desorb faster. Alkanethiols desorb with a two step kinetics (first fast then slow) and desorb as disulfides. The study also shows that using alkanethiols with aromatic rings and multi sulfur anchoring improves the thermal stability of the SAM which may be very valuable for the immobilization of DNA for *in situ* PCR purposes. Because most studies concern long alkanethiols that are not soluble in water, no results where reported for alkanethiols in water.

The elaboration of more complex monolayer structures relies on the knowledge from the alkanethiol studies. Though, there are many aspects of the immobilization of DNA oligos via a thiol-modification that are specific to these molecules. First, DNA-oligos are larger molecules than most of the alkanethiols studied. Second, nucleic acids are charged molecules and thus interact more strongly than alkanethiols do during the formation of SAM. Finally, for biosensor applications it can be desirable to form SAM on polycrystalline gold instead of single crystalline

gold. The focus of thiol-modified nucleic acids SAM formation is to achieve a high coverage and to retain the binding specificity/efficiency of the immobilized nucleic acid. Moreover, this immobilization technique has a direct commercial interest for making biosensors.

- **On single crystalline gold**, a densely packed monolayer of 15'mer dsDNA was adsorbed on Au(111) yielding a coverage of 2.5 10^{11} molecules/mm^2 [60] [5]. Those were adsorbed directly as duplexes meaning that no *in situ* hybridization of the DNA layer is involved.

- **On polycrystalline gold**, the most valuable results with respect to applicability to biosensors were published by Herne *et al.* [57] and Steel *et al.* [70]. In those studies thiol-modified DNA is adsorbed together with mercaptohexanol (MCH) to form a mixed-layer. MCH is a 6 carbon long alkanethiol with an hydroxyl group. MCH adsorbs on gold in between the thiol-DNA oligos and displaces the un-specifically bound DNA strands. Thus only the DNA bound to the gold via a strong sulfur-gold bond remains on the surface and those remaining molecules are bound to the surface only via their modified end which makes them available for hybridization. 25'mer capture probe coverage as high as 5.2 ± 0.8 10^{10} molecules/mm^2 was demonstrated and the hybridization efficiency was 100 % [6]. One notice that though the specific area of polycrystalline gold is expected to be larger than for single crystalline gold because of the roughness, the coverage reported on this surface is almost a factor ten lower. This indicates that the packing of DNA molecules (their occupancy of binding sites on gold) in this study is probably as low as 1 % if one consider that the specific area is 10 times larger than on single crystalline gold.

The formation of a mixed layer of DNA oligos and MCH is *a priori* well suited for cantilever-based sensor applications.

Cleaning methods for gold

The presence of contaminants on the gold surface prior to the adsorption of thiolated molecules influences strongly the SAM formation. Therefore is the cleanliness of the gold surface a critical issue [71, 72]. Those contaminants are most probably hydrocarbon compounds adsorbed from air onto the gold surface thus minimizing the surface energy of the bare gold surface. Several cleaning methods have been reported and are summarized below:

[5] adsorbed for 12-48 hours at 0.1 mM in 5 mM phosphate/50 mM NaCl at pH 7.

[6] Adsorbed 4 hours from a 10 μM in 1 M phosphate buffer at pH 3.8 on polycrystalline gold evaporated on silicon (100), then washed and incubated 1 hour in MCH at 1 mM in water. The same authors also reported the same procedure at pH 7.

- **Piranha solution**, a mixture of hydrogen peroxide and sulfuric acid (1:3 H_2O_2:H_2SO_4), is a convenient and well established method for gold electrodes and surfaces on mica. However, this is not a suitable method for cleaning gold surfaces integrated in an assembly including polymer parts since polymers are also strongly oxidized. This method was successfully used for cleaning silicon chips with gold layers.

- **Oxygen plasma** cleaning is a dry process relying on the formation of oxygen radicals by electron discharge in oxygen and is suitable for cleaning assemblies with polymers. However, the temperature of the plasma is an issue, since high power produces a plasma with temperatures that can exceed the melting point of certain polymers [7].

- **Ozone** cleaning is a dry process also based on oxygen radicals which takes place at temperatures below 100 °C. It is performed in a commercial system based on the exposure to UV light in an oxygen containing atmosphere (air). The exposure to 185 nm radiations from a mercury arc lamp produces ozone from oxygen which is subsequently dissociated into oxygen radicals by a 254 nm radiations. Oxygen radicals are strong oxidizing agents.

- **Aqua Regia** solution, a mixture of nitric acid and hydrochloric acid, is a gold etchant made of concentrated acids and is thus a priori not suited to gold surface integrated in a sensor. However, the Aqua Regia can be diluted and thus the activity of the acid reduced. In contrast to the other three methods, aqua regia cleaning modifies the morphology of the gold surface which can be an advantage with respect to surface stress changes measured on a cantilever sensor since the surface area is increased. However the Aqua Regia etch can be difficult to control and can limit the re-use of the sensor as the gold layer is etched away [73].

Among these four methods, UV/ozone cleaning was further investigated for cantilever-based sensors. Under cleaning processes based on a strong oxidant agent such as piranha solution, oxygen plasma or ozone, the organic contaminants as well as the gold surface itself are oxidized. A gold oxide as thick as 1.7 nm is formed under a one hour ozone treatment [71]. As the gold oxide is not stable, it is reduced spontaneously. In order to avoid the re-deposition of contaminants, gold surface can be conserved in ethanol.

Investigation of UV/ozone cleaning

UV/ozone cleaning is investigated using a commercially available system (PR-100, UVP Inc.). The cleaning system consists of a mercury arc lamp and a stage where the sample is placed. The lamp provides UV radiations at 185 nm and 254

[7] 10 minutes at 500 W typically deforms a 1 mm PMMA plate which indicates a plasma temperature above 100 °C

nm (respectively 1.5 mW/cm^2 nominal and about ten times more at the distance between the sample and the lamp, approx. 1 inch).
In order to investigate the contamination of gold and thereafter the effect of the UV/ozone cleaning, several methods have been used including various spectrometry and hydrophobicity measurements. Spectrometry such as XPS provides an accurate information about the amount and the composition of the contaminants but this is a time consuming method and the time necessary to provide the vacuum conditions necessary to the experiment can also be a source of contamination by oil traces from the pumps in the not-yet established vacuum. On the other hand the evaluation of the hydrophobicity of the gold surface is a quick method. Indeed, a clean gold surface is hydrophilic and gold contaminated by hydrocarbons is hydrophobic. A measurement of the contact angle of a gold surface with water thus provides a good evaluation of its cleanliness. Simpler but only qualitative are the so-called steam test and water-break test. In both tests the morphology of a thin film of water deposited on the surface either by dipping the gold surface in water or by condensation of steam is revealing the hydrophobicity of the gold surface. If the film is homogeneous, the surface is hydrophilic, if the film appears blurry, the water forms droplets which indicates a hydrophobic surface (like steam condensation on a window) [8].

The cleaning of polycrystalline gold samples coated with alkanethiols was investigated by steam test and water break test. gold coated with alkanethiols is a good model for a gold surface contaminated by adventitious carbon because it is hydrophobic and is an organic monolayer as contaminants are expected to be. A silicon wafer coated with 100 Å of chromium and 600 Å of gold was cut into pieces and immersed in an octadecanethiol (ODT) solution in ethanol at a concentration of 100 μM for over 12 hours. The sample were then rinsed and conserved in ethanol. One sample was used as reference and others were cleaned an increasing amount of time in the UV/ozone cleaner. On each sample the steam test and water break test were declared positive if the water film was transparent and negative if the film was blurry indicating a hydrophobic surface.
The results in table 3.1 show that an ozone cleaning of 20 minutes is sufficient to remove a SAM of ODT assembled on gold. One should notice that this time span includes the 10 minutes necessary for the lamp to warm up before the system reaches its maximum ozone concentration. The recontamination of the gold surface in air was detected very rapidly after the end of the cleaning (less than a minute) but this is very dependent on the storage conditions. For samples that became hydrophobic (both tests negative) after one hour in air, a 5 minutes ozone cleaning was sufficient to yield clean hydrophilic surfaces (both tests positive). Finally, the steam test was seen to be the most sensitive. Since the amount of water deposited on the surface is smaller, the water film is thinner and isolated

[8] In *Operating Instruction Manual, UVP, Inc.*

Time in minutes	0	5	10	20	30	60
Steam test	-	?	?	+	+	+
Water-break test	-	+	+	+	+	+

Table 3.1: Hydrophobicity tests on ozone cleaned polycrystalline gold. The tests are positive when the water film is transparent indicating a hydrophilic/clean surface.

droplets can thus form more easily. In the case of a gold layer on cantilever-based sensor, the gold layer can be deposited as a batch process or on a single cantilever just before use. This strongly influences the cleanliness of the gold. In the laster case, the deposition on a chip basis provides a freshly deposited gold that is clean but the characteristics of the gold would vary from one chip to the other and the process is time consuming. In the first case, the gold layer is most probably patterned by photolithography and is thus exposed to various chemicals including resist that can contaminate the surface. It is shown later that for the cantilever-based chips, an ozone cleaning of 15 minutes preceded by a 10 minutes warming up of the cleaning system was enough to achieve reliable immobilization of thiol-modified DNA oligos [9].

Stability of free thiol modifications

Thiol-modified DNA-oligos are typically synthesized as hetero disulfides (figure 3.3 A) where a nucleic acid strand and a radical group R are linked by a disulfide bridge. DNA-oligos with a free thiol modification (figure 3.3 B) are obtained by reduction of the disulfides and removal of the R group. Free thiols are not stable in solution and tend to dimerize to form disulfides which are stable. Both disulfides and free thiols adsorb on gold. This was demonstrated for alkanethiols which suggests that, at least on Au(111), free thiols are adsorbed on gold as dimers and eventually desorb as disulfides [66, 74]. The adsorption of nucleic acids based disulfides was demonstrated by XPS and cyclic voltametry

[9] See the measurements by fluorescence and the comparison of RIE, plasma and ozone cleaning.

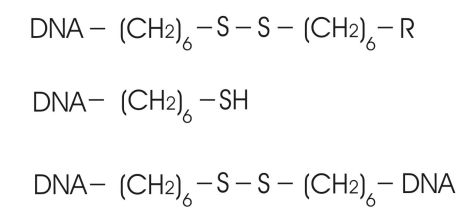

Figure 3.3: Thiol-modified DNA oligos are synthesized as disulfides (**A**) where typically R is a dimethoxytrityl (DMT) group. After reduction the DNA-oligo carries a free thiol group (**B**). DNA-oligos with free thiol groups tend to form homo-dimers (**C**).

for hetero-dimers (figure 3.3 A) and homo-dimers (figure 3.3 C) [63, 75]. Thus practically, thiol-modified DNA-oligos can be adsorbed as disulfides or free thiols in order to produced a monolayer of DNA-oligos on gold. Surprisingly, only the free thiol form is utilized by the biosensor community. In section 3.2, we demonstrate that using commercially available deprotected thiol-modified oligos is successful. Freshly deprotected thiol-modified oligos are also used. Two protocols are available. One consisting of the cleavage of the disulfide bridge by DTT, the precipitation of DTT and DMT residues with $AgNO_3$ and the purification by centrifugation. The second protocol consists of the cleavage of the disulfide bridge by DTT and gel filtration of the thiol-oligos. This protocol minimizes the loss of DNA during the purification and yield even higher coverage than commercially deprotected oligos (see appendix B).

3.2 Investigation of thiol-Gold immobilization method for PCR applications

Although thiol-Gold chemistry is widely used for biosensors and has potential as immobilization chemistry for micro-array fabrication, the stability of DNA-oligos immobilized on gold surfaces has not been as thoroughly investigated as DNA-oligos immobilized on chemically treated glass surfaces [44]. The thermal stability of immobilized DNA capture probes is of special interest since a high stability is a key issue for performing solid phase heat requiring processes such as the PCR. In order to investigate the suitability of thiol based immobilization chemistry for cantilever-based sensor for PCR applications, DNA hybridization assays were made by immobilizing thiol-modified DNA-capture oligos on gold-coated substrates, and subsequently submitting the arrays to heat cycling. The assays were prepared using a reliable immobilization protocol, previously reported in the literature involving the formation of a mixed layer of DNA-capture oligos and 6-mercapto-1-hexanol (MCH) [57].
Three sets of experiments are presented. First the technique of making DNA micro-arrays on gold for fluorescence scanning is investigated. Second, the density of functional DNA-capture oligos present before and remaining after heat cycling was investigated by radio-labeling and fluorescence scanning on macro-arrays made of 1 μL spots. Third, the density of hybridization during a PCR heat cycling was investigated by fluorescence scanning using micro-arrays. The results of radio-labelling and fluorescence scanning on the macro- and micro-arrays are summarized and the stability of such assays is discussed in section 3.2.4.

3.2.1 Oligonucleotides microarrays and fluorescence scanning on gold

In this section, the experimental protocol for making DNA-hybridization assays on gold is presented. Then, contact printing is characterized and fluorescence scanning on gold is calibrated. These results are later on used for making DNA-arrays on gold and quantifying hybridization to the arrays by fluorescence scanning.

Principle of DNA micro-arrays

DNA micro-arrays utilize DNA hybridization assays attached on a solid substrate and fluorescence scanning as read-out. Micro-arrays were developed on glass substrates and alternatively on polymer surfaces and consist of arranging on a solid surface a 2 dimensional array of dots, each dot consisting of one type of DNA-capture oligos attached to the surface and having a known base sequence [76, 77, 78]. Primarily this hybridization assay is intended for hybridization with complementary DNA reporters tagged with fluorescent labels. The reporter DNA solution can either contain one or several DNA sequences tagged with either one or different type of fluorophores having different characteristic wavelength (color). The arrays are then read by fluorescence scanning, the fluorescence of each dot indicating the amount of fragments with the corresponding sequence that was present in the DNA reporter sample. Later, in the development of DNA-microarrays, those were used for performing *in situ* enzymatic reactions as ligation, extension by polymerase or restriction in order to increase the sensitivity and the specificity of the assay and thus detect single nucleotide polymorphism (SNP) or making large gene expression arrays, the two main applications of DNA and RNA micro-arrays.
As depicted in figure 3.4, making DNA hybridization assays in a micro-array format for fluorescence scanning requires to:

1. Immobilize DNA-capture probes on gold in a DNA array format

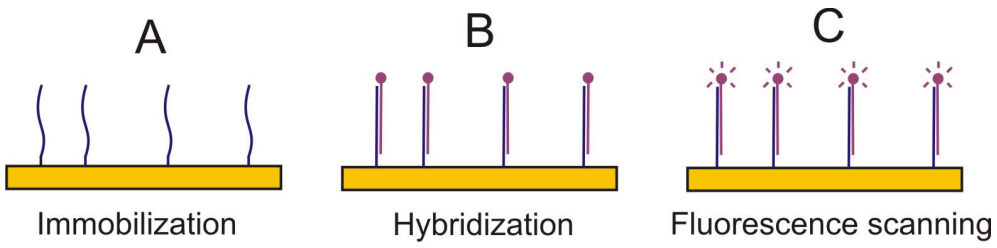

Figure 3.4: (**A**) DNA-capture probes are immobilized on the substrate. (**B**) The array is hybridized to fluorescent tagged reporter DNA. (**C**) The array is read-out by fluorescence scanning and the fluorescence of each dot of the array is quantified.

2. Hybridize fluorescent tagged reporter DNA to the array
3. Read-out the array by fluorescence scanning
4. Quantify the number of hybridized DNA

In addition to those steps, the application of DNA-arrays to *in situ* PCR requires that the array is heat cycled. The above mentioned steps are established for glass substrates but are not for gold substrates. Glass is preferred to gold as DNA array support because of the relative novelty of thiol-based immobilization techniques compare to organo-silanes based methods which are used on glass and because of the quenching of fluorescent dyes by metallic surfaces. Briefly, the proximity of the metallic surface causes the fluorescent dye to transfer an electron to the surface instead of emitting a photon after being excited. This thus reduces considerably the fluorescence signal obtained from the DNA array. On the other hand the choice of a metallic surface as substrate for fluorescence detection can provide an increase of fluorescence signal as depicted in figure 3.5. Because fluorescent dyes emit light spherically (in any directions not depending on the direction of the excitation light), imaging a fluorescent dye on a reflective surface can in principle enable to collect the fraction of light emitted toward the surface and reflected within the angular acceptance of the optics. A fluorescence scanner having a depth of focus in the μm range provides that both the dye and its image are in focus, the light reflected being effectively collected. On the other hand the reflection on the surface is not total and introduces scattering due to the surface roughness (in case the roughness is in the order of magnitude of the wavelength). If the surface roughness is in the range of the wavelength then figure 3.5 left is a wrong picture and figure 3.5 right is more relevant. Nevertheless, a part of the fluorescence emitted toward the surface is scattered with an angle comprised in the cone of admittance of the optics and is thus collected. In addition, the excitation light is also more reflected on a gold surface which can increase the background signal depending on the quality of the wavelength discrimination capability of the scanner.
We chose to make DNA-micro arrays on gold in order both to investigate the feasibility of DNA micro-arrays on gold and to gather knowledge about the suitability of thiol-based immobilization technique for PCR applications. In the following the steps 1 to 5 are established and characterized for gold surfaces.

Preparation of gold surfaces

Standard microscope glass slides (75 x 25 mm, Knittel Gläser, VWR, Germany) were used as substrates for making arrays. The slides were cleaned in piranha solution for one hour and conserved in water until they were coated with 100 Å of chromium followed by 600 Å of gold in an E-beam evaporating system (Alcatel, France). Slides were conserved in Milli-Q water and cleaned for 40 minutes in a

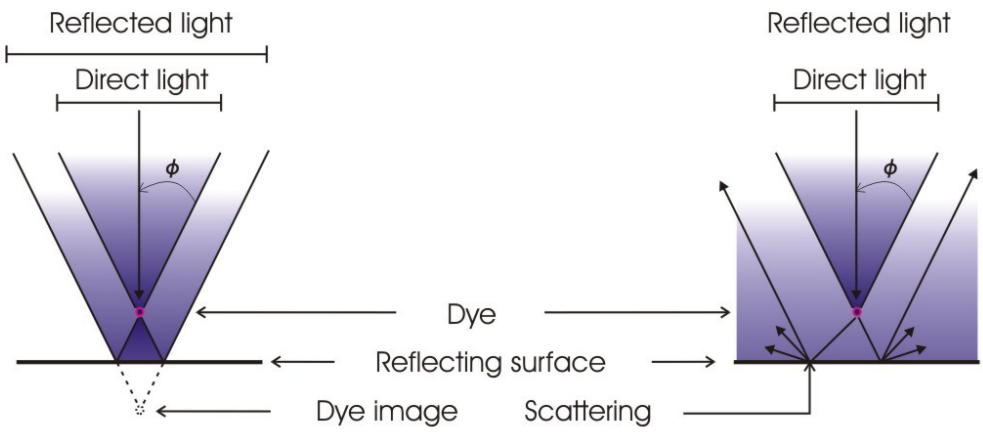

Figure 3.5: In the ideal case of a flat surface (**left**), the light emitted by a fluorescent dye and reflected on the metallic surface is collected by the optics. In the case of a rough surface (**right**) the light is scattered, partly within the cone of admittance of the optics. In both cases the light collected by the fluorescence scanner is increased.

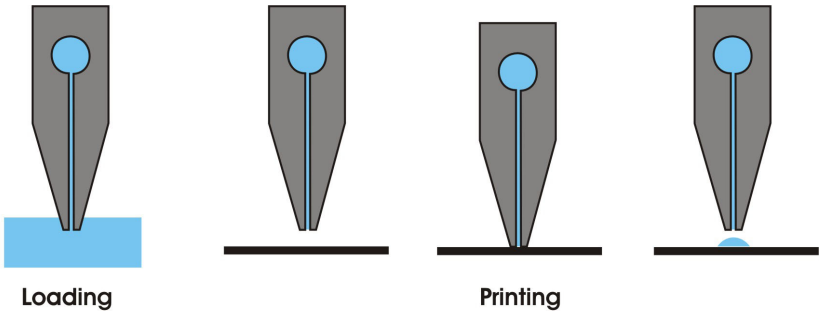

Figure 3.6: In contact printing the stylus is loaded by capillary forces with the solution to print. A drop of solution is printed on the surface each time the stylus is brought in contact with it.

PR100 UV/Ozone cleaning system (UV Products, UK) prior to spotting of the DNA-capture oligos (Q-Array spotter, Genetix, UK).

Contact printing: calibration of the spot volume

Contact printing is used for delivering small volumes of DNA-capture solution onto a surface in an automated way. In contact printing, a stylus having a vertical slit with a reservoir is dept into the solution to print. By capillarity the solution enters the slit and the reservoir (figure 3.6). The stylus is then brought in contact with the surface. At each contact with the stylus, a small portion of the solution is delivered onto the surface. In order to determine the volume of solution delivered by contact printing on a gold surface and the amount of

Fluorophore density in pmol/mm^2	Area in mm^2	Volume in nL	Molar density at 10 μM in molecules/mm^2	Molar density at 50 μM in molecules/mm^2
1.0925 ± 0.100 10^{-1}	4.7 ± 0.5 10^{-2}	1.035 ± 0.225	[1.305 ± 0.145] 10^{11}	[6.545 ± 0.745] 10^{11}

Table 3.2: The fluorophore coverage of two micro-spots made by contact printing were calculating using the calibration of the fluorescence density vs. fluorophore coverage made with macro-spots of 1 μL.

capture probes available per binding site, a dilution series of Cy 5' labeled target DNA-oligos (0.001 - 10 μM) was made in spotting solution and spotted onto gold-coated slides. Replicate spots were made either by contact printing using the robotic pin spotter or by hand using a standard automatic pipette (Eppendorf, Germany). The volume of the pipetted spots were adjusted to 0.5 and 1 μL. All the dilution series where imaged at 80% laser and photo-multiplicator tube (PMT) power. The spots were allowed to dry and for the macro-array spots, the density of fluorescence in digital light units (DLU) per mm^2 was plotted against the density of Cy 5' thus providing a calibration curve of the fluorescence density vs. the density of fluorophores (figure 3.7). Next, by measuring the fluorescence density of the spots made by contact printing and reading the corresponding fluorophore density on the calibration curves made for macro-spotted 0.5 and 1 μL spots, the volume delivered by the robot pin spotter was calculated.
Two calibration curves made with 1 μL and 0.5 μL spots both showed a saturation level and a linear part in a log-log plot (squares in Figure 3.9). The fluorescence density of the replicate spots made by contact printing was very homogenous. In order to calculate the volume spotted, spots made by contact printing with the 5 μM solution were chosen since their fluorescence density was within the linear range in the log-log plot (10^8 to 10^9 DLU/mm^2) (Figure 3.7). The density of the Cy 5' groups in the 1 μL and 0.5 μL spots was found to be 1.070 and 1.115 10^{-1} pmol/mm^2 and the spot area was 4.2 and 5.2 10^{-2} mm^2 respectively (Table 3.2). The volume of Cy 5' solution deposited by robot contact printing on each of the two spots was derived from the density of Cy 5', the area extracted from the fluorescence image and the concentration of the solution (5 μM). The volumes deposited by contact printing were found to be 1±0.2 nL.

A homogeneous fluorescence signal was obtained from the spots as shown in figure 3.8. Assuming the spot volume and the surface to volume ratio to be constant when using spotting solution or thiol-modified capture probe solution, the print volume on gold is 1 nL and the spot diameter is 120 μm (Table 3.2). Similar results were published for contact printing of oligo solutions on silanized glass by Cheung *et al.* [53]. In this study they assumed that the solution deposited on the surface forms hemispherical spots and thus calculated the volume of the spots from their diameter. The results of table 3.2 clearly show that for equivalent diameters of 120 μm the volume of the spots on gold is half of the value calculated

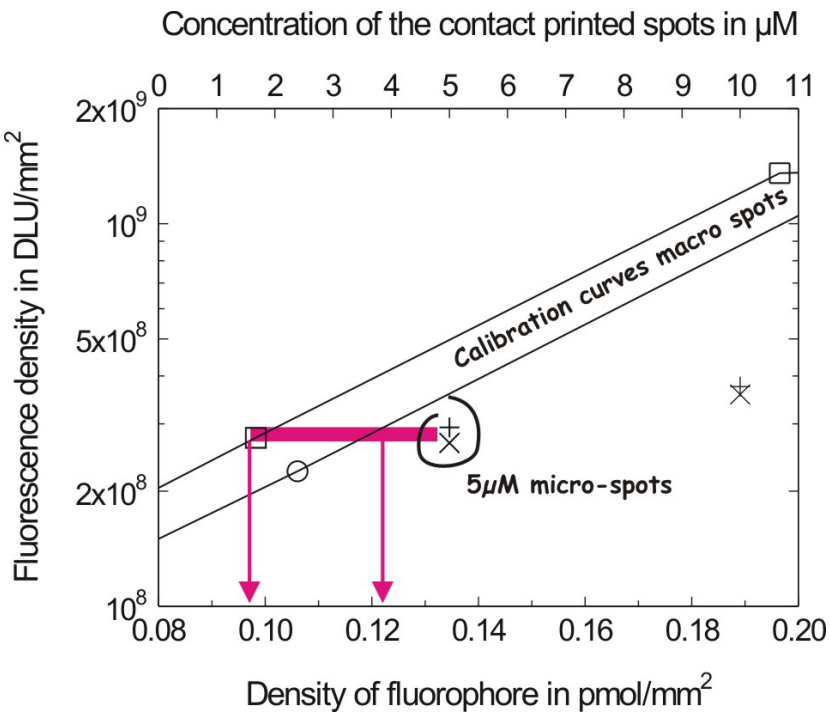

Figure 3.7: The figure shows how, by reporting the fluorescence density of the 5 μM spots made by contact printing (**crosses**) on the calibration curve made with the 0.5 and 1 μL spots (**squares** and **circles**), the fluorophore density in the micro-spots was extracted. Thus, the volume of solution deposited on each micro-spot by contact printing was calculated using the concentration of the solution and the area of the spots.

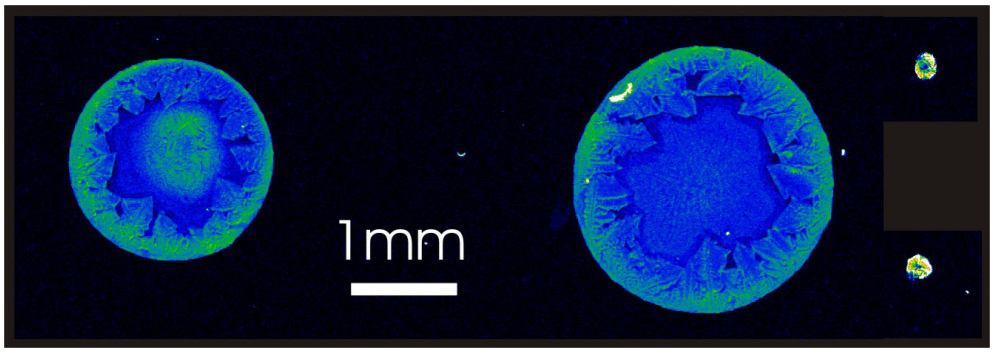

Figure 3.8: Fluorescence image of the 0.5 μL spots (**left**), the 1 μL spots (**middle**) and two 5 μM spots made by contact printing (**right**) on gold with Cy5' labelled reporter DNA in spotting solution. The spots are those used in figure 3.7.

with the hemispherical shape (1.9 nL). This must be due to the hydrophilic nature of clean gold surfaces lowering the contact angle much below the 90 ° required for

forming a hemispherical drop. From the point of view of microarray fabrication, gold is not a suitable surface in the sense that clean gold which is required for thiol immobilization is very hydrophilic which prevents large volume to surface ratio during the spotting. Another reason for density of fluorophore to be lower might be the spreading of the spots during the incubation in a wet atmosphere on the gold surface. The volume of printed/spotted solution and the surface area to volume ratio of the spot was used to calculate the minimum concentration of DNA-capture probes needed for achieving a saturation of the available binding sites on the surface. Achieving a DNA-capture probe density in the range of 10^{10} to 10^{11} molecules/mm^2 over a spot area in the range of 4.2 to 5.2 10^{-2} mm^2 and for a spot volume of 1 nL requires a concentration of 50 μM (Table 3.2). It is here considered that some of the DNA-capture probes do not bind to the surface and are washed off.

Heat cycling

Arrays were enclosed by a plastic frame (GeneFrame^{TM}, Abgene, UK), placed in a thermal cycler (Peltier Thermal Cycler 200, MJ Research, USA) and denatured five minutes at 95 °C. The heat cycling for PCR consisted of a one-minute denaturing step at 95 °C, a one-minute annealing step at 55 °C and a one-minute extension step at 72 °C respectively, for a maximum of 31 cycles. Heat cycled arrays were washed twice for five minutes in water before phosphorimaging or subsequent hybridization with Cy 5' labeled target DNA-oligos and fluorescence imaging.

Fluorescence scanning settings

In the following experiments, the fluorescence scanning was performed using a Scanarray Lite 5000 (Packard Biochip Technology, USA) and the areas and fluorescence intensities were extracted from the images (Optiquant, Packard Biochip Technology, USA). The arrays were scanned with a 5 μm resolution at laser/PMT settings 80 % (micro-arrays) or 70 % (macro-arrays). Similar settings were used when scanning the dilution series of Cy'5 labeled target oligos hybridized to each type of array (*i.e.* the corresponding calibration curve). Each spot was fitted within a circular cell. The total fluorescence intensity in DLU and the area in mm^2 was extracted. For each spot, a cell of the same size as the spot was placed next to the spot and used for extracting the local value of the fluorescence background, which was then subtracted from the fluorescence intensity of the spot. All fluorescence density values listed in the following are the net values.

Calibration of fluorescence on gold

In order to quantify the density of target DNA-oligos hybridized to the DNA hybridization assays requires a standard curve showing the relation between the flu-

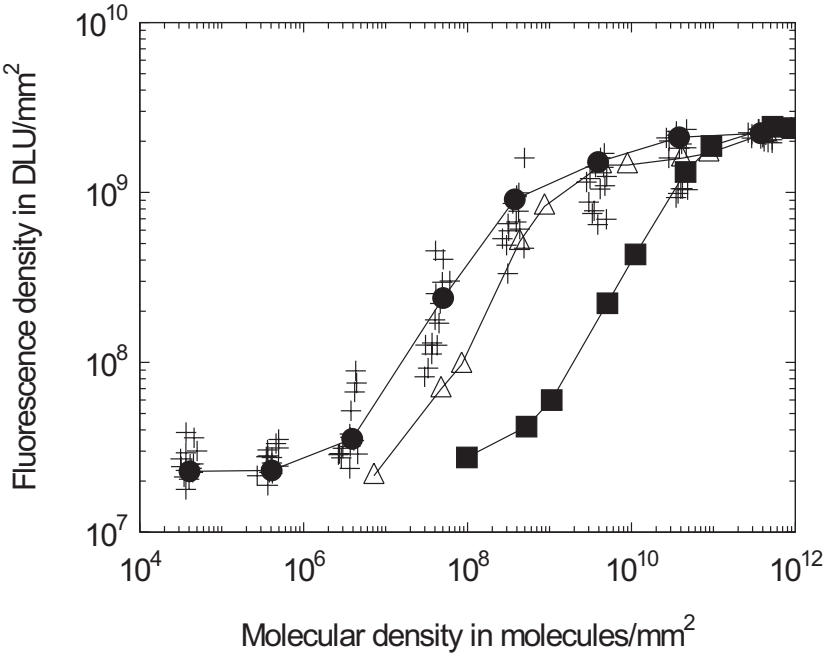

Figure 3.9: Two dilution series of a batch of Cy 5' labeled target DNA-oligo solution were spotted on seven glass slides coated with gold and MCH (**crosses**). Each slide was submitted to a different number of heat cycling in buffer. The representative standard curve (**black circles**) is the average of two selected standard curves and is used for quantification of hybridization on the micro-arrays. A dilution serie of the target DNA Cy 5' batch spotted on bare gold yields a standard curve shifted toward higher fluorophore density (**squares**). A second standard curves on MCH coated gold for a different Cy 5' labeled DNA-oligos batch is shown (**triangles**) and is used for quantification of hybridization on the macro-arrays.

orescence intensity and the number of fluorescent Cy 5' labeled target DNA-oligos hybridized to the surface, assuming one label per target oligo. The fluorescence intensity of the fluorescent label on gold coated with MCH was calibrated with respect to the density of fluorescent labels. The influence of the MCH coating of the gold on the fluorescence signal was investigated as follows.

Gold-coated slides were incubated overnight in 1 mM MCH. Slides were submitted to respectively 5, 10, 15, 20, 25 and 31 heat cycles as described, in a 1xPCR buffer and washed in Milli-Q water. Two dilution series of Cy 5' labeled target oligos in spotting solution ranging from 10 μM to 1 pM were macro-spotted in one μL volumes on each slide. The spots were allowed to dry, scanned and the fluorescence density of the spots was plotted against the density of the fluorophore (crosses in figure 3.9). The fluorescence density was calculated from the concentration of the dilution and the measured spot area. From the replicate experiments a standard-calibration curve was selected (black circles in figure

3.9). Four dilution series of the same batch of Cy 5' labeled target DNA were spotted on bare gold (squares in figure 3.9). For comparison, one dilution series of another batch of Cy 5' labeled target DNA was spotted on an MCH coated gold surface and quantified in the same manner (triangles in figure 3.9).

At high molecular densities, the fluorescence density saturated at 3.10^9 DLU/mm^2 and at lower molecular densities, the fluorescence density of the dilution series inflected to a common value, reflecting the saturation and the detection limit, respectively, at the laser and PMT power values used (80 %). In the intermediate range the logarithm of the fluorescence density increases linearly with the logarithm of the molecular density. This part of the calibration curves can be used for an efficient calibration of the fluorescence density as a function of the molecular density. In figure 3.9, squares represent the curve that was fully linear within a large range and was thus taken as a well diluted standard curve on bare gold. The coating of the gold surface by MCH is expected to strongly decrease the quenching of the fluorophore by the gold surface since MCH can prevent the fluorophore to be in contact with the gold. The fluorescence signal should thus be higher on MCH-gold than on gold at equivalent fluorophore density. On figure 3.9, all the curves corresponding to the dilution series imaged on MCH-gold show higher fluorescence values consequently shifting the linear range towards lower molecular densities (circles on figure 3.9). This shows that coating the gold surface by MCH reduces the quenching of the fluorescence of Cy 5', approximatively by one order of magnitude. For all curves, the number of heat cycles and the respective position of the curves are not correlated. Thus, two curves that are fully linear within a large range are averaged and considered as a representative calibration curve for Cy 5' labeled oligos on gold covered with MCH (circles). A similar experiment with a second batch of Cy 5' labeled oligos was performed. This new standard curve (triangles) had the same saturation level and the same slope within its linear part as the first standard curve. The shift of the new standard curve towards lower fluorophore densities indicates that all Cy 5' groups contained in the solution were not active and that the second batch of Cy 5' labeled oligos contained a lower percentage of active Cy 5' groups. It is thus necessary to establish a new standard curve for each batch of Cy 5' labeled oligos to be investigated in order to perform reliable quantification of the density of fluorophore molecules.

In conclusion, it is possible to perform a reliable quantification of the density of hybridized Cy 5' labeled target oligos on MCH coated gold surface by making several dilution series for the same batch of fluorophore labeled oligo and thereby establishing a calibration curve. The calibration curve is characteristic of a given fluorophore solution therefore a new calibration curve shall be made for each new batch of Cy5 labelled oligo. In the following the first curve (circles) is used for quantification of hybridization coverage on the micro-arrays and the second curve

(triangles) for the quantification on the macro-arrays.

3.2.2 DNA-capture oligo and hybridization coverage on macro-arrays

DNA macro-arrays were made on gold using radio labelled DNA-capture probes as described in figure 3.10. The arrays were submitted to 31 PCR heat cycles and hybridized to targets labelled with a fluorescent label. Thus, before and after heat-cycling, the DNA-capture probe coverage was quantified using radio-imaging and the hybridization coverage was quantified using fluorescent scanning.

Radio-labelling

The radio labelling technique is a well established technique to quantify molecules immobilized on solid surfaces. In a first approach the labelling of the DNA-capture oligos with a fluorescent dye and the quantification of the coverage by fluorescence scanning was envisaged. But the labelling by a Cy'3 or 5' dye was shown to influence the binding behavior of the labelled oligos. On the other hand, the labelling of a DNA oligo with a radioisotope containing base (adenine containing γ^{32} P) does not inhibit or enhance the binding of thiol-modified capture probes on gold. Moreover, high sensitivity of the radioactive phosphore imaging enables us to obtain an accurate quantification of the DNA-capture probe coverage.

Method

The DNA capture oligos used in those experiments were alternatively labeled with a thiol-function in the 3' end, leaving the 5' end available for radiolabeling. DNA-capture probes were thus labeled with γ^{32} P ATP (Amersham Pharmacia,

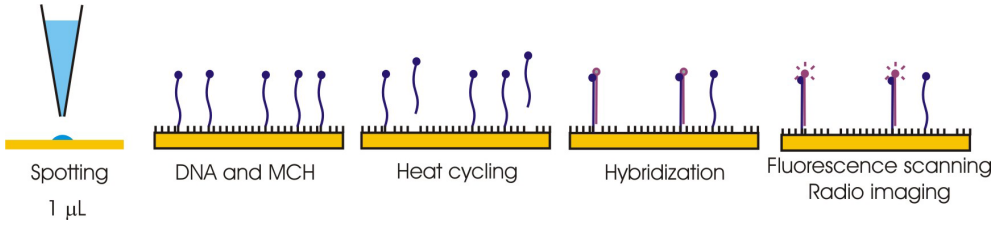

Figure 3.10: Experimental procedure for the DNA macro-arrays: radio-labelled and non labelled DNA-capture probes are immobilized on gold coated slides in 1 μL spots. The arrays are incubated in MCH. The slides are submitted to 31 heat cycles in solution. The arrays are hybridized to fluorescent labeled DNA-reporter. The DNA-capture probe coverage is quantified by radio-imaging and the hybridization coverage by fluorescence scanning.

USA), using 10 units/L T4 Polynucleotide kinase (New England Biolab, USA) in the buffer provided by the manufacturer (7 mM Tris-HCl, 1 mM $MgCl_2$, 0.5 mM DTT, pH 7.6 at 25°C). In a modified labeling procedure the DNA-oligos were labeled using the same amount of kinase in a DTT-free buffer (7 mM Tris-HCl, 1 mM $MgCl_2$, pH 7.6 at 25 °C). The oligos were desalted after labeling using a Microspin G-25 column (Amersham Pharmacia, USA). Three different capture-DNA oligo solutions were prepared and spotted manually onto gold surfaces prepared as described in section 3.2.1. Solution ♯1: 50 μM of 3' thiol oligos spiked with 0.03 μM of radio-labeled oligos prepared using the standard labeling procedure, solution ♯2; 50 μM of 3' thiol oligos spiked with 0.03 μM of radio-labeled oligos prepared using the DTT-free labeling procedure, solution ♯3; 50 μM of 5' thiol oligos, all in 1 M potassium phosphate (pH 7). The arrays were incubated for one hour in a humid atmosphere followed by three washes, ten minutes each in a 0.1 % SDS solution at 40 °C, and finally washed two minutes in Milli-Q water at 40 °C. The arrays were incubated overnight in a 1 mM solution of MCH and washed four times five minutes in Milli-Q water after incubation. Two arrays were heat-cycled and two arrays (one heat cycled and one not heat-cycled) were hybridized to a complementary fluorescent target as described in section 3.2.2. Dilution to 10, 1, 0.1 μM of the oligo solution ♯1 and ♯2 were prepared and spotted onto a silica membrane in order to be imaged and compare the yield of the labeling reaction in both conditions. All macro-arrays and the silica membrane were imaged by phosphorimaging for 45 hours (Instant Imager, Packard Bioscience Company, USA).

DNA-capture probe coverage on the macro-arrays

Since DTT is a thiol-containing molecule that can compete with thiol-modified DNA for the adsorption on the gold surface, modified radioactive-labeling procedure in which the labeling was performed in DTT free buffer was also used.
In order to calibrate the density of counts per minute (CPM) and the molecular density, the dilutions of solutions spiked with radio-labeled oligo were imaged on a silica gel. The density of counts per minutes was plotted against the density of oligo for the solution ♯1 (circles) and ♯2 (squares) in figure 3.11. The linear fit yields the calibration equation used for converting CPM density to DNA-capture oligo coverage:

$$Molecular\ density = 0.416\ 10^{10} \times CPM\ density + 0.321\ 10^{10} \qquad (3.2\text{-}1)$$

where the CPM density is in counts/minute/mm^2 and the molecular density in molecules/mm^2.
The solution of capture probes labeled in a buffer containing DTT yields a 17±3.5 % lower coverage than the coverage achieved using capture probes labeled in a DTT-free buffer. The capture probe densities achieved with the DTT-free solution are shown in figure 3.12. The grey bars represent the densities of capture

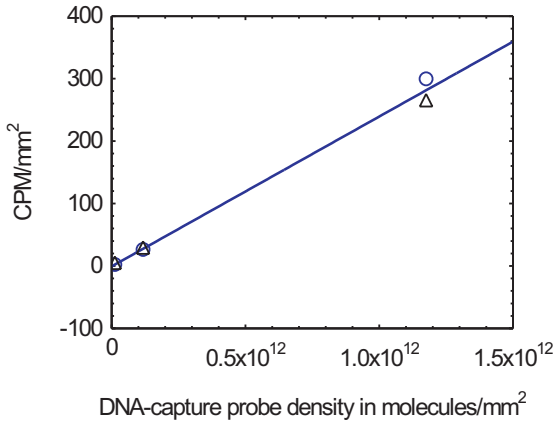

Figure 3.11: Calibration curve for the thiol-modified DNA-capture probe solution ♯1 (**circles**) and ♯2 (**squares**). The linear fit is shown.

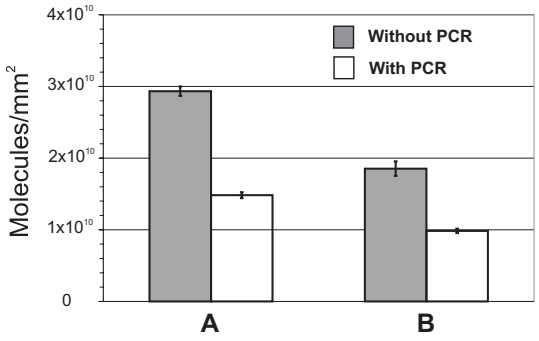

Figure 3.12: A. Density of radio-labeled DNA-capture probes immobilized on gold (**grey bars**) and subsequently submitted to 31 heat cycles (**white bars**). **B.** As in A, but further hybridized to a complementary oligo and washed.

probes on the arrays that were not submitted to heat cycling, the white bars for the arrays that were subjected to heat cycling. A 56 % reduction in DNA-capture probe density was found for the arrays that were heat cycled, compared to the arrays that were not heat cycled. Macro-arrays that were further hybridized to a complementary target and washed showed a 42 % lower density of DNA-capture probes than the arrays that were not hybridized and washed.

Hybridization coverage on the macro-arrays

In order to quantify the hybridization density, Cy5' labeled target oligos were hybridized to heat cycled macro-arrays and reference macro-arrays. The arrays were allowed to hybridize for one hour in darkness with 150 μL of hybridization

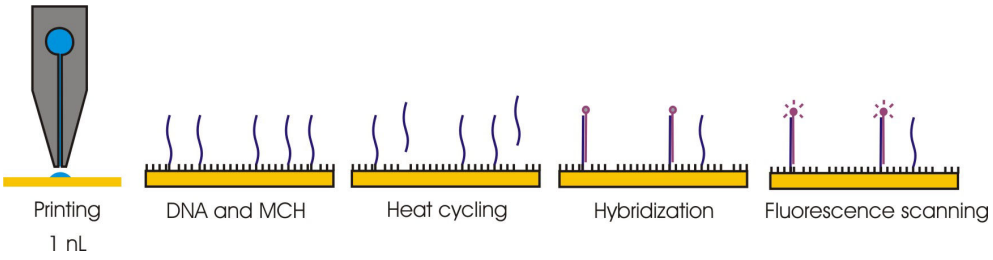

Figure 3.13: Experimental procedure for the DNA micro-arrays: the DNA-capture probes are immobilized on gold coated slides in 1 nL spots and incubated in MCH. The slides are submitted to PCR heat cycles in solution. The arrays are hybridized to fluorescent labeled DNA-reporter. The hybridization coverage is quantified by fluorescence scanning.

solution, comprising of ten times excess of Cy 5' labeled target DNA-oligos in 5x SSC + 0.1 % SDS. The arrays were washed in 1x SSC + 0.1 % SDS solution four times for five minutes and dried under a nitrogen flow. Besides being imaged by phosphore imaging, the arrays were imaged by fluorescence scanning in a dry state. The hybridization coverage on the macro-arrays are reported in figure 3.15.

3.2.3 Hybridization coverage on micro-arrays

The DNA micro-arrays were made as described in figure 3.13. Six different DNA-capture probe solutions were spotted on each micro-array: three dilutions of thiol-modified DNA-capture probes (1, 10 and 50 μM in 1 M potassium phosphate, pH 7) and three dilutions of DNA-capture probes without thiol function (as above). Each probe solution was spotted in 24-replicates at 45-55 % relative humidity and incubated for one hour in the same humidity. Micro-arrays were processed as above for macro-arrays. Reference micro-arrays were conserved in water, while other micro-arrays underwent respectively 5, 10, 15, 20, 25 and 31 heat cycles. After completion of heat cycling, each micro-array was conserved in water. All micro-arrays were washed, hybridized, and imaged by fluorescence scanning as described for macro-spotted arrays.
The fluorescence images of the microarrays are typically as depicted in figure 3.14 for one reference array and for the array submitted to 31 heat-cycles. Almost only the 50 μM spots are visible on the arrays but for other experiments, the 10 μM spots were also visible. Both thiol-modified and unmodified spots are visible and the large amount of more or less bright particles on the array was responsible for the large error range on the data and causes sometimes the unmodified spots to be brighter than the modified spots. This was very dependent on the MCH incubation step and the washing procedures but difficult to avoid.
It is of great interest to profile the loss of hybridization density during heat cycling. The density of hybridized DNA-oligos was investigated as a function of the

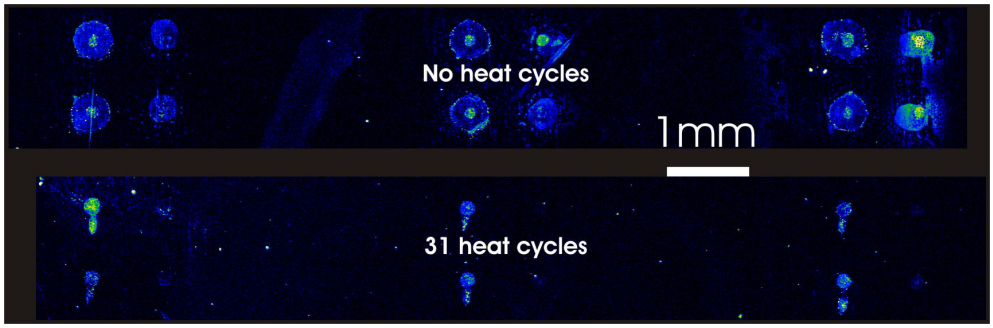

Figure 3.14: Fluorescence image of 3 sub-arrays of 50 μM spots on a reference array (**top**) and on the array submitted to 31 heat cycles (**bottom**) showing the decrease of the "unmodified" spots compare to the "modified" spots as well as the disappearance of the secondary spot marks both probably due to unspecific adsorption.

number of heat cycles, and presented in figure 3.15. It is seen that most of the decrease in the density of hybridization occurs before the 10^{th} heat cycle while the capture probe density can be considered constant for the micro-arrays submitted to a larger number of heat cycling. The hybridized Cy 5' target densities were obtained using the corresponding calibration curve (circles on figure 3.9). Comparing the average target density on the micro-arrays submitted to 10, 15, 20, 25 and 31 cycles, to the average target density on the reference micro-arrays, showed that the Cy 5' target density is decreased by 95 %. The densities of hybridization to the macro-arrays are reported on figure 3.15 (black triangles, circles and squares corresponding respectively to the capture probe solution 1, 2 and 3). Data obtained from hybridization of DNA-target to the macro-arrays are within the range of the micro-arrays (bars on figure 3.15) showing a 43 to 99 % loss in target hybridization density. The densities of DNA-capture probes measured by phosphorimaging are also plotted on figure 3.15 for the 3' thiol DNA-capture probe labeled with the standard and with the DTT-free procedure (white triangles and white circles). On the reference array that was not heat cycled, the DNA-capture probes density is within the error range of the hybridization density measured by fluorescence scanning on the micro-arrays (bars). On the array that was heat cycled, the capture probe density is no longer within the hybridization density range measured on the same array and the micro-arrays (bars), indicating higher loss of target hybridization density than capture probe density.

3.2.4 Summary and discussion

This study aims at establishing and characterizing a protocol that will provide a layer of immobilized DNA-capture oligos on a gold surface, stable to heat cycling like in PCR reaction. The protocol includes a stringent wash of the gold

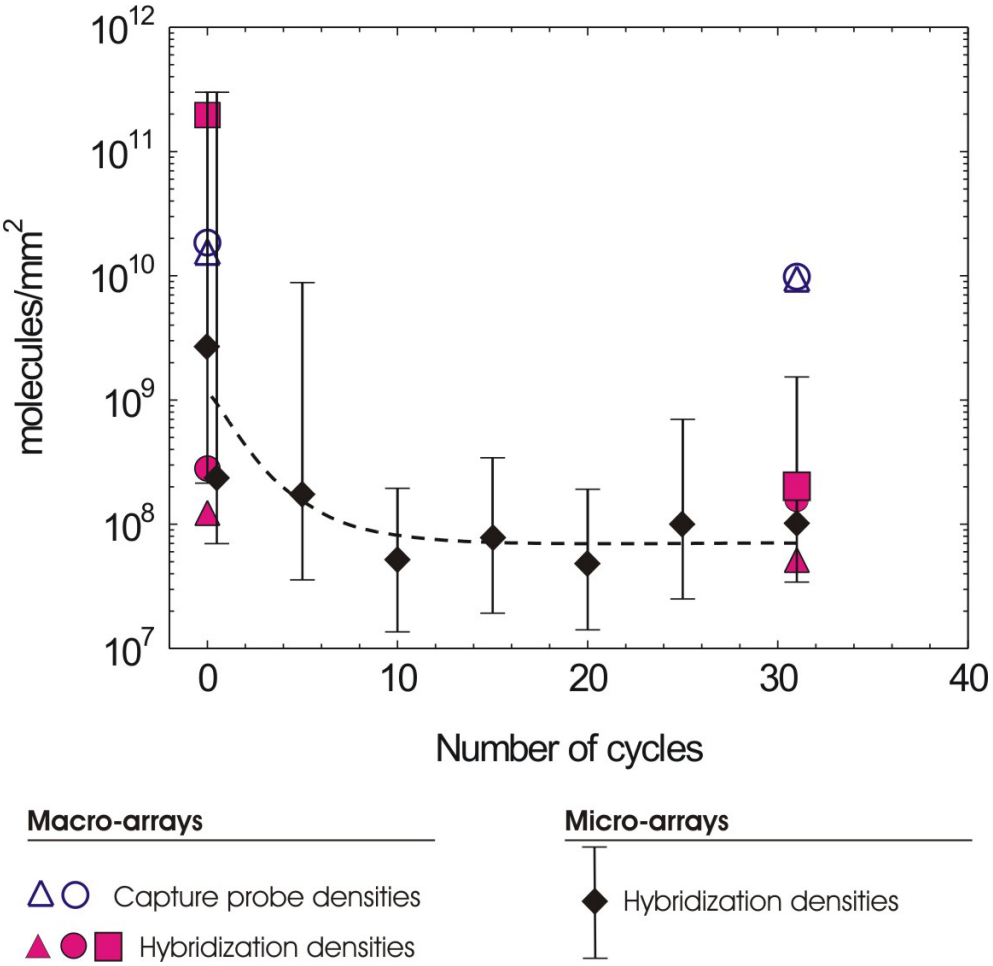

Figure 3.15: On two **macro-arrays**, the densities of the radio-labeled DNA-capture probes immobilized at a concentration of 50 μM are shown (**white triangles** and **white circles**). The arrays were hybridized to a 10 μM hybridization solution. The hybridization densities to the 5' thiol DNA-capture probes (**black squares**) and DNA-capture probes labeled in DTT containing buffer (**black triangles**) and DTT free buffer (**black circles**) are shown. On the **micro-arrays**, the density of target DNA-oligo probes hybridized to thiol-modified capture probes (50 μM spots) (**diamonds with bars**) is plotted against the number of heat cycles. Each micro-array consists of 24 replicas and all the micro-arrays were hybridized in a 13 pM hybridization solution. The dashed line represents the trend line of the decrease in density of hybridization to micro-arrays along the heat cycling.

surface after the incubation with the DNA-capture probes in order to wash off non-specifically bound capture probes and thus to reduce the fraction of capture probes that desorb from the surface during the heat cycling. Furthermore, the protocol includes an incubation of the arrays with MCH. While the adsorption of the MCH is taking place on the gold surface, it displaces non-specifically

bound DNA strands [57], which is expected to both increase the fraction of capture probes that can hybridize and displace the capture probes that were not attached to the surface by a sulfur-gold bond. The efficiency of the wash and the effect of MCH incubation to minimize the fraction of non specifically adsorbed capture probes on the micro arrays could be detected by comparing the hybridization signal obtained for the spots made with non-modified and thiol-modified DNA-capture probes. The low target density of non-modified DNA-capture probes attached to the surface, and the high target density from the thiol-modified DNA-capture probes, on microarrays that are heat cycled at least five times indicate that the protocol provides a layer of specifically bound DNA-capture probes (lower array on figure 3.14).
The density of DNA-capture probes as well as the density of target DNA-oligo probes hybridized on the arrays are in good agreement with densities in the range of (1-10) 10^{10} molecules/mm^2 reported elsewhere for similar substrates [57, 70]. Therefore further increasing the concentration of DNA-capture probes was not investigated. In all experiments the fluorescence background signal obtained from areas outside the spots was low as shown on figure 3.14. This indicates that the washing procedures were efficient to remove target DNA-oligos that unintentionally adsorbed either on the MCH-coated gold surface or on the gold left exposed by the eventual desorption of MCH molecules during heat cycling. Thus, we believe that the number of detected Cy 5' groups is equivalent to the number of target DNA-oligos hybridized to the micro-arrays. On another hand, the phosphorimaging results presented in figure 3.12 suggest that the washing procedure necessary to reduce the background fluorescence also reduces the DNA-capture coverage by 42 %.

Heat cycling influence on the hybridization density
Results from the experiment depicted in figure 3.15 indicate that up to 95 % of the immobilized DNA-capture probes were unable to hybridize with their complementary target DNA-oligos. Two factors may account for the fact that less target DNA-oligos can hybridize to the capture probes after heat cycling.
First, 55 % of the capture probes are desorbed from the gold surface during heat cycling as measured by phosphorimaging (Figure 3.12). Other reports have shown the heat induced desorption of surface bond molecular layers: desorption of DNA-capture probes immobilized on chemically modified glass substrates [44], solvent induced desorption of alkanethiol-based self-assembled monolayer (SAM) immobilized on polycrystalline gold [69] and release of surface bond DNA-capture probes in gel, possibly induced by the temperature induced breakage of disulfide bonds [79]. However, none of these studies allow us to conclude on the processes leading to desorption of the DNA-capture probes; either the rupture of the attachment of the DNA-capture probes at the sulfur to gold bond or inside the gold matrix or within the molecule itself.
Secondly, although DNA-capture probes are still present on the surface, they can

be denatured by the proximity of the metallic gold surface during the heat cycling and thus rendered unable to hybridize with their targets. However, the micro-arrays were incubated in MCH after the immobilization of the capture probes, providing a soft coating of the gold, possibly limiting the interaction between the DNA strands and the gold surface. In figure 3.15, the density of DNA-capture probes measured by phosphorimaging before heat cycling is contained in the error range of the density of hybridization to the same type of array. After heat cycling, the 55 % lower capture probe density is only a factor 2 reduction compared to the hybridization reduction of a factor 10. This indeed indicates the presence of intact DNA-capture probes that cannot hybridize to the target DNA. Both observations suggest a process that further reduces the hybridization ability of the target oligos without involving desorption or cleavage of the DNA-capture probes. One explanation could be a process known as the Ostwald ripening. The Ostwald ripening of vacancy islands on a Au(111) surface covered by alkanethiols was observed by Scanning Tunneling Microscopy and Atomic Force Microscopy at 298 K [80]. This study concerns densely packed monolayers of alkanethiols on gold and thus cannot conclude about the diffusion of the alkanethiols on the surface but it suggests that the thiols diffuse on the surface together with the gold atoms they are tethered to. Aside from the desorption of the DNA-capture probes that reduces the overall coverage, the 2D diffusion of the thiol-modified DNA-capture probes and the formation of islands of very densely packed DNA-capture probes can further reduce the fraction of DNA-capture probes able to hybridize with complementary targets, due to steric constraints and electrostatic repulsion [81] as shown in figure 3.16.
More than the overall loss of functional capture probes on the surface during PCR cycling, the qualitative aspect of the decay of coverage is interesting. The results depicted in figure 3.15 show that after the tenth heat cycle, the density of functional DNA-capture probes on the gold surface is constant. A similar desorption of alkanethiols on polycrystalline Gold in solution with a double kinetics has been reported by Garg *et al.* [69]. In this model the monolayer is first desorbing with a fast rate and then with a slower rate. Though the authors report an influence of the structure of the adsorbed molecule on the two rates, the double kinetics model could account for the stabilization of the density of DNA-capture probes in our study and thus for the trend line depicted in figure 3.15.

In the perspective of making a sensor for real time detection of a target DNA sequence amplified by a PCR process, it is desirable to keep the density of capture probes constant while the concentration of DNA target in the solution is increasing. Such a situation would yield an increasing density of target DNA hybridized to the sensor surface. In that sense, the trendline in figure 3.15 shows that the immobilization of thiol-modified capture probes on a gold-coated surface is a suitable technique for the fabrication of micro-arrays or biosensors where the monitoring of *in situ* PCR amplification is involved. However, the remaining

10^8 hybridization per mm^2 after 10 heat cycles might not be enough to produce a sufficient surface-stress for the detection by cantilever-based sensor.

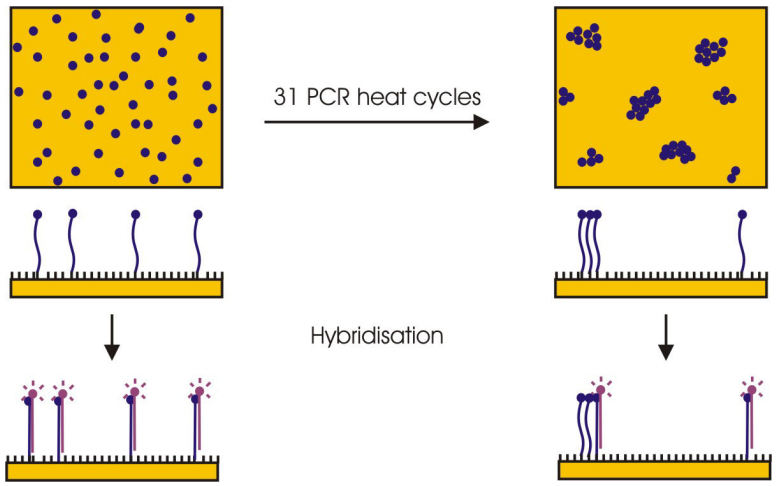

Figure 3.16: The process known as Ostwald ripening could account for a decrease of hybridization density after heat cycling without a reduction of the overall density of DNA-capture probes on the gold surface.

Chapter 4

Cantilever-based sensor for monitoring *in situ* PCR

A cantilever-based sensor system for monitoring DNA concentration in real PCR conditions was designed and successfully tested for heat and buffer robustness. First, two ways of encapsulating the cantilever-based sensor are presented. Second, the set-up for characterization and experiments is presented before the performances of the two encapsulations are investigated.

4.1 Introduction

4.1.1 Requirements

In order to monitor *in situ* the amount of template DNA during its amplification by polymerase chain reaction (PCR), one needs to build a cantilever-based sensor that fulfils the following requirements. The sensor should sustain the conditions of buffer and temperature required by a PCR reaction. A typical PCR reaction is performed in a buffer containing 15 mM of Tris-HCl , 50 mM of potassium chloride and 1.0 to 4.0 mM of magnesium chloride at pH 8.0. The number of temperature cycles of a PCR reaction is in the order of 30 at temperature of 55°C, 72°C and 95°C. The conditions can be summarized as follows:

- a salt concentration ranging from 0 to 1 M for monovalent ions (K^+, Na^+, Cl^-) and from 0 to 10 mM for magnesium ions.
- at least 30 heat cycles from room temperature up to 95°C.
- a pH in the range of 6 to 8.

In addition, the different materials used for building the reaction chamber of the sensor should be PCR compatible meaning it should not inhibit the PCR reaction by binding one of the reagents for example. It is also desirable to make the sensor

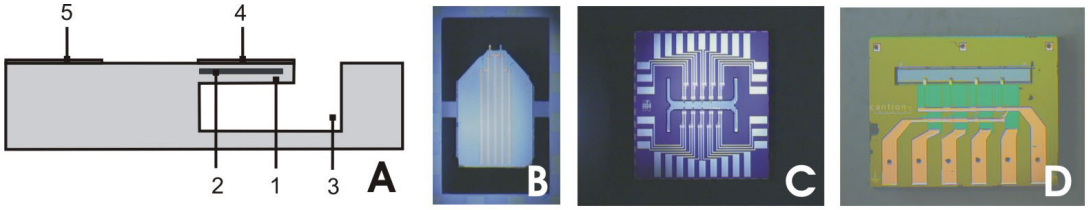

Figure 4.1: (**A**) On a cantilever chip there is (1) cantilevers with (2) their buried piezoresistor, placed in (3) the channel. Some cantilevers are coated with (4) a gold layer. (5) The contacts are placed further away from the channel on the body of the chip. Optical images of (**B**)a Fagpakke chip with 2 cantilevers, (**C**) a BioProbe chip with 10 cantilevers and (**D**) a Cantion chip with four cantilevers (see specifications in table 4.1).

easy to use *e.g.* loading with solutions and placing into a temperature controlled device.

4.1.2 Principle

The core element of a cantilever-based sensor for monitoring PCR is a silicon-based device comprising micro-cantilevers with an integrated piezo-resistive read-out. The basic idea is to encapsulate the silicon chip so that (1) the cantilevers, active parts of the sensor, are placed in a tight reaction chamber containing the solution with the reagents necessary to the PCR reaction and (2) the electrical contacts of the silicon chip are protected from the solution.

4.1.3 Available cantilever-based silicon chips

Several generations of micro-cantilever chips with integrated piezo-resistive read-out were developed and can be potentially used for building a sensor for monitoring PCR (see overview in figure 4.1). Here is a review of those chips. Three different generations of cantilever-based chips with piezoresistive read-out that can be used as a basis chip for building an in-situ PCR sensor were developed within the BioProbe project at MIC and at Cantion A/S.

The first type of chip also called Fagpakke carries two cantilevers, one coated with gold and the other uncoated. The cantilevers are free-hanging from the edge of the body of the chip and were first designed as probes for AFM [5, 6, 7]. The electrical contacts in metal (gold or aluminium) are not encapsulated on chip and the major challenge for using this chip in solution is to enclose the cantilevers in a reaction chamber and to encapsulate the electrical connections. For room temperature applications, the electrical connections on this kind of chips were encapsulated in vacuum sealing wax by dipping the chips in melted

wax [82]. Encapsulation was also made with glue, deposited on the body of the chip and allowed to flow on the surface. The glue stops at the edge of the body of the chip leaving the cantilevers free hanging [75, 83]. Finally, electro depositable photoresist was used to encapsulate the electrical contacts only [75]. The electro-deposition of EAGLE resist was the most promising solution for the PCR application. This method makes it possible to enclose the silicon chip and a ceramic substrate in the reaction chamber, as any electrical contact would be encapsulated in resist during the electro-deposition. Although promising, EAGLE resist encapsulation is not compatible with the required temperature and ionic strength conditions. Improving the quality of the encapsulation requires higher deposition voltage, which is incompatible with the optimization of the sensitivity of the cantilever-based chip that requires thinner encapsulation layers of the resistor.

On the second type of chip, also called BioProbe chip, ten cantilevers are integrated in a micro channel and the electrical contacts encapsulated under a SU8 polymer layer thus enclosing the cantilevers inside a reaction chamber of about 0.1 μL. Attempts to use the SU8 layer as a reaction chamber failed. This is due to the poor adhesion of SU8 to silicon nitride and the repetitive strain caused by the expansion and contraction of the SU8 layer under heat cycling. On the Fagpakke and Bioprobe chips, cantilevers can be externally connected in pairs in a Wheatstone bridge by wedge bonding as shown is figure 4.2 A.

The third type of chip was fabricated by Cantion A/S. Four cantilevers are integrated in a channel. Two cantilevers are coated with gold and two others are not coated. The four cantilevers and their respective substrate resistors are connected on chip in such a way that pairs of cantilevers are in a Wheatstone bridge configuration as shown in figure 4.2 B. The cantilever piezoresistors have long extensions buried under silicon nitride in order to place the gold contacts further away from the channel (500 μm) thus making them more convenient to encapsulate. Three generations of Cantion chips were tested. Table 4.1 summarizes the characteristics of the in total five different types of cantilever chips.

Type of chip	**Fagpakke**	**BioProbe**	**Cantion 1**	**Cantion 2**	**Cantion 3**
Number of cantilevers	2	10	4	4	4
Chip dimensions mm	3.5 x 2.5	6.0 x 6.0	2.5 x 3.5	2.5 x 3.5	2.5 x 3.5
l, w, t μm	200 x 50 x 1.30	200 x 50 x 1.30	200 x 50 x 1.30	200 x 50 x 1.30	200 x 50 x 1.30
Piezoresistor material	p^+ Poly-Si	p^+ Poly-Si	p^+ Poly-Si	p^+ Si	n^+ Si
Back-side material	Poly-Si	SiN_x	SiN_x	SiN_x	SiN_x

Table 4.1: Cantilever-based silicon chips available from the BioProbe project and Cantion A/S. l, w and t are respectively the length, width and thickness of the cantilevers.

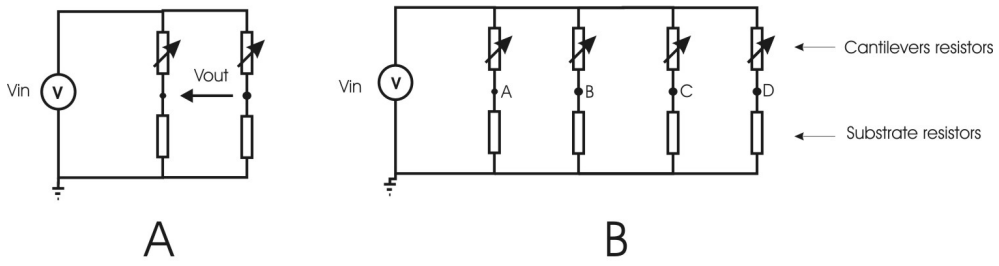

Figure 4.2: (**A**) On the Fagpakke and Bioprobe chips, pairs of cantilevers with their substrate resistors can be connected externally in a Wheatstone bridge. (**B**) On Cantion type chips, four cantilevers and four substrate piezo-resistors are connected on chip. Pairs of cantilevers are connected in a wheatstone bridge fashion.

4.1.4 Dicing silicon-based chips comprising micro-cantilevers

Dicing the Bioprobe and Cantion chip becomes an issue as the dimensions of the cantilever are reduced. During dicing, the free hanging cantilevers breaks as a result of either the vibrations or the water jet used to cool down the saw. Therefore photoresist is used as a mechanical protective coating that fills the channel and embedd the cantilevers. After dicing, the photoresist is easily removed in acetone as it is not hard baked. The resist processing is as follows:

1. The wafer is spin coated with photo-resist (AZ5200 series). The recipe used is a thick resist recipe which produces a 4 μm thick resist layer on a 4" plane wafer.

2. The resist is baked for 2 minutes at 90 °C (soft bake).

3. The chips are diced out.

4. Before use, the chips are cleaned in acetone (5 minutes) and rinsed in ethanol (99% pure) to remove acetone traces.

This procedure prevents the cantilevers from breaking during dicing. This also protects the surface from silicon particles produced during the dicing. Thus the surface of the chip is clean for bonding, gluing and eventually evaporating metal layers.

4.2 Design based on glue sealing

The idea for the first basic design of the sensor system is based on experiences from earlier attempts to make a sensor by encapsulating two-cantilever chips with electro-depositable resist and by using the SU-8 layer on the 10-cantilevers chips

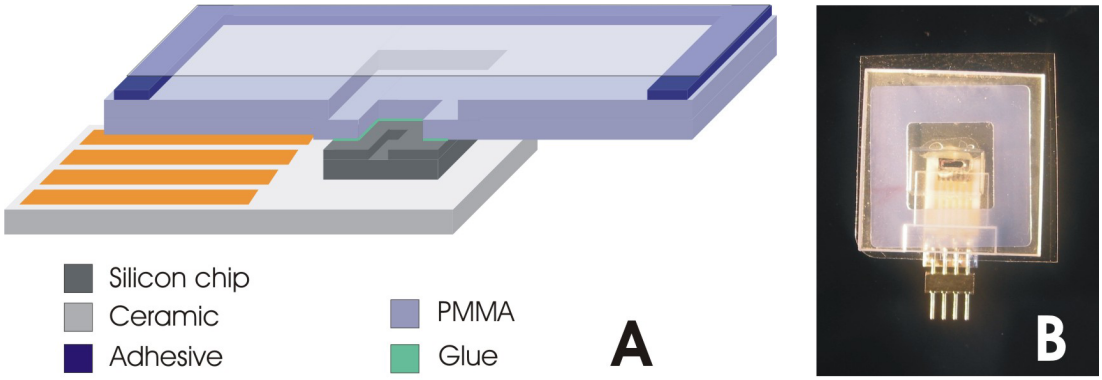

Figure 4.3: (**A**) 3D view of the PCR sensor glue-based design. (**B**) Optical image of an encapsulated sensor with the adhesive frame on top of the sensor.

as reaction chamber. First, the reaction chamber is made large to avoid the localization of air bubbles near the cantilever. Secondly, glue or polymer with a better adhesion than SU8 or electro-depositable resist to the silicon nitride surface is used to encapsulate the wiring and to seal the chamber. Finally, the sensor should be easy to load with a solution without entrapping air bobbles and it should be possible to exchange the solution. Figure 4.3 A shows the different elements of the sensor. The silicon chip is glued on a ceramic carrier with gold wiring and contact pads allowing simple electrical connections to the power supply and the data acquisition system.
This design was mainly used for encapsulating the 10 cantilever chips. Two of cantilevers are used for measurements and are connected in a Wheatstone bridge (figure 4.3 B) and to the ceramic contact pads.

A PMMA plate is glued onto the silicon chip. A hole through the PMMA part constitutes the reaction chamber. The chamber is closed by applying an adhesive frame (Gene Frame^{TM} 10x10 mm) and a lid. The chamber volume is about 50 μL.

4.2.1 Selecting the glue

The key issue in making the sensor is the assembly of the plastic chip with the silicon chip with the glue that also encapsulate the electrical connections on the silicon chip. The glue was selected for its adhesion properties to both surfaces (PMMA and silicon nitride), for its stability in water and ionic solutions, for having a high working temperature and for its viscosity. Mechanically the glue is subjected to the strain developed during the temperature cycling and caused by the PMMA having a much higher thermal expansion coefficient (5 to 10 10^{-5} K^{-1}) than the silicon (2.6 10^{-6} K^{-1}). Therefore the glue should have very good

Glue	Type	Hardness D	Elongation at failure	Viscosity	Temp. max
NOA 61	UV	85	35 %	300 mPa.s	125 °C
Dymax 3069	UV	55	175 %	25000 mPa.s	180 °C
Dymax 3072	UV	60	200 %	25000 mPa.s	175 °C
Dymax 3073	UV	45	115 %	30000 mPa.s	-
Araldite 2022	metacrylate	75	50-75 %	60000 mPa.s	90 °C

Table 4.2: Characteristics of glues.

adhesion properties to both PMMA and silicon nitride. The glue should remain stable up to 100 °C which is also the glass transition of PMMA and the highest temperature the sensor would be used at. The viscosity of the glue when non-cured is a key issue because the glue is dispensed directly on the silicon chip. The glue flows onto the chip surface and stops at the sharp edges of the channel only if its viscosity is greater than 300 cps. Thus the wiring on the chips are encapsulated and the cantilevers remain free of glue. A glue of a much lower viscosity would actually cover the cantilevers, because it has a much lower surface tension. The different glues that were tried are listed in table 4.2.

The glues were tested by assembling a fully functional sensor and measuring the output voltage of the sensor in a 1 x PCR solution at temperatures from 20 to 70 °C. The output of the sensor is recorded until the encapsulation fails which usually means that the output voltage of the sensor changes dramatically. Such measurements are presented in section 4.6. In order to confirm that the electrical contacts are then not any longer encapsulated, the sensors were tested under a microscope by applying an increasing voltage. Bubbles usually appear where the electrical contacts are in contact with the solution. The sensor are also tested for leaking by pressing on the chamber lid. The UV-curable glue NOA61 (Norland) gave the best result for this design, although it does not have the highest temperature range or the highest elongation at failure which are desirable according to the criteria given above. This indicates that the critical property is the adhesion strength to silicon nitride.

4.2.2 Fabrication of the PMMA plate

PMMA is an acrylic polymer (Riacryl XT 1030). PMMA has a melting temperature of 111 °C, slightly above the PCR temperature range but rather low which makes the laser machining possible. Moreover, PMMA has a fairly low thermal expansion coefficient (7.7 10^{-5} linear in the range of 23-100 °C). The PMMA plate is machined in a 1 mm thick plate using a CO_2 laser (see figure 4.4). CO_2 laser etching is a versatile process enabling fast and inexpensive prototyping of plastic parts. The final shape of the chip is obtained by machining the PMMA plate from both sides successively. On the front side of the plastic chip, the chamber groove is machined. On the backside, the hole through the chip and extra grooves

Figure 4.4: The PMMA plate is made by laser machining. First a groove is made on one side. Then a hole through and grooves for fitting the wires and ceramic are machined on the other side.

for fitting the bonding wires and the ceramic carrier under the plastic chip are machined. Making a groove on the front side reduces the thickness of PMMA that is cut for making the hole through the plate. This reduces the aspect ratio of the hole and thus avoids having a hole with a conical shape that would trap any gas bubbles down on the cantilevers. After being machined, the chips are baked out for one hour at 90 °C in order to release the residual strain accumulated in the PMMA during the laser machining. If not baked, cracks appear in the PMMA when rinsed in acetone or ethanol. This also prevents the relaxation of the structure when the sensor is fully assembled which would induce strain in the bond between the glue and the plastic chip.

4.2.3 Adhesive frames

GeneFrame (ABgene, Switzerland) is a commercially available adhesive frame for making PCR chambers on glass slides. It seals properly a chamber on glass or plastics and is PCR compatible. Once applied on glass, the GeneFrame reaches its full adhesion when annealed five minutes at 95 °C. The adhesive frame is placed on top of the PMMA part and the lid closes the reaction chamber of the sensor. The adhesive frame is also easily removed which enables to perform different measurements with different solutions on the same sensor *e.g.* a blank test on a pure buffer and then a measurement of a solution containing complementary DNA.

4.2.4 Assembly protocol

All the steps of the assembling protocol are listed below:

1. The chip is mounted on a ceramic carrier with standard epoxy glue and electrical connections are made by wire bonding.

2. The back side of the PMMA chip is cleaned with ethanol and acetone using a cleaning paper (cleanroom paper).

3. The PMMA chip is cleaned 40 minutes in UV/ozone. An oxygen plasma cleaning could also be used for that purpose.

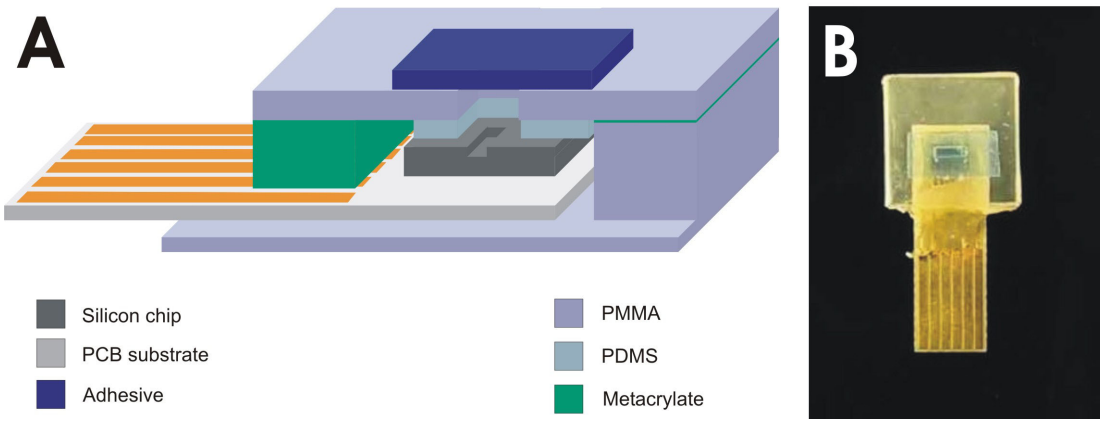

Figure 4.5: (**A**) Scheme of the PDMS-based sensor assembly and (**B**) picture of the encapsulated sensor.

4. The UV curable glue is deposited on the chip and on the PMMA chip. Then both are assembled and aligned under microscope. The glue is cured 40 minutes in a Stratalinker UV oven with 365 nm light tubes (NEC Black Light).

4.3 Design based on PDMS encapsulation

In the design described above the major cause of failure of the chip is the bond between the glue and the cantilever chip. The idea for a more robust design is to make a sealing that is not relying on glue but on Poly(dimethyl-siloxane) (PDMS). PDMS is a soft, hydrophobic and bio-compatible polymer. Applying even a light pressure on a PDMS structure against a surface makes a tight sealing. The principle of the design is to use a PMMA structure assembled to press the silicon chip and a PDMS frame against each other. The design is depicted in figure 4.5. This encapsulation method was successfully used on the different four cantilever silicon chips.

4.3.1 PDMS frame

PDMS is a polymer obtained by mixing a base with a hardening compound. The hardener is mixed in a ratio of 1:10 to the base and mixed thoroughly (DuPont, Sylgard 184 PDMS). PDMS is further mixed a few minutes in ultrasound which also removes air bubbles. In order to make a thin layer of PDMS, 1 to 3 mL of PDMS is deposited on a 7 x 9 cm PMMA plate and allowed to flow on the surface overnight at 4 °C. Next, PDMS is crosslinked at 80 °C for four hours. The PDMS frame can be cut with a scalpel or by CO_2 laser cutting. After being

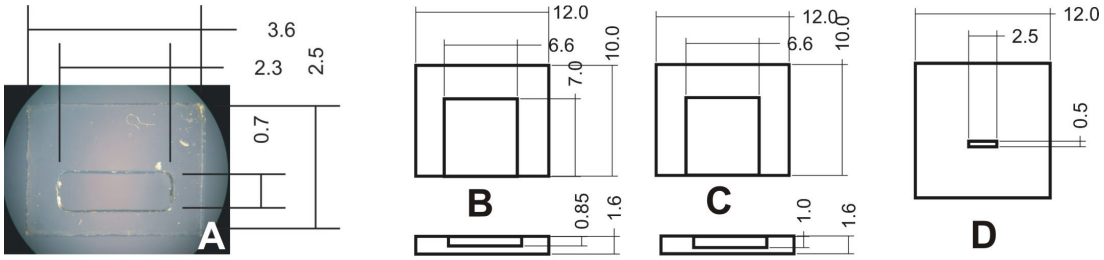

Figure 4.6: (**A**) PDMS frame, PMMA part I for (**B**) poly-Si chips and (**C**) SOI chips and (**D**) PMMA part II. Dimensions are in mm.

cut by hand with a scalpel the PDMS frame is ready to be used and pressed on the chip. After laser cutting, sooth from the etching is re-deposited on the surface of the PDMS. These sooth particles are removed by rinsing several times in ethanol. This procedure yields a clean PDMS surface (Figure 4.6 A).

The surface of the PDMS frame that was in contact with the PMMA plate during the laser cutting is preferably pressed against the silicon chip because it is the cleanest, while the other side is then pressed against the PMMA upper part of the sensor.

4.3.2 PMMA parts

The two PMMA parts are fabricated using a CO_2 laser. Part I is a plate with a groove where the PCB chip carrier is glued. The depth of the groove is adjusted according to the thickness of each type of silicon chip so that the top side of the silicon chip fits with the top side of the PMMA part I. The second PMMA part is a 1 mm thick plate of PMMA with a hole slightly larger than the channel of the silicon chip. Both PMMA parts were baked at 90 °C for one hour in order to release the internal stress of the material. The PMMA part II was treated with ultrasound in ethanol in order to remove the PMMA residues from the surface.

4.3.3 Assembly protocol

The assembling protocol is as follows

1. The silicon chips are glued with epoxy on the printed circuit board (PCB) substrate.
2. Electrical connection are made by wire bonding.
3. The epoxy substrate is glued with epoxy onto the PMMA part I and cured.
4. PDMS frame is adjusted on the silicon chip under a microscope.

5. PMMA part II is glued on the part I with the metacrylate glue and pressed with a clamp (Wolfcraft, Germany). The assembly is cured at room temperature for one hour.

6. GeneFrame adhesive is used to seal the chamber when the chamber is loaded with solution.

4.4 Set-up for a cantilever-based PCR sensor

Performing *in situ* PCR monitoring requires that one can perform accurate heat cycling on the sensor, measure the output of the sensor as well as the temperature inside the chamber of the sensor. The data are collected from a data acquisition software developed on the Labview platform (National Instrument). The diagram of the set-up is as depicted in figure 4.7.

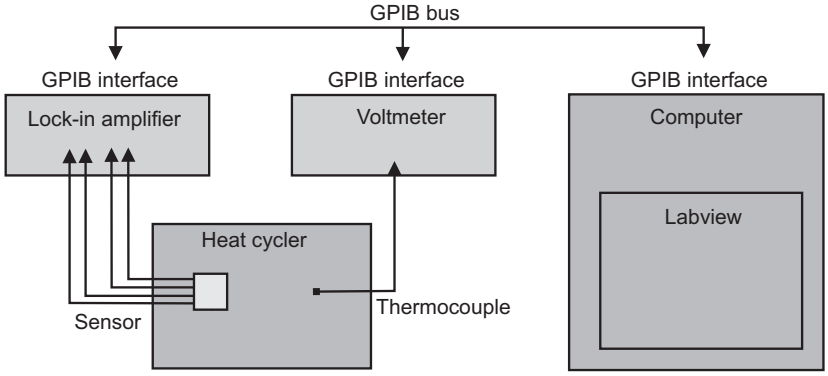

Figure 4.7: Diagram of the set-up.

4.4.1 DNA engine thermal cycler

PCR is a well-established and key technique of modern molecular biology. Like other techniques such as micro-arraying and gel electrophoresis, PCR has been automated in order to process large amounts of samples in parallel. PCR is based on accurate heat cycling of the sample and machines have been designed in order to heat cycle samples both fast and accurately. The typical requirements for heat cycling for PCR are a temperature accuracy below 0.1 °C. The maximum heating/cooling rate should be preferably higher than 0.5 °C/s in order to be able to perform a whole PCR process (30 cycles) in a couple of hours. State of the art PCR heat cyclers are based on Peltier element heating/cooling devices. Briefly, a Peltier element is a junction of two different conducting materials (*e.g.* doped semiconductors). When a current flows through the junction the temperature of the junction decreases or increases depending on the direction the current

is passing through the junction. The temperature can be easily and accurately stabilized because the Peltier element is an active heating and cooling element (reversible) in contrast to a Joule effect device that has a passive cooling. Furthermore, it is possible to use a good thermal conductor as a base material for the device guarantying fast heating/cooling rates.

Two kinds of sample holder can be coupled to the DNA engine PTC200 (MJ Research, USA). One holder is designed for microscope glass slides and consists of shelves which both sides are temperature controlled. The maximum sample thickness is 2.5 mm. The other holder consists of two plates where the temperature of the bottom plate is controlled and the second plates is a lid that can be pressed onto the sample with a screw. Here, the sample thickness can be as large as a couple of centimeters but the top plate is not heat controlled. In the following the two sample holders are referred to as two-sides heating element and one-side heating element respectively. The one-side heating element has mostly been used together with the sensors encapsulated with PDMS.

In order to ensure that the temperature of the sensor and of the Peltier element is the same, the sensor is placed on the bottom plate and covered with an aluminium plate (figure 4.8A). The thermal contact between the plate and the Peltier element is made by an aluminium piece. The thermal contact of the aluminium and the sensor to the Peltier element is improved by using heat transfer silicone paste (Electrolube, UK). Between the aluminium plate and the top plate, some foam and a 8 mm PMMA plate are stacked in order to make thermal isolation. The equivalent thermal circuit shows that placing a high thermal resistance on top of the chip and a low thermal resistance in parallel with the sensor makes the temperature of the sensor homogeneous and equal to the Peltier element temperature (figure 4.8B).

4.4.2 Lock-in amplifier and cables

The output signal of the sensor is the voltage output from the Wheatstone bridge consisting of four piezo-resistors, two placed on cantilevers and two on the substrate. A previous study has shown that using a lock-in amplifying technique combined with a proper electrostatic shielding of the measurement set-up can improve the quality of such a measurement by reducing the electrical noise [83]. Briefly, the lock-in technique consists of multiplying the output signal by the reference signal, which the circuit is excited with. When the AC signal is filtered out of the resulting multiplied signal, remains only a DC voltage proportional to the component of the output signal having the same frequency as the reference signal. This means that the components of the output voltage that have different frequencies (noise) are filtered out. The noise was measured for sensors encapsulated according to the PDMS design. A sensor was encapsulated and loaded with

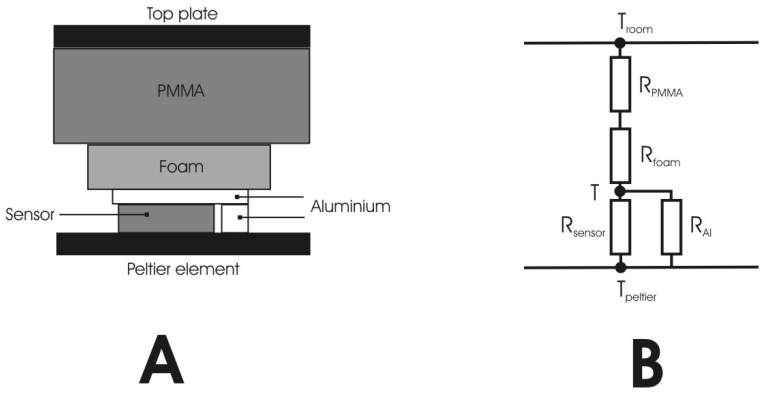

Figure 4.8: **A** The sensor is placed between the peltier element and the top plate of the heat cycler together with a PMMA plate, a piece of foam, an aluminium plate and an aluminium piece. **B** The equivalent one dimensional thermal circuit.

Coatings of the cantilevers	Gold/Gold	Gold/Nitride	Nitride/Nitride
n-type SOI	1 ± 0.1 μV	0.75 ± 0.25 μV	1.5 ± 0.25 μV
p-type SOI	0.4 μV	2 μV	1 μV

Table 4.3: Noise levels for two cantilevers in a Wheatstone bridge for a Cantion 3 chip (same sensor) and a Cantion 2 chip (3 different sensors).

a buffer solution (1xPCR). The cantilever chip is a Cantion 3 chip (see table 4.1) and the output signal was measured for each of the three combination of gold coated and uncoated cantilevers at 20 °C. The experiment was repeated for three Cantion 2 chips (table 4.1) in another buffer solution (PBS buffer pH 7.4 at 37 °C). The results are presented in table 4.3.

The noise level is the voltage peak to peak measured over 100 seconds. The results listed in table 4.3 show noise levels as low as 0.4 μV but the typical noise of a sensor is in the range of 0.4 to 2 μV. The noise level is chip dependent and not coating dependent as the noise levels on the same chip are in the same range while quite different when measured on different chips. The doping of the chip (n^+ or p^+) does not influence the noise level either.

4.4.3 Temperature measurement

The temperature of the Peltier element is monitored online using a thermocouple. The thermocouple is maintained on the surface of the heat cycler and thermal contact is improved by using thermal conducting silicone paste (Heat Transfer silicon, Electrolube, UK). The voltage of the thermo-couple is monitored using a voltmeter (Keithley 2000) connected via the General Purpose Interface Bus

(GPIB) to the computer. The read-out of the thermocouple is made from the data acquisition program running under Labview and the sensitivity and offset point of the thermocouple are calculated during the measurement from the acquisition program by measuring the voltage at two different temperatures. The temperature can be re-calibrated from the set of data after the experiment using the data treatment program.

4.4.4 Data acquisition

Labview was chosen as data acquisition platform via a GPIB protocol, also known as IEEE 488, because ready-to-use Labview components for controlling most of the instruments via this protocol are available. The amplifier is configured through the front panel by adjusting the sensitivity, the time constant *etc.* The data acquisition program is basically a recursive program that builds an array of data in this order: time in second, output voltage in volts, phase in degrees and temperature in degree Celsius. Time is recorded from the internal clock of the computer. The output voltage and the phase are recorded via the GPIB interface from the two output channels of the lock-in amplifier. The temperature is calculated using the values of the sensitivity and the offset point of the thermocouple stored in a local parameter of the program and from the output voltage of the thermocouple recorded via the GPIB interface. At the completion of the program, the data are saved in a text file under four columns in the order time, voltage, temperature and phase.

The sampling time is about 250 ms at the fastest and is mainly limited by the GPIB interface of the voltmeter which is slower than the GPIB interface of the lock-in. The sampling time increases with the total acquisition time; 250 ms for the first 10 000 s and 350 ms after 50 000 s of acquisition and up to 670 ms was observed. This aspect of the data acquisition is an issue of the data treatment. Indeed, when later calculating the slope of the voltage change from a constant number of data points, the time constant of the slope calculation increases with time. In other words, the time constant of the derivation is not constant. This reduces the noise on the output voltage slope data but this can also filter-out some of the signal if the time constant of the signal is too low. Ideally the time constant of the slope calculation should be at least ten times lower than the time constant of the change of slope we want to detect. The melting of DNA has a width at half maximum of about 10 °C. At a heating rate of 0.2 °C/s this represents 50 seconds.
In the latest version of the program the data are saved in a text file at each iteration and the front panel viewing the graphs are refreshed from a binary file periodically, both reducing the memory demand of the program and making the sampling time independent on the acquisition time. The sampling time is here 160 ms. It is though possible to set the sampling time through the front panel

of the program thus reducing the amount of data collected. Figure 4.9 shows the front panel of the program.

4.4.5 Data treatment

The data acquisition produces a file containing the time, the output voltage, the temperature and the phase of the output signal in an array t_i, V_i, T_i, P_i. The data treatment program is a Labview based program with three main modules/functions.
In the first module the data can be formatted and the temperature recalibrated. The beginning and the end of the data file can be removed leaving only the portion of interest of the data to be further treated. Then the temperature is re-calibrated using a linear correlation of the temperature values of the file and the reference temperature values (typically 20 and 80 °C).
As described earlier, we are interested in visualizing the slope of the output voltage versus the temperature during the heating and cooling periods. The second module is dedicated to smoothening the profile of the data by averaging the voltage over 2n points. Each voltage value V_i of the array is replaced by the average of $[V_{i-n};V_{i+n}]$. The third module calculates the slope values for each data point by making a linear fit of the portion $[V_{i-n}; V_{i+n}]$ vs. $[t_{i-n}; t_{i+n}]$ of the output voltage corresponding to 2n data points. As heating and cooling rates are linear with time, the linear fit against time is equivalent to the linear fit against temperature during the heating/cooling periods. When the temperature is constant, the slope of the signal against time indicate the drift of the chip and is thus a valuable information. The calculation of the slope against the temperature yields asymptotic values at the temperature plateaus disturbing the later visualization of the results. When the "smoothen" function is activated the signal as a function of time is displayed and if the slope calculation is activated, the program displays the output slope against temperature $\frac{\Delta V_i}{\Delta t_i}(T_i)$. Figure 4.10 shows the front panel of the program. Two other functions can be used to remove the beginning of the data until the first heat cycle starts and to average over several cycles the signal or the slope for a single temperature value.

Figure 4.9: User interface of the data acquisition program. Output voltage, phase and temperature are recorded simultaneously.

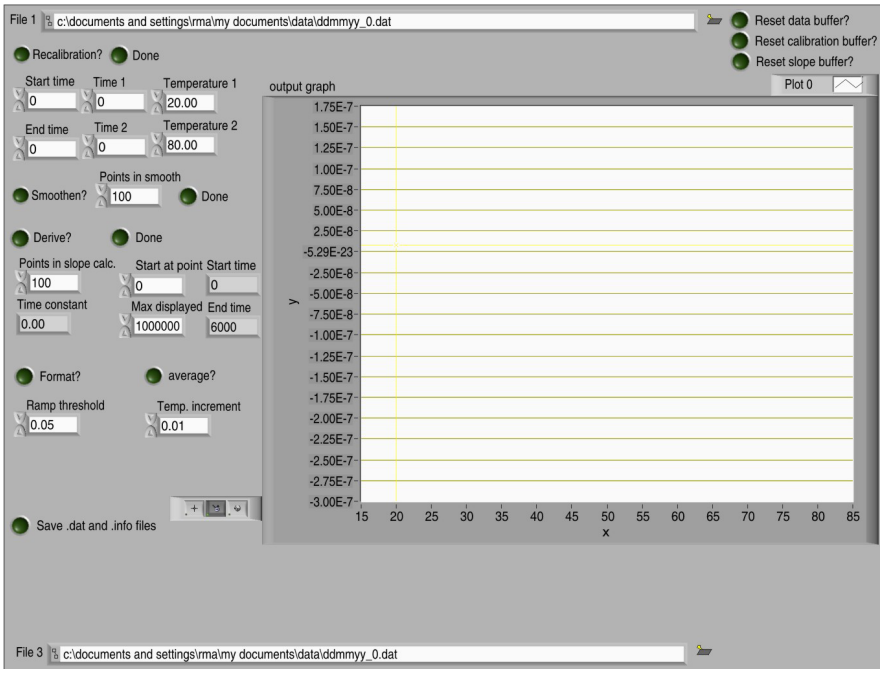

Figure 4.10: User interface of the program dedicated to the data processing.

4.5 Flow device

The measurements we are aiming at are static measurements meaning that no flow of liquid through the chamber of the sensor is involved during the detection. Never the less, flowing solutions on the sensor is necessary in order to perform isothermal hybridization detection and in order to wash the sensor in a controlled way. Therefore a device enabling to flow solutions at a given flow rate was developed for the sensors encapsulated in PDMS. Based on conventional drilling and CO_2 laser machining, a device made of PMMA was made with one inlet and one outlet, with easy connections to commercial micro-fluidics and tubing (UPChurch scientific). The connection of the inlet and outlet to the chip is made via a PDMS layer with two holes that define the inlet and outlet of the sensor chamber which is otherwise an open channel. The flow device as well as the PDMS frame and their alignment to the sensor are shown in figure 4.11. Using this device it is easy to exchange chip and to flow aqueous solutions at rates up to 50 μL/min without breaking the cantilevers. As the volume of the sensor chamber is only 3 μL, a flow of 10 μL/min was sufficient to wash the sensor in order to remove salt traces and 50 μL/min was used for thoroughly washing the sensor after incubation with thiol-oligos or oligos labelled with fluorescent dye.

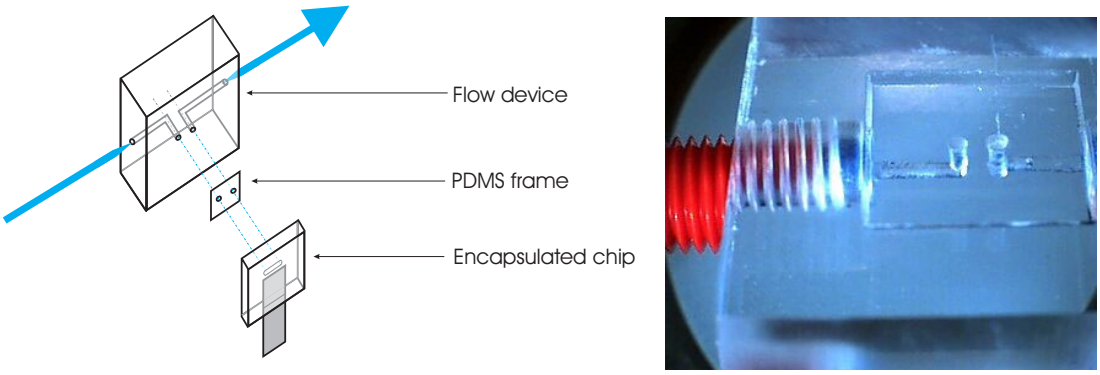

Figure 4.11: Flow through device for the encapsulated sensor.

4.6 Performances of the sensors

4.6.1 Principle of the characterization

The goal of the chip encapsulation presented in section 4.2 and 4.3 is to fabricate a sensor that remains functional during PCR conditions. Therefore the sensors are tested as follows:

- The reaction chamber is filled with a buffer solution.

- The sensor is then placed inside a temperature controlled device.
- The temperature is cycled between two temperatures (typically 20 °C and 70 °C).
- The output voltage of the sensor is recorded until the encapsulation fails

4.6.2 Design based on glue sealing

Two temperatures heat cycling

The most comprehensive results obtained for this design were obtained with a sensor based on a Cantion 1 chip (see table 4.1). The sensor was successfully heat cycled 10 times in 1xPCR buffer between 20 and 70 °C. The sensor was placed in a two-side Peltier element heat cycler. Temperature is maintained constant at 20 °C and 70 °C for five minutes and the heating/cooling rate was 0.2 °C/s. On the chip, one cantilever was coated with Gold and one was uncoated. The output voltage is shown in figure 4.12.

The shape of the output signal stabilizes after 4000 seconds corresponding to the first three heat cycles. Surface stress release taking place on the cantilever can account for such variations of the output signal thermal profile. After the third heat cycle the output signal change due to the temperature change is linear with temperature and corresponds to a sensitivity of -7.8 $mV.K^{-1}$ after amplification by the lock-in amplifier. This corresponds to a sensitivity of -16 $\mu V.K^{-1}$. The

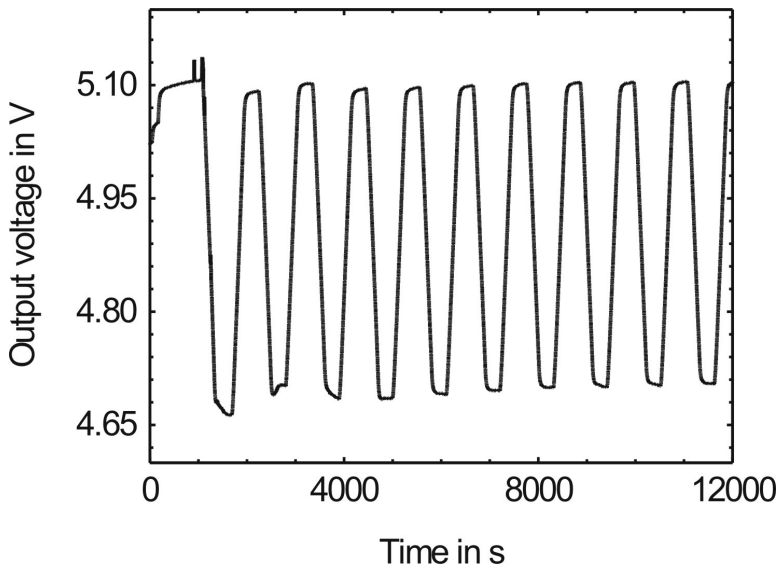

Figure 4.12: Output voltage of a glue encapsulated sensor heat cycled 10 times in solution.

large thermal sensitivity of the sensor is not only due to the difference in bimorph effect between the two cantilevers. A large part of the signal is due to mismatch of resistance and Temperature Change of Resistance (TCR) of the four resistors included in the Wheatstone bridge. This will be discussed further together with the sign of $\frac{\Delta V}{\Delta T}$ in section 4.6.3.

PCR-like heat cycling

The sensor was also successfully heat cycled in the same buffer as in real PCR five times before the sensor failed. Again the heating/cooling rate was 0.2 °C/s and the temperature was stable for one minute at successively 55 °C, 72 °C and 95 °C. Because the PCR-like heat cycling was performed on the sensor that was already heat cycled in buffer, the shape of the output signal cycle is stable from the first cycle which confirms the hypothesis of a surface stress release taking place on the silicon chip when the sensor was submitted to the first heat cycles.

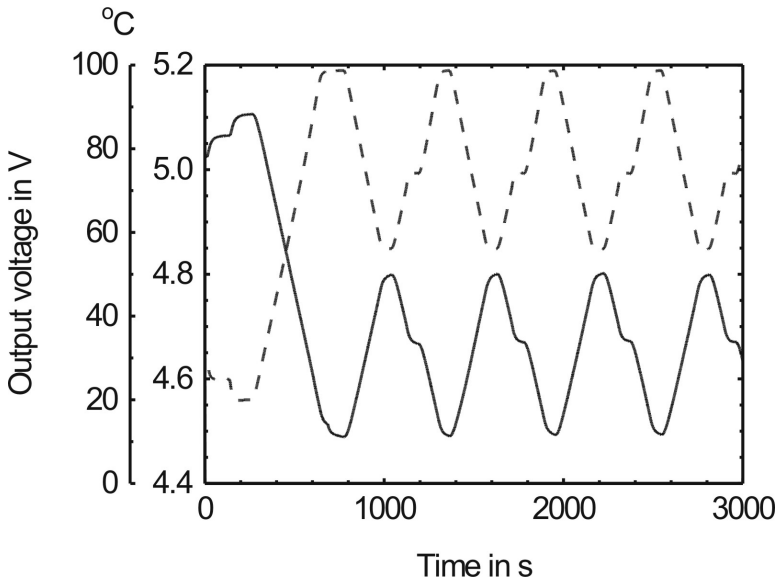

Figure 4.13: Output voltage of an encapsulated sensor during PCR-like heat cycles.

4.6.3 Design based on PDMS sealing

Two temperatures heat cycling

A sensor encapsulated with PDMS was heat cycled ten times between 20 and 70 °C at a rate of 0.2 °C/s in 1xPCR solution. The minimum and maximum temperature is maintained constant for 5 minutes. The output signal of the sensor is shown in figure 4.14 and a close up of one cycle can be seen in figure

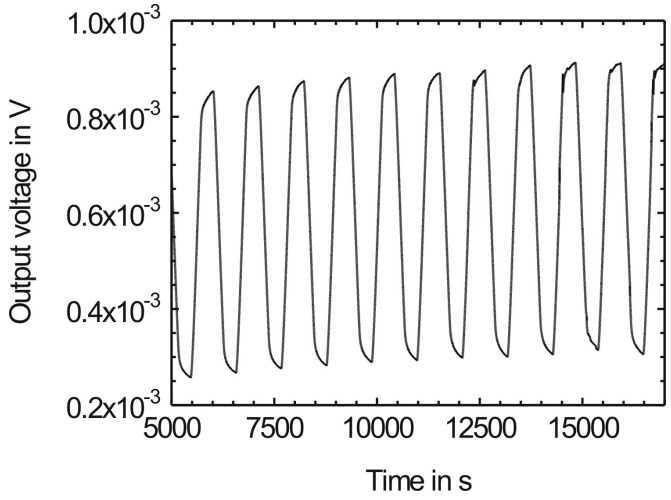

Figure 4.14: Output voltage of a PDMS-based sensor during heat cycling at 20 and 70 °C.

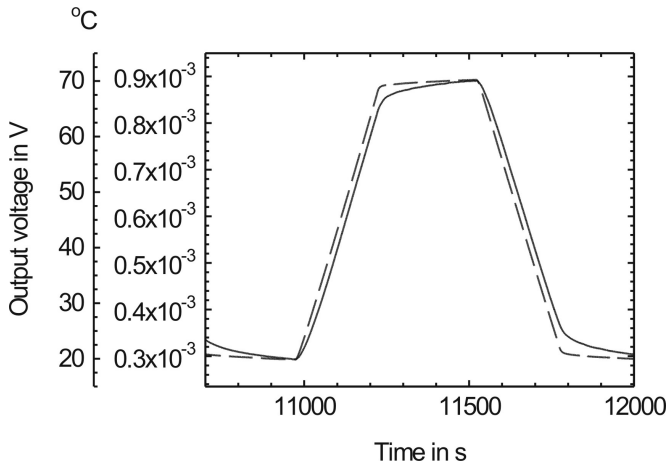

Figure 4.15: Output voltage of a PDMS-based sensor during one heat cycle between 20 and 70 °C. The dashed line shows the temperature of the peltier element.

4.15. There is drift on the signal but this is a due to the silicon chip, not to the encapsulation. On figure 4.15, there is drift of the temperature at each plateau and this is due to a bad thermal contact between the thermo-couple and the Peltier element (see section 4.4.3). The behavior of the sensor is quite similar to that shown in figure 4.12 for the glue-based encapsulation. The change in output voltage upon a 50 °C change is about 597 μV and corresponds to a sensitivity of 12 μV.K^{-1}.

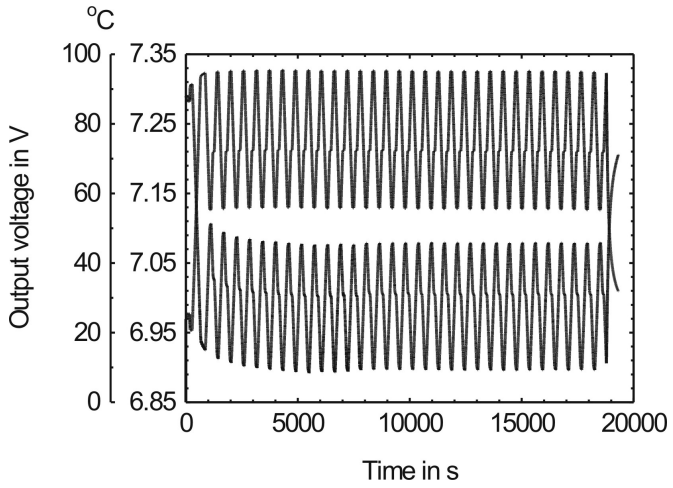

Figure 4.16: Output voltage of a PDMS-based sensor during 31 PCR-like heat cycles. The top curve is the temperature as measure by the thermo-couple.

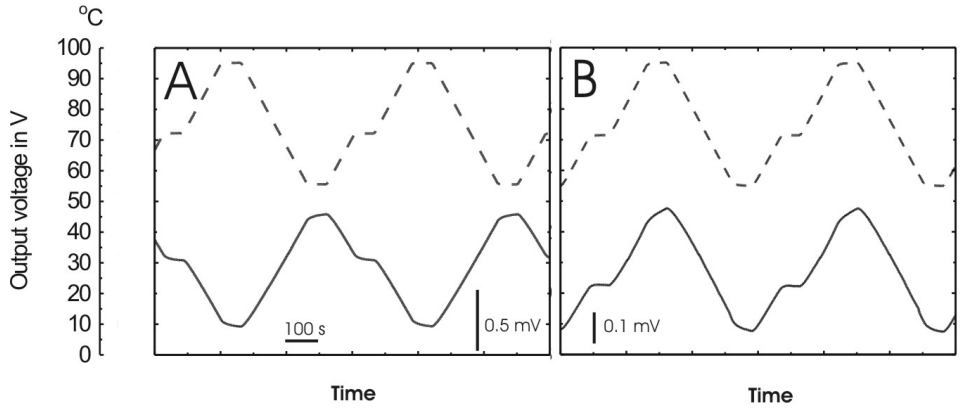

Figure 4.17: Output voltage (**continuous**) and temperature (**dashed**) corresponding to cycles 20 and 21 in figure 4.16 (**A**) and for a second sensor (**B**).

PCR-like heat cycling

A PDMS-encapsulated sensor was successfully tested in real PCR conditions. 31 PCR-like heat cycles were performed on a PDMS encapsulated sensor in 1xPCR solution. The sensor is placed in the one-side Peltier element. One cantilever is coated with gold and the second cantilever is uncoated. The cycling parameters are: 1 minute at successively 95, 55 and 72 °C with 0.2 °C/s heating/cooling rate. As seen in figure 4.16, the sensor output voltage (bottom curve) is measured during 31 temperature (top curve) which indicates that the sensor remains functional.

The figure 4.17 A shows the 20^{th} and the 21^{st} cycles on the same sensor. The

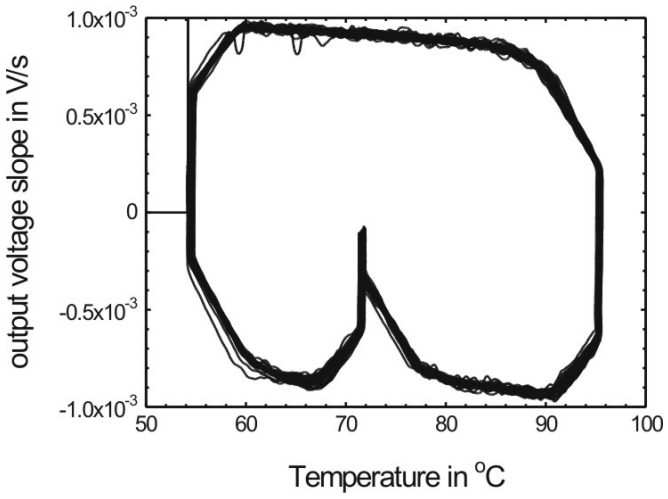

Figure 4.18: Slope of the output voltage of the sensor during 31 PCR-like heat cycles vs. the temperature.

water used for preparing the solution was degassed 5 minutes by bubbling helium through it. The experiment was repeated for a second sensor (figure 4.17 B) in non-degassed solution and identical measurements were obtained. Thus, the degassing of the solution is not an issue here. On the second sensor, drift is observed at the highest and lowest temperature but this is believed to be a chip-dependent effect as this is not observed for the first sensor. Moreover, $\frac{\Delta V_{output}}{\Delta T}$ is positive for the second chip and negative for the first chip which will be discussed later.

Ultimately, output voltage slope variations during the heating/cooling phases should be detected, thus indicating the surface stress signal due to melting/hybridization of DNA. The signal slope vs. temperature diagram of the measurement shown in figure 4.17 B is calculated using the data treatment software presented earlier. The diagram is shown in figure 4.18. The diagram confirms that the slope is rather constant over a large temperature range during the heating phase which can make it possible to distinguish variations of the slope due to the bimorph effect and due to surface-stress changes.

Temperature ramp performances

The chip was filled with 1xPCR solution prepared of degassed water and set in the one-side Peltier element PCR cycler. Temperature cycles between 20 and 70°C were performed with increasing ramping speed: successively 0.1, 0.2, 0.4, 0.6, 0.8 and 1 °C/s and thus for four times. In order to controle how fast the temperature of the sensor can be changed, the slope of the temperature and output voltage are plotted against the temperature (figure 4.19). The scales are

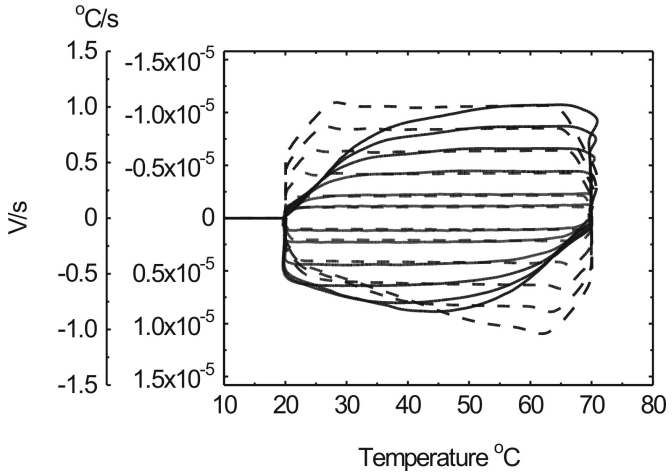

Figure 4.19: First order derivative of the signal (**continuous**) and temperature (**dashed**) between 20 and 70 °C. Heating/cooling ramp is adjusted to 0.1, 0.2, 0.4, 0.6, 0.8 and 1 °C/s. The sensor is heat cycled in 1xPCR.

adjusted so that the first plateau of the two curves are matching. The signal slope is inverted so that a positive slope of the signal corresponds to the positive slope values of the temperature. The sensor signal can reach stable signal slope at heating (cooling) rate as high as 1 °C/s (-0.6 °C/s) but is limited by the second order ramping speed of the temperature. This means that the heating/cooling rates of the sensor cannot be changed as fast as the temperature of the thermal cycler. This suggests that the sensor should be heated/cooled at rates as low as 0.2 °C/s in order to have a constant signal slope in the largest temperature range. From the temperature curve one can also gather information about the thermal cycler itself. At low temperatures, the cooling rate of the cycler is limited which is probably due to a disfunction in the ventilation. At high temperatures one can notice that the temperature of the thermal cycler overshoots of a couple of degrees.

Heat cycles on two gold coated cantilevers

For DNA detection it is desirable to have a reference cantilever and a measuring cantilever as identical as possible. This implies that the reference cantilever should as well be coated with gold. Therefore the heat cycling was performed on a PDMS encapsulated sensor with two cantilevers coated with gold. The temperature was cycled at 0.2 °C/s between 20 and 80 °C and maintained at 80 °C for 1.5 minutes. Figure 4.20 displays the temperature (dashed) and the output voltage (continuous) during the fourth heat cycle performed on the sensor loaded with 1xTE + 0.1 M NaCl buffer.

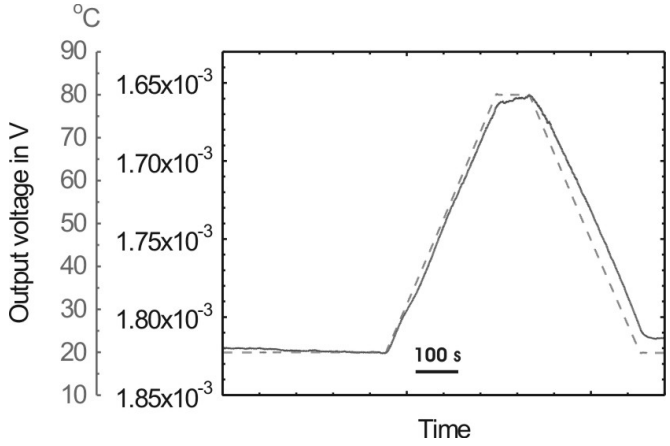

Figure 4.20: Output voltage (**continuous**) and temperature (**dashed**) between 20 and 80 °C. Heating/cooling ramp is 0.2 °C.s^{-1}. The sensor is heat cycled in 1xTE + 0.1 M NaCl.

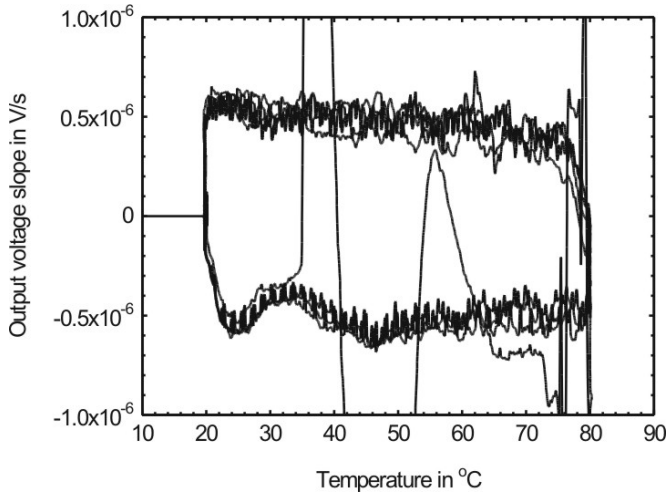

Figure 4.21: The slope of the output voltage depicted in figure 4.20 is plotted against the temperature.

The output voltage change due to the 50 °C temperature change is about 160 μV. $\frac{\Delta V}{\Delta T}$ is negative and about 3.2 μV/K. The slope of the signal $\frac{\Delta V}{\Delta T}$ is constant but this is an example of a "good" sensor in that sense. For most of the sensors $\frac{\Delta V}{\Delta T}$ varies in this temperature range or even changes sign. Moreover, for eight sensors that have been cycled successfully in solution, the sensitivity ranges from 1.0 to 2.9 μV/K. Therefore it appears necessary to heat-cycle a sensor in buffer before using the sensor for detection in order to have a reference heat profile of the sensor. The slope of the output voltage is plotted against the temperature(figure 4.21).

About the sign of $\frac{\Delta V}{\Delta T}$, the TCR and the bimorph effect

For the sensors used in figure 4.17 left and figure 4.12, $\frac{\Delta V}{\Delta T}$ is negative and for the sensor used in figure 4.14, $\frac{\Delta V}{\Delta T}$ is positive. On those three sensors, the voltage V_{AB} is measured. The cantilever A is coated with gold and the cantilever B is not coated. Therefore the cantilever A is expected to bend more downwards than the cantilever B due to a larger bimorph effect. In the electrical configuration described in figure 4.2 B and according to the discussion introduced in section 1.1, the larger bending of A should yield an increase of the output voltage V_{AB}. This is true if disregarding the variations of the temperature coefficient of resistance (TCR). The resistance of a resistor varies with the temperature as

$$R = R_0(1 + \alpha\ (T - T_0)) \tag{4.6-1}$$

where R_0 is the resistance at the reference temperature T_0 and α is the TCR. The linear approximation is true for small temperature variations and the TCR can be written as:

$$\alpha = \frac{1}{R}\frac{\Delta R}{\Delta T} \tag{4.6-2}$$

$\frac{\Delta R}{\Delta T}$ is the slope of R vs. T. In case of our piezoresistor, α increases with the temperature and the doping [84]. The output voltage of the wheatstone bridge is then the measurement of the mismatch in bimorph effect of the cantilevers and in TCR on the four resistors. In order to investigate the TCR and the bimorph effect for the n-doped SOI piezoresistors used, the relative change of resistance for a cantilever resistor and its corresponding substrate resistor was measured from 10 °C to 90 °C. The relative change of resistance of the substrate resistor is due solely to TCR effect and on the cantilever both the TCR and bimorph effect contribute:

$$\left.\frac{\Delta R}{R}\right|_{substrate} = \left.\frac{\Delta R}{R}\right|_{TCR} \tag{4.6-3}$$

$$\left.\frac{\Delta R}{R}\right|_{cantilever} = \left.\frac{\Delta R}{R}\right|_{TCR} + \left.\frac{\Delta R}{R}\right|_{bimorph} \tag{4.6-4}$$

The measurement were carried out for a gold coated cantilever and an un-coated cantilever [1]. On figure 4.23, the relative change of resistance for the four piezoresistors are plotted. The bimorph contribution for each cantilever (the gold coated and the uncoated) is obtained by subtracting the relative resistance change of the substrate resistor from the relative change of resistance of the cantilever resistor. It is seen that the bimorph contribution is more than one order of magnitude smaller than the TCR contribution even for a gold coated cantilever and represents only 6 % of the relative change of resistance on the gold cantilever

[1] On different chips because three cantilevers must be broken off in order to access directly the resistance of one resistor.

(table 4.4). In case of the gold coated cantilever the bimorph contribution is positive and for the un-coated cantilever it is negative and two orders of magnitude smaller than the TCR contribution. The sign of the variations of a given chip is probably due to TCR coefficient differences between the four piezo-resistors in the bridge and not due to the bimorph effect difference between the two cantilevers. Moreover, the measurement was repeated on the same chip with and without encapsulation. The encapsulation does not induce resistance changes in the substrate resistors.
α is calculated from the resistance of the substrate resistors. As it may not be obvious on figure 4.23, $\frac{\Delta R}{R_{10°C}}$ is not linear with ΔT for temperatures up to 90 °C. This suggests that α is not constant. α is thus calculated for each data point as:

$$\alpha_i = \frac{1}{R_{i-1}} \frac{R_{i+1} - R_{i-1}}{T_{i+1} - T_{i-1}} \tag{4.6-5}$$

where T_{i+1}-T_{i-1} is 20 °C. α is plotted in figure 4.24 and the average α values are shown in table 4.4. α increases with the temperature as expected according to figure 4.22 but the variations are small compared with the variations observed for p-doped piezo-resistors [84]. This is due to the higher doping of the n-doped resistors (figure 4.22). In conclusion, far the best solution for optimizing a cantilever based sensor for PCR would be to suppress the TCR effect. According to figure 4.22 this could be realized by either lowering the doping so that the minimum of resistivity is in the PCR temperature region or to use a very high doping to reduce further the TCR. Using another piezo-resistive material with a lower TCR is also a possibility.

Cantilever coating	$\frac{\Delta R}{R_{10°C}}$ cantilever	$\frac{\Delta R}{R_{10°C}}$ substrate	Bimorph effect	Average α value
gold	6.53 %	6.14 %	0.39 %	7.50 10^{-4} K^{-1}
No coating	6.86 %	6.93 %	-0.06 %	8.48 10^{-4} K^{-1}

Table 4.4: Relative change of resistance at 90 °C compared to the values at 10 °C for a Gold coated cantilever, an un-coated cantilever and their respective substrate resistors. Assuming that the substrate resistors are only submitted to TCR effect, the bimorph contribution is calculated for each cantilever. The average TCR values over the temperature range is calculated as in equation 4.6-5 for the substrate resistors.

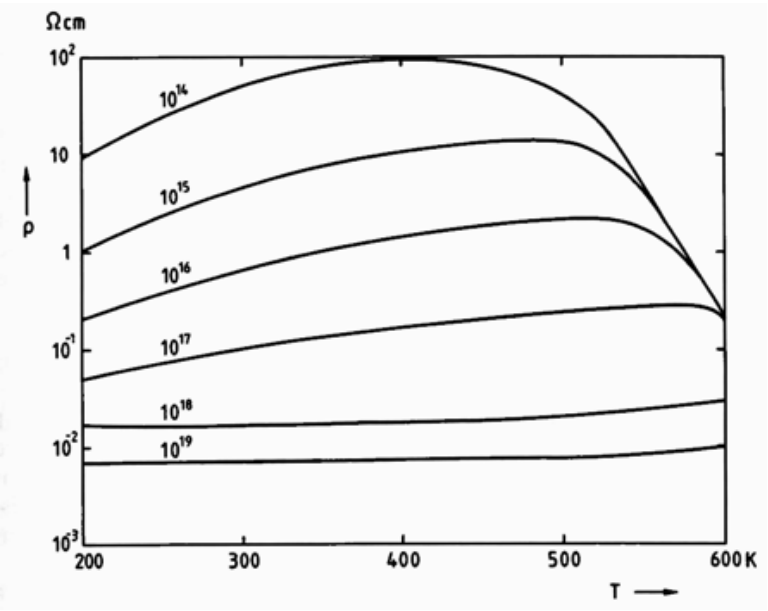

Figure 4.22: The resistivity of n-doped single crystalline silicon as a function of temperature for increasing doping. The slope of the curve α increases with temperature in the 10 to 100 °C range and decreases as the doping increases. Reprinted from [85].

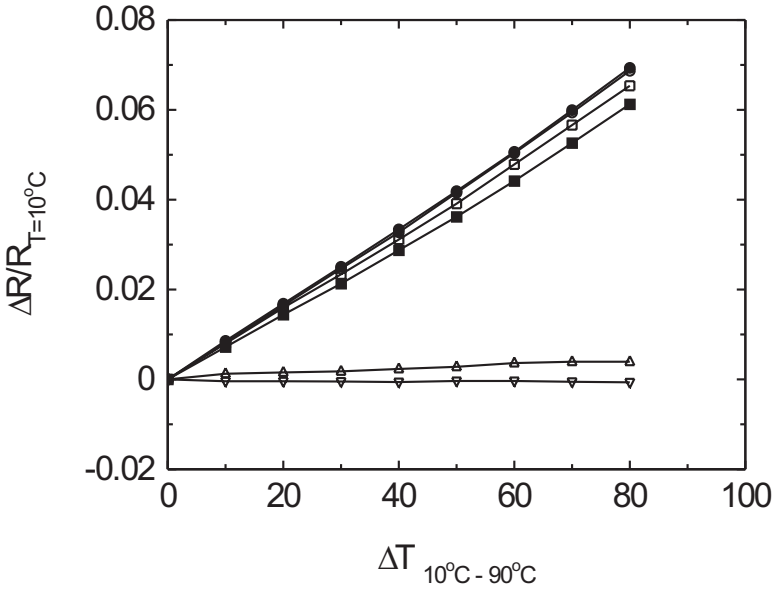

Figure 4.23: The relative change of resistance for a gold coated cantilever (**white squares**) and its substrate resistor (**dark squares**), for an uncoated cantilever and the corresponding substrate resistor (respectively **white and dark circles** which are on top of each other). The bimorph contribution for the gold coated cantilever (**upright triangles**) and the uncoated cantilever (**inverted triangles**) is also shown.

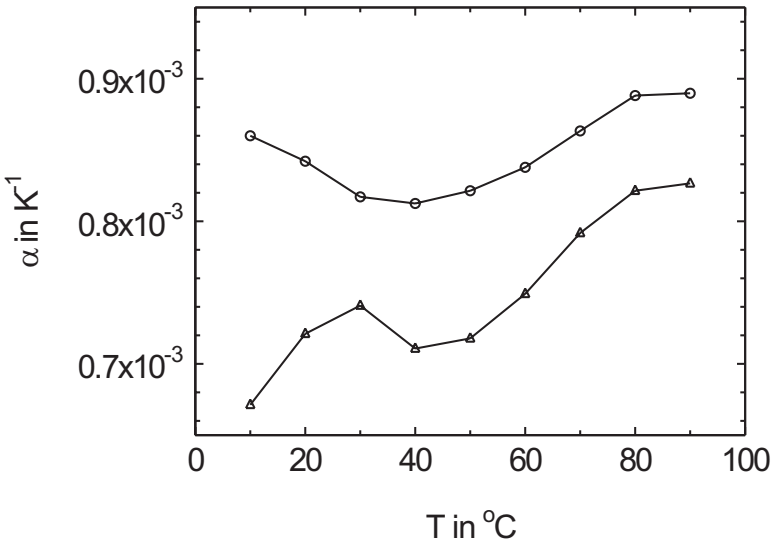

Figure 4.24: α values calculated from the resistance of the substrate resistor coupled to the gold-coated cantilever (**triangles**) and the un-coated cantilever (**circles**).

Chapter 5

DNA immobilization on cantilever-based sensor

In chapter 3 the immobilization of DNA-capture probes on gold is characterized. In the previous chapter, the encapsulation of a cantilever silicon chip is described and characterized in order to build a cantilever-based sensor for measuring hybridization/melting of DNA. In the present chapter, the immobilization procedure is implemented onto the cantilever-based sensor with the optimization for surface stress sensing as the final goal.

5.1 Challenges

The silicon chip carrying the cantilevers is shown in figure 5.1 together with the dimensions relevant for the immobilization of DNA-capture probes. Our goal in this section is to immobilize DNA on a cantilever-based sensor in order to maximize the surface stress signal due to the DNA interaction taking place on its surface. It is therefore necessary to achieve

- A high coverage on the top side of the measuring cantilever (A).
- A low coverage on the back side of the measuring cantilever and on the reference cantilever (A and C).

It is thus necessary to localize the solution containing thiol-modified DNA on the chip and perform an efficient wash of the surfaces after incubation in the immobilization solution. In addition, the final goal is to perform both steps *in situ*, meaning inside the chamber of the encapsulated sensor.

5.2 Fluorescence on chip

The method was first transferred to cantilever carrying silicon chips and validated by making fluorescence detection of hybridization on the gold surfaces of

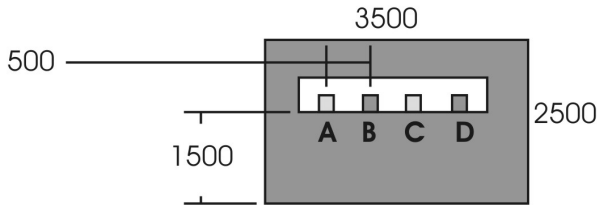

Figure 5.1: There are 4 cantilevers on the chip. The cantilevers A and C are coated with gold. Dimensions are in μm.

the chips. The chips were taken as diced out from the wafers, exactly as found before being encapsulated, as described in section 4.1.4. By not encapsulating the chips before performing the immobilization and fluorescence imaging, the imaging is eased a lot. It is assumed here that the encapsulation of the chips would not further contaminate the gold surface such that this couldn't be cleaned by the methods described in the following. This is reasonable since the gold surfaces are not submitted to any liquid or other gas than atmosphere during the encapsulation. The fluorescence was imaged on the gold contact pads rather than on the gold-coated cantilevers because it is more convenient to adjust the focus on those plane and large areas than on small and bending cantilevers. The gold layers of the cantilevers and contact pads were assumed to be equivalently treated during the processing of the chips.
In a first step, different cleaning methods were compared in order to confirm the choice of UV/ozone cleaning. Three silicon chips with gold contact pads were cleaned for 10 minutes by reactive ion etching (RIE) at 100 W followed by 40 minutes of UV/ozone cleaning, 10 minutes of UV/ozone and 10 minutes of oxygen plasma at 500 W respectively. The second chip was submitted to an ethanol dip an dried in nitrogen flow right after the UV/ozone treatment. Each chip was then immersed in a solution of 50 μM of thiol-modified DNA-capture probes in 1 M potassium phosphate pH 7.0 for one hour, subsequently rinsed in ten times 2 mL Milli Q water, hybridized to Cy5' labelled complementary oligos at 1 μM in 5xSSC + 0.1 % SDS for one hour and finally rinsed in ten times 2 mL in 1xSSC + 0.1 %SDS. The chips were then imaged in solution at PMT and laser settings of 70 %. The fluorescence image of the gold contact pads and the silicon nitride surface in between are displayed in figure 5.2. As expected the cleaning by RIE followed by a long UV/ozone cleaning yields the best results; the fluorescence signal is strong and homogeneous on all the gold surfaces which is due to the physical action of ionic bombardment that efficiently removes not only contaminants but also a thin layer of gold thus leaving a clean gold surface. Unfortunately this procedure cannot be adapted to the cantilever-based sensor as it damages the electrical properties of the sensor. The two other cleaning procedures also yield good results, the best being the rather short UV/ozone cleaning.

This "soft" cleaning procedure is well suited for cantilever-based sensor and was used in the following.
The method was further validated by performing the hybridization on a chip in 1xPCR buffer (E and D respectively in figure 5.2) and in 1xTE + 0.1M NaCl (data not shown) instead of 5xSSC buffer. The imaging of the fluorescence yielded similar results in those buffers. Subsequently to the imaging of the fluorescence, the chip was treated by 30 % urea solution, washed in water and imaged again (F in figure 5.2). The fluorescence signal had disappeared showing that the Cy5' labelled targets were hybridized to thiol-modified DNA capture oligos that were successfully immobilized on the chip.
The thiol-based immobilization shows a very good selectivity between the silicon nitride and the gold surface as illustrated by the contrast between the gold contact pads and the areas in between. This was confirmed on a fourth chip with aluminium contact pads and all four cantilevers present. The fluorescence on the gold coated cantilever is much stronger than on the uncoated cantilevers and than in figure 5.3 A. Later on, freshly deprotected thiol-modified DNA was used in the same conditions (30 minutes UV/ozone cleaning, incubation overnight and hybridization in 1xTE + 0.1 M NaCl buffer) yielding even higher coverage and a similar selectivity. The fluorescence picture of the gold wires chip is shown in figure 5.3 B. The higher coverage is achieved mainly because freshly deprotected thiol-modified oligos were used.

5.3 Immobilization on encapsulated sensors

The last step of this chapter is the implementation of the thiol-based immobilization on the fully encapsulated sensor. It is crucial to derivatize one gold-coated cantilever at a time in order to use two gold-coated cantilever, one as measuring and one as reference cantilever. Thereby the reference is mechanically very similar to the measuring cantilever. This was realized for the sensors encapsulated in PDMS as described earlier in chapter 4.

The cleaning by UV/ozone treatment is well suited for the encapsulation as all the materials involved are stable during this rather "soft" cleaning. The localization of the thiol-DNA on the chip was realized by pipetting 0.3 μL of thiol-modified DNA solution in the extremity of the channel. Doing such, only the one or two first cantilevers were immersed in the solution and even for long (overnight) incubation in a wet atmosphere (figure 5.4). This is due to the hydrophobicity of the PDMS that prevents small volumes of aqueous solution to cover the entire chamber. The cleaning of the sensor by the oxidizing ozone treatment was not enough to render the PDMS hydrophilic. Even though it depends on how the PDMS layer is placed on the chip during the encapsulation, it is possible to localize a thiol-oligo containing solution on one or two cantilevers at a time inside

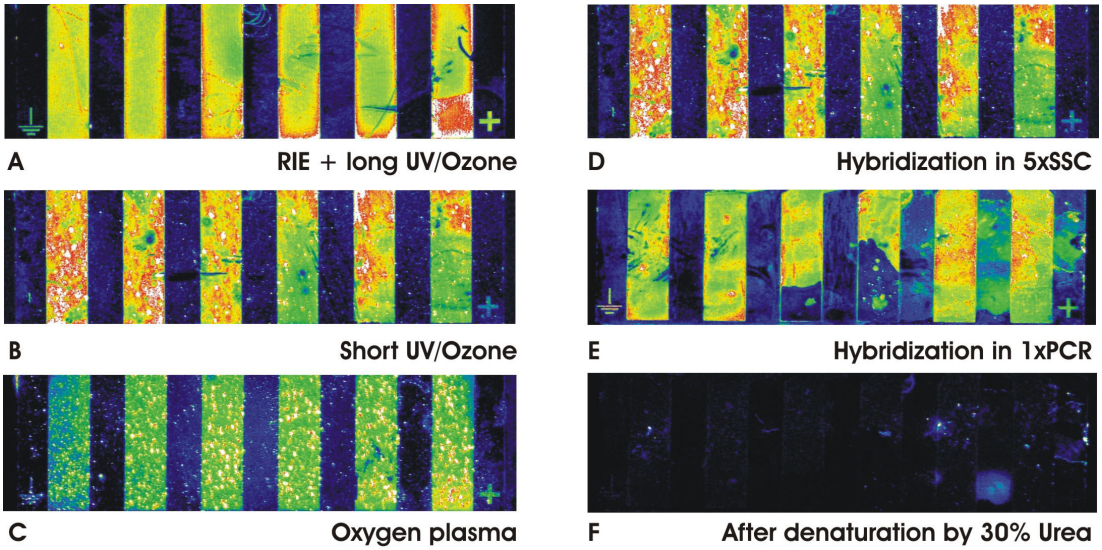

Figure 5.2: Fluorescence image of cantilever-chips cleaned by (**A**) 10 minutes of RIE at 100 W followed by 40 minutes of UV/ozone cleaning (**B**) 10 minutes of UV/Ozone followed by an ethanol dip (**C**) 10 minutes of oxygen plasma at 500 W. After immobilization of thiol-modified DNA-capture oligo the chips were washed and allowed to hybridize to Cy 5' labelled complementary targets in 5xSSC + 0.1 % SDS (**A to D**), in 1xPCR (**E and F**) and denatured in Urea solution (**F**). The chips were imaged in solution.

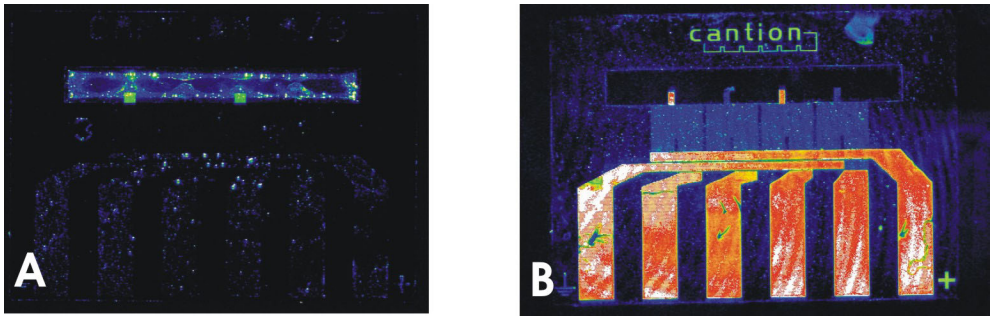

Figure 5.3: **A** Fluorescence image of a Cantion poly chip with aluminium wires cleaned by procedure in figure 5.2A, derivatized and hybridized. The fluorescence on the two gold cantilevers is stronger than on the two uncoated cantilevers and than on the aluminium (contact pads) or silicon nitride (everywhere else) surfaces. **B** Image of a second chip with gold wires immobilized with freshly deprotected thiol-modified oligos.

the chamber of an encapsulated sensor.
The conditions of the immobilization as well as of the subsequent washing procedures are critical for achieving a high coverage on gold and reducing the coverage of other surfaces respectively. Therefore they were optimized step by step in

order to achieve high coverage/low background. The following conditions were investigated:

- Immobilization on a chip that is not encapsulated
- Immobilization on a chip where the solution is localized on cantilevers using a PDMS frame
- Immobilization on an encapsulated sensor
- Immobilization and subsequent wash in an encapsulated sensor

The hybridization and the washing thereafter were on purpose made *ex situ* in order to get the best possible signal to background ratio. The results of the first immobilization technique are shown in figure 5.3. The results of the three other techniques are shown in figure 5.5. The immobilization with a PDMS frame yield a high coverage on the gold cantilever and a low background but does not enable to localize the solution on only one gold cantilever (figure 5.5 top). This is only possible if the immobilization is performed in a encapsulated sensor were the PDMS frame is pressed against the chip (figure 5.5 middle). Both chips were washed *ex situ* by 10 times 2 mL of water in a PCR tube which provides an efficient washing of the silicon nitride surfaces and accounts for the low fluorescence observed on these. The washing step can be performed successfully *in situ* by washing the chip for 30 minutes at 10 μL/min and then 50 μL/min with 0.1% SDS solution. This yield also a good selectivity between the gold cantilevers and the other surfaces (figure 5.5 bottom) apart from the fact that the second gold coated cantilever was also exposed to the thiol solution. Those results were obtained on different cantilever chips using 0.3 μL of freshly deprotected thiol-DNA at a concentration of 50 μM, one hour immobilization, one hour hybridization in 1 μM Cy5' labelled targets in 5xSSC + 0.1% SDS and subsequent wash in 10 times 2 mL of 1xSSC + 0.1% SDS. For each experiment the immobilization was performed on several chips and on a reference chip were the thiol-DNA was immobilized on the gold contact pads.
The fluorescence on the cantilevers shown in figure 5.5 was quantified and the ratio between the gold cantilever and the first un-coated cantilever (ratio A/B) and between the two gold cantilevers (ratio A/C) are reported in figure 5.6. Ratio A/B is highest (17) for the chip that was washed *ex situ* (top chip in figure 5.5). It is a bit lower (6.5) if the immobilization and wash are made *in situ* (the bottom chip). The A/C ratio is very good for the chip where the thiol-solution was localized and is about 160. The surface of the non-coated cantilever is a good representation of the back side of the gold-coated cantilever. Therefore, the ratio "A/B" indicates the relative amount of DNA-capture probes immobilized on the top side of the first gold cantilever and the ratio "A/C" indicates the relative amount of DNA-capture probes immobilized on the "measuring" cantilever compared to the "reference" cantilever. Of course the fluorescence intensity is not

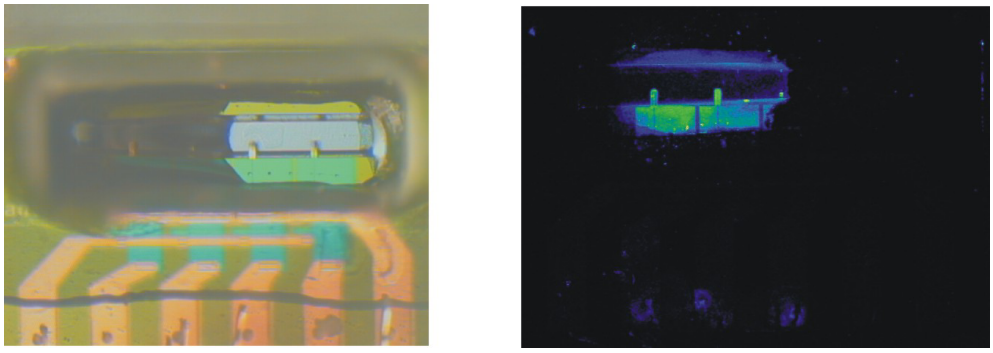

Figure 5.4: (**Right**) Optical image of the solution covering the two first cantilevers to the left of the sensors chamber. The solution volume is about 0.3 μL. (**Left**) Fluorescence image after hybridization to fluorescent labelled target DNA of a chip immobilized this way. Though the immobilization is not specific it shows which area was in contact with the thiol-oligos solution.

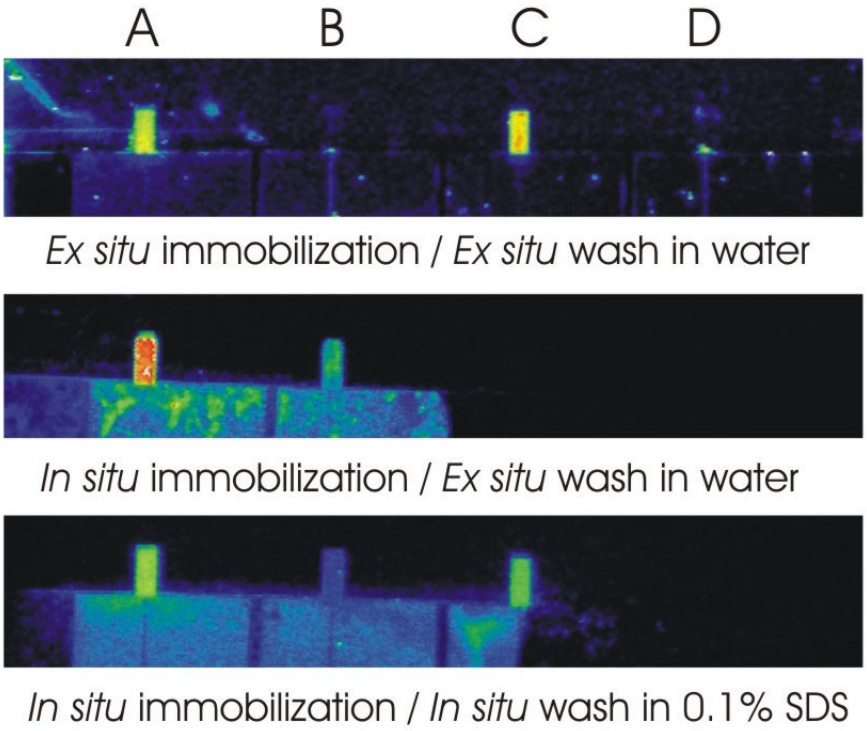

Figure 5.5: Fluorescence images of the four cantilevers (A, B, C, D) corresponding to (**Top**) a chip that was functionalized with a PDMS frame and washed in water (**middle**) a chip that was functionalized encapsulated and washed in water after the encapsulation is removed and (**bottom**) a chip that was both functionalized and washed encapsulated. The last chip was washed in 0.1% SDS.

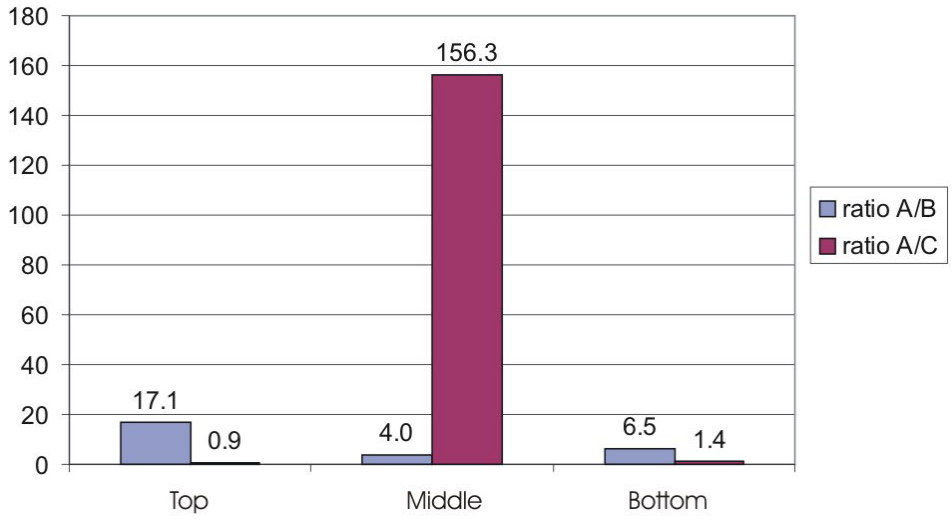

Figure 5.6: Fluorescence intensity ratio between the first gold cantilever and the adjacent uncoated cantilever (ratio A/B) and the two gold coated cantilevers (ratio A/C) corresponding to the figure 5.5 top, middle and bottom.

proportional to the hybridization coverage as shown in section 3.2 but the ratios give an idea of the efficiency of the procedure. Figure 5.6 tells us that one can expect a hybridization coverage of the top side of the measuring cantilever about 10 times higher than on its back-side and more than 100 times higher than on either side of the reference cantilever.

5.4 Fluorescence detection on encapsulated sensors

It is highly desirable to check that the immobilization of DNA-capture probes on the gold cantilever is successful before using the sensor. Therefore I investigated a method for making fluorescence scanning of encapsulated sensors which is none destructive meaning that it does not require to remove the encapsulation. It seemed difficult to use the confocal laser scanner for that purpose as the typical focal distance (1.5 mm) is very close to the thickness of the encapsulation (1 mm of PMMA and about 200 μm of PDMS) and imaging in solution would require a cover glass that increases the working distance even more. Instead, a CCD based scanner was used (ArrayWoRx, Applied Precision, Germany).

The scanner is adjusted in order to scan the backside of a typical 1 mm thick glass slide. It is thus possible to make a holder for the sensor that would place

the bottom of the sensor chamber in the focal plan of the CCD camera. As shown in figure 5.7 A, the holder is made of two pieces of glass slide in order to provide vacuum compatible surfaces for the scanner arm and a PMMA plate with a hole that fits the sensor top plate. As the sensor is inserted in the holder with the top surface aligned with the top surface of the holder and covered with a cover glass, the bottom of the sensor chamber (the surface of the silicon chip with cantilevers) is in the focal plan (figure 5.7B). This works only if the chamber is loaded with solution, in air the cantilevers are not in focus. Figure 5.7 C shows a fluorescence image of a chip covered on purpose with an excess of Cy'5 fluorescent dyes and imaged at Cy'3 and Cy'5 wavelength. Both channels are adjusted for brightness, contrast and intensity separately after the acquisition in order to visualize the Cy'5 signal in the sensor chamber. Therefore no quantification of the fluorescence signal is made and only the fluorescence of different cantilevers on a same sensor can be compared. By hybridizing the newly functionalized sensor with Cy'5 labelled target DNA-oligos, the fluorescence detection is used for validating the immobilization procedure on every sensor before test without destructing the sensor. After the detection the labelled target can be either removed by an appropriate wash (in DI water or in Urea solution) and tested further for micro-cantilever based detection with unlabelled target DNA. This shows that it is possible to detect by fluorescence if the functionalization of the cantilever is successful.

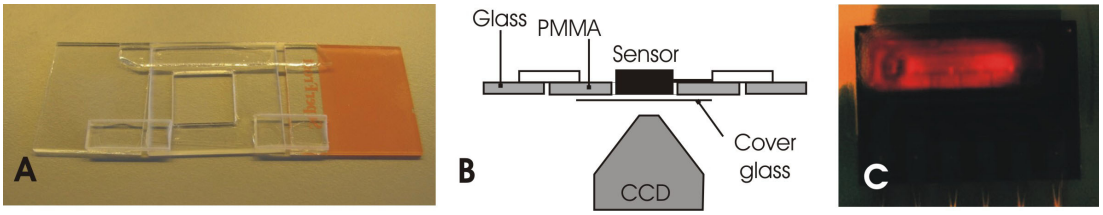

Figure 5.7: The holder for introducing an encapsulated sensor into the CCD scanner (**A**) is made of glass and PMMA. The sensor is placed face down in the holder window (**B**) and covered with solution and a glass cover. (**C**) A fluorescence image of the sensor. The inside of the sensor chamber is coated with an excess of Cy5' in order to visualize the cantilevers.

Chapter 6

Measurements by cantilever-based sensor

6.1 Isothermal hybridization: gold-coated/uncoated cantilevers

The detection of DNA-hybridization in a continuous flow of solution is, together with the hybridization detection by injection, the state of the art of DNA detection by cantilever-based sensor. It consists of recording the bending of a cantilever coated with DNA-capture probe from an instant t where the solution is switched from a pure buffer solution to a solution containing the complementary DNA. The detection is triggered by the introduction of the target DNA.
In all the experiments reported in the literature, the sensor is taken from a "no DNA" to a "complementary DNA" state, both unspecific binding and specific binding were observed both causing bending of the cantilever. The elimination of the unspecific binding signal is the main problem for cantilever-based sensing. Introduction of a reference cantilever coated with non-complementary DNA sequence [12] was proven the most efficient solution though it is more difficult to realize than using a non coated reference cantilever because it requires the functionalization of one cantilever at a time.
Even though hybridization detection by cantilever with integrated read-out has not been demonstrated yet, Cantion A/S has developed a promising instrument based on the very same silicon chips that are used for building the sensor described in this thesis. Therefore it is an obvious choice to investigate the hybridization in continuous flow with this instrument and the Cantion encapsulation of the cantilever-chip. As the immobilization of different DNA sequences on different cantilevers was not developed at the time of those investigations, an alternative approach involving one gold-coated cantilever and one non-coated reference cantilever is proposed here. It consists of introducing a solution of complementary DNA after that the sensor was stabilized in a solution of non-complementary

DNA, that is taking the sensor from a "non-complementary DNA" to a "complementary DNA" state and thus avoiding the signal due to non-specific adsorption of DNA.

6.1.1 Method

The measurement system consists of a syringe pump (Harvard Research, USA), a 6-port valve (Vici) with a 100 μL sample loop, an encapsulated cantilever-chip placed in a plug-and-play instrument (Cantion A/S, Denmark) and a waste bottle all connected by PTFE tubing. The valve and the instrument are controlled by a software developed by Cantion and running on a computer. An electrode at ground potential is placed in the solution in the waste bottle. All the components are depicted in figure 6.1. When the valve is closed the solution from the pump is pumped directly to the sensor placed in the instrument. When the valve is open, the solution is pumped through the sample loop.
According to the protocol provided by Cantion, the sensor was cleaned 15 minutes by UV/Ozone and the channel was filled with freshly deprotected thiol-modified DNA-capture oligo solution at 10 μM in 1 M potassium phosphate pH 7.0. The sequence is the 25'mer long BRCA1 probe sequence described earlier. All four cantilevers are then immersed in solution. The sensor was incubated in a humid atmosphere overnight. The sensor was then flushed in Milli-Q water for 30 minutes at 10 μL/minute in order to wash away the non-specifically bound DNA-capture oligos. Eventually the sensor was incubated in the solution of non-complementary oligo in order to shorten the stabilization time once placed in the instrument. The non-complementary sequence is a 10'mer sequence: 5'-TGC ACT AGA CCT-3'. It is diluted at 2 μM in 1xTE + 0.1 M NaCl pH 7.0. The complementary sequence is diluted at 1 μM in the same buffer. The non-complementary sequence is twice shorter than the complementary sequence

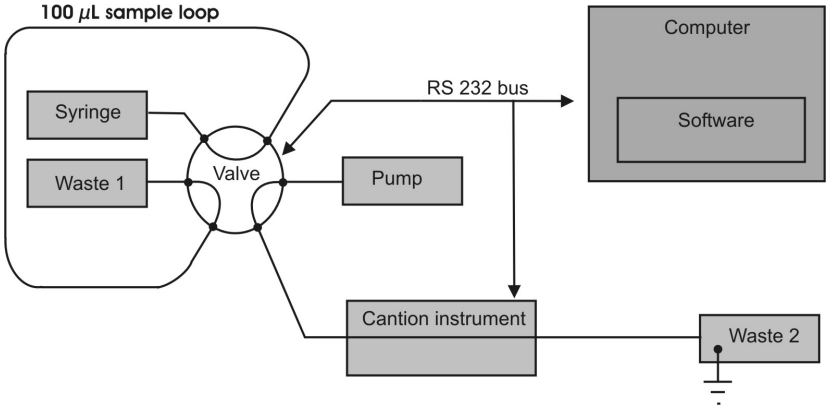

Figure 6.1: Set-up used for the isothermal hybridization measurements in a flow.

and is thus diluted at a twice higher concentration in order to keep the amount of DNA constant during the experiment assuming that unspecific adsorption is rather dependent on the total amount of bases than the concentration of oligos. The flow rate is maintained constant at 10 μL/minute. At the beginning of the experiment, the non-complementary solution is injected until the output signal is stable. Then the valve is open and the 100 μL of complementary solution runs through the system. Then the flow is back to the non-complementary solution. The four output channels of the sensor are the output signal of four pairs of cantilevers: A and B, C and D, A and C, B and D, noted A-B, C-D, A-C and B-D respectively. Cantilevers A and C are coated with gold and B and D are not coated.
The internal connections of the read-out is such that the introduction of 10 mM 6-mercapto-1-hexanol (MCH) yields a negative change of the A-B and C-D output voltage which is interpreted as due to a compressive stress change.

6.1.2 Results

The output voltage of the four channels were recorded while the sensor is successively exposed to the flow of non-complementary solution, complementary solution and non-complementary solution at constant flow rate and temperature

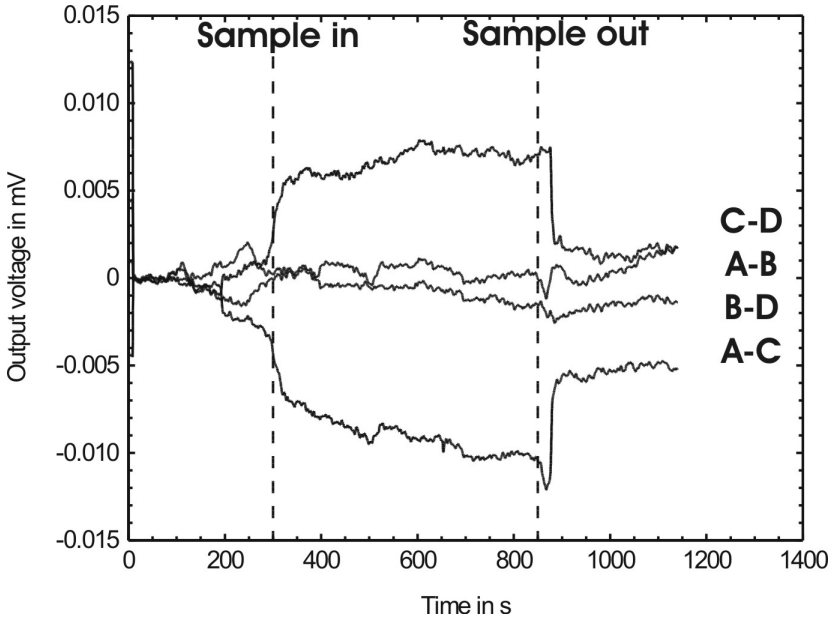

Figure 6.2: Measurement of hybridization in a continuous flow of 10 μL/min. The solution with non-complementary DNA is injected until t=300 s where the 100 μL sample of complementary DNA is introduced. The solution is back to non-complementary DNA solution at t= 850 s.

(figure 6.2). Right at the introduction of the complementary oligo solution the C-D signal increases and A-C decreases almost symmetrically while the A-B and B-D remains at the base line.
The increase in output voltage for C-D suggests a tensile stress change on C that can be due to the interaction of the complementary oligo with the DNA-capture probes immobilized on C. The constant signal for the two non-coated cantilever B and D confirms that there is no unspecific adsorption of DNA at the replacement of the non-complementary DNA by the complementary DNA. Though, no signal is observed for A-B and a decrease of signal almost symmetrical to the C-D signal is observed for A-C which is the pair of gold coated cantilever. This suggests that, for some reason, no complementary DNA adsorbs on A while it adsorbs on C. Those results are consistent if we assume that no thiol-modified capture probes were immobilized on A while it was successfully immobilized on C. Never the less, the experiment shows that using a non-complementary DNA solution before introducing the complementary sequence can attenuate the non-specific binding signal during this type of experiment.
The amplitude of the signal is about 8 μV and is interpreted as a tensile stress. The sensitivity of the cantilever chip is 1300 N.m^{-1}.V^{-1} under 2.5 V [1]. The signal then corresponds to a tensile stress of 10 mN.m^{-1}. Fritz *et al.* reported a compressive stress of 5 mN.m^{-1} for the hybridization of 12'mer at 0.75 M sodium ions [12][2] while Wu *et al.* reported a tensile stress of 5.6 mN.m^{-1} for 20'mer in 0.1 M sodium ions [10][3]. More than the differences in salt concentration and sequence length between those two experiments, the use of a reference cantilever or not is matter of discussion and can probably explain the radical disagreement about the sign of the surface stress and its origin.
At the end of the complementary DNA sample, the solution is back to non-complementary DNA solution. The output voltages of A-C and C-D then drop back to their baseline considering the drift during the measurement. This suggests that the complementary DNA adsorbed on C is desorbed again and was thus due to unspecific adsorption but B-D remained unchanged. This can also suggests that the signal observed during the injection of complementary DNA is due to the difference in length of the non-complementary and the complementary DNA. The experiment need to be reproduced with a 25'mer non-complementary sequence in order to confirm the specificity of the signal.

[1] According to the value communicated by Cantion A/S. See chapter 1.

[2] The hybridization was made in 5xSSC buffer, pH 7.0.

[3] Based on the calculation with Stoney's formula for 15 nm deflection of a 200 μm long and 0.5 μm thick cantilever with E=180 GPa/m^2 and ν=0.25. the hybridization was performed in 0.1 M sodium phosphate pH 7.0.

6.2 Isothermal hybridization: two gold coated cantilevers

The experiments performed using the Cantion instrument were repeated using sensors packaged as described in section 4.3.3 and the immobilization procedure described in chapter 5.

6.2.1 Method

Basically the experimental method is the following:

1. Encapsulation of a sensor according to 4.3.3.
2. Functionalization of one gold cantilever as described in 5.3.
3. Equilibration of the sensor in a flow of non-complementary DNA oligos.
4. Introduction of complementary DNA oligos while recording the output voltage (cantilever A and C) of the sensor.

The set-up is as described in figure 6.1 except that the valve is controlled manually and the sensors output is only recorded for the cantilevers A and C, the two gold coated cantilevers. The device described in section 4.11 is used for flowing a solution through the chamber. As the encapsulation was originally designed for static experiments, the chamber is not optimized for flow experiments. This means that the flow inside the chamber may not be laminar. Never the less, the relatively small volume of the chamber (about 3 μL) provides that the solution inside the chamber is renewed fast enough at flow rates used in the experiments (10 μL/minute). Moreover, the noise of the measurements is not dramatically increased.

The non-complementary sequence is, this time, a 25'mer sequence. The sequence is 5'- TGC ACT AGA CCT TGC ACT AGA CCT A-3'. The maximum consecutive bases complementary with the DNA-capture probes and the target oligos is 4 (TGCA) in both cases. This provides that at room temperature, at salt concentration of 0.1 M sodium ions, no hybridization occurs between the non-complementary oligos and the target or the capture probes on the cantilever. Moreover, this enables to have a constant concentration of DNA during the whole experiment, the only thing changing at the introduction of the target DNA being the base sequence. The buffer solution is 1xTE + 0.1 M NaCl pH 7.0. Non-complementary and target DNA are dissolved at a concentration of 1 μM in the same buffer solution rigourously.

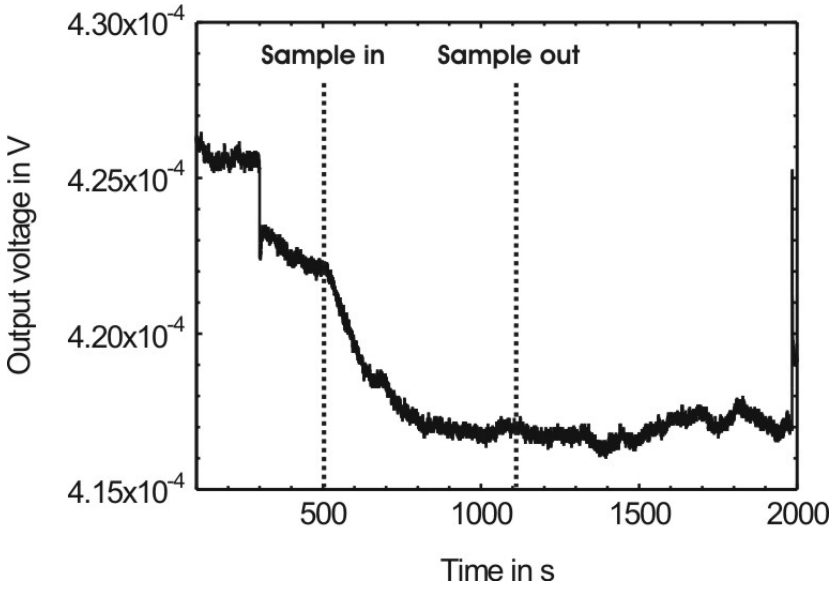

Figure 6.3: Measurement of hybridization in a continuous flow of 10 μL/min. The solution with non-complementary DNA is injected until t=520 s where the 100 μL sample of complementary DNA is introduced. The solution is back to non-complementary DNA solution at t=1120 s.

6.2.2 Results

During the measurement depicted in figure 6.3, non-complementary DNA solution is injected until t=300 s where the valve is open. At t= 520 s the solution of complementary DNA enters the reaction chamber which yields a decrease of 5 μV of the output voltage. After 300 to 400 s the signal is stable and remains stable. At t= 1120 s the flow is back to a non-complementary DNA solution. Signals at t= 300 s and t= 1985 s are due to the opening and the closing of the valve.

The change of output voltage corresponds to a tensile stress of 16.3 mN/m. Both the sign and the amplitude agree with the work published by Wu *et al.* [10]. Though a factor three larger surface stress is measured, the surface stress value is a calculated value and is thus highly dependent on the theoretical framework adopted to model the deflection or voltage change of the cantilever. More interesting is that

- The signal stabilizes at a fixed value. This indicates that the process causing the cantilever to bend is ending. The hybridization of complementary DNA to a DNA-capture probe layer is expected to end at the saturation of the DNA layer.
- The signal remains constant after that target DNA is replaced by non-complementary DNA inside the system. This is also consistent with the

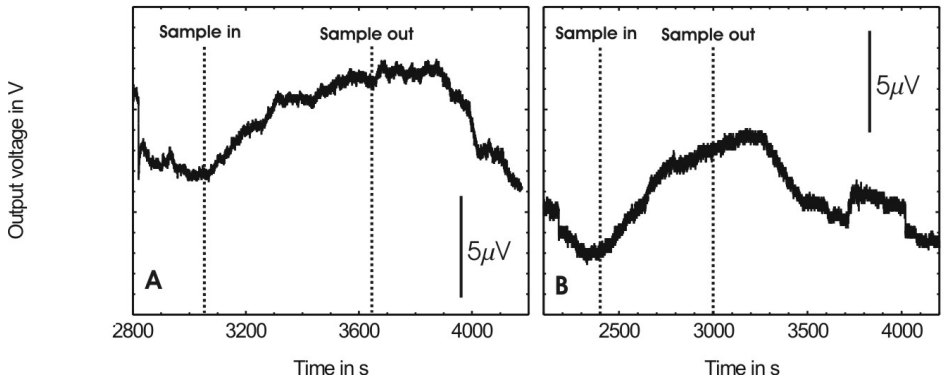

Figure 6.4: (**A**) Signal at the second injection of complementary DNA. The solution with non-complementary DNA is injected until t=3040 s where the 100 μL sample of complementary DNA is introduced. The solution is back to non-complementary DNA solution at t=3640 s. (**B**) a similar injection on the same chip after denaturation by Urea.

hypothesis of a DNA specific interaction.

In order to show that the signal is specific to the complementary DNA, a second sample of complementary DNA was introduced. Unlike the first sample injection, it didn't yield a decrease of the output voltage, neither did the output voltage remain unchanged. The second injection of complementary DNA yields a positive change of ouptput voltage with a characteristic shape as shown in figure 6.4A. Unlike the first signal, the output voltage does not reach a stable value and the signal decreases back toward the baseline when the flow is switched to non-complementary DNA solution. After washing the sensor in 30 % urea and water, only increasing signals with the same shape were obtained, with amplitudes varying from 10 to 3 μV (figure 6.4B). This suggests that the sensor has lost its sensitivity after being washed in a strong flow of urea and water.

The measurement was repeated two times with different sensors (figure 6.5). In both cases a permanent 4 to 5 μV decrease of voltage was obtained at the first introduction of complementary DNA. At later introduction of complementary DNA, the two sensors reacted differently. In one case the unspecific signals were increasing, in the other case decreasing; in both cases the shape was the same as described in figure 6.4, meaning that after 200 seconds the voltage returns back to its level before the introduction of the complementary DNA. This suggests that the signal follows the concentration of complementary DNA inside the sensors chamber. The delay of 200 seconds can be interpreted as the time necessary for the concentration of complementary DNA to decrease. The fact that there is no laminar flow inside the chamber can account for this long mixing time.

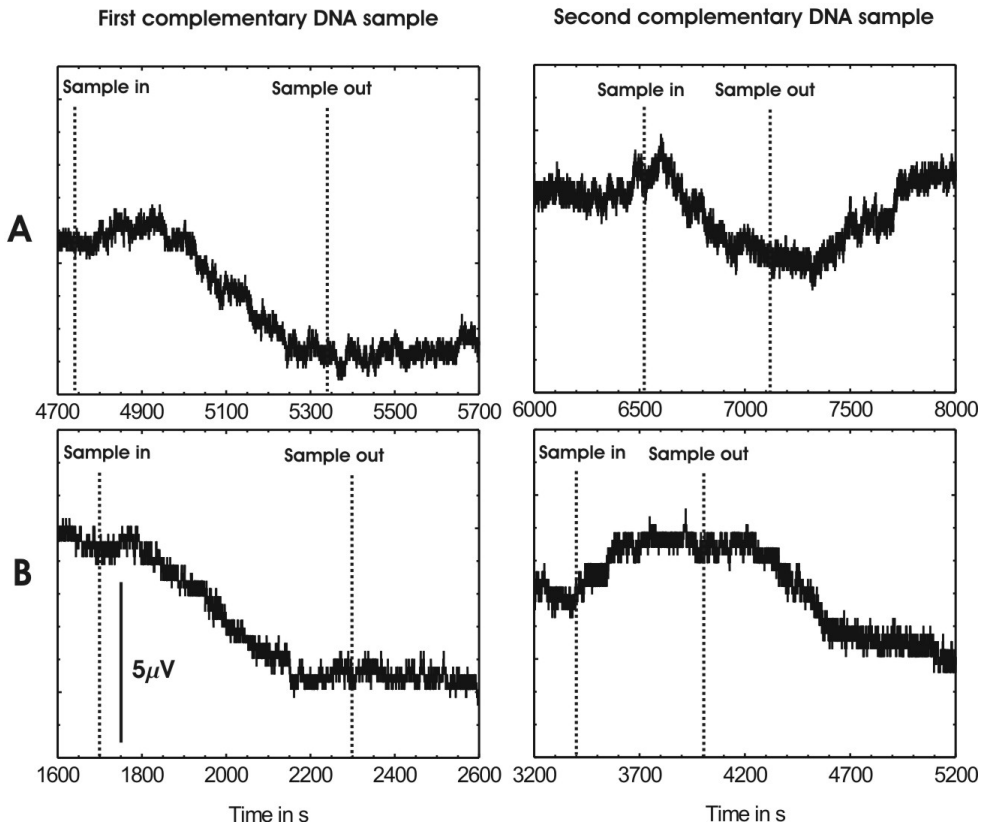

Figure 6.5: Signal obtained at the first (left) and second (right) introduction of complementary DNA sample for two different sensors (A and B). The voltage scale is identical on all graphs.

6.2.3 Discussion

The change of output voltage is about 5 μV. The temperature sensitivity of such a sensor coated with ssDNA is about 2.5 μV/K. If caused by a change of temperature, the voltage change should correspond to a temperature change of 2 °C. This is too large considering that all the set-up is stabilized at room temperature. The two types of signals obtained are qualitatively different. Assuming that the voltage change observed is due to the adsorption of DNA on the cantilevers, it can be seen as a convolution of specific adsorption of DNA (through hybridization to DNA-capture probes immobilized) and unspecific adsorption (through hydrogen bonding). In the following, the coverage of DNA-capture probes on a surface is called the number of specific sites and the coverage sites available for the unspecific adsorption of ssDNA is called the number of unspecific sites (see figure 6.6). Those numbers are denoted, on each sides of the cantilever A and C:

- on the top side of A there are $N_s^{A\ top}$ of specific sites
  and $N_u^{A\ top}$ of unspecifc sites

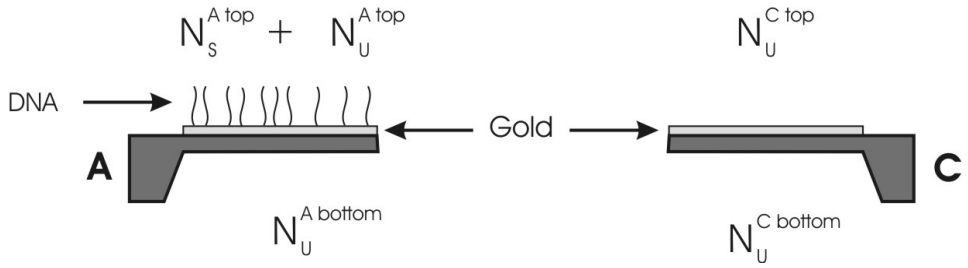

Figure 6.6: The top side of the cantilever A is coated with DNA-capture probes. This yield a coverage $N_s^{A\ top}$ of specific binding sites . On all the surfaces, there are sites available for the unspecific adsorption of ssDNA. The number of these sites are denoted $N_u^{A\ top}$, $N_u^{A\ bottom}$, $N_u^{C\ top}$ and $N_u^{C\ bottom}$.

- on the bottom side of A there are $N_u^{A\ bottom}$ unspecific sites
- on the top side of C there are $N_u^{C\ top}$ unspecific sites
- on the bottom side of C there are $N_u^{C\ bottom}$ unspecific sites

As shown by the fluorescence images in figure 5.5, there are also DNA-capture probes immobilized on the bottom side of A and we assume that $N_s^{A\ top}$ is actually the difference of the coverage of DNA-capture probes between the top and the bottom side of A: $N_s^{A\ top} \geq 0$.

The fluorescence images have also shown that no DNA-capture probes are immobilized on the cantilever C which means that there are only unspecific sites on cantilever C, but since the top side is coated with gold and the bottom side is silicon nitride: $N_u^{C\ top} \neq N_u^{C\ bottom}$.

Moreover, the coverage of unspecific sites on the bottom sides of cantilever A should be lower than on the bottom side of cantilever C since there are also some specific sites on the bottom side of cantilever A: in principle, $N_u^{C\ bottom} \geq N_u^{A\ bottom}$.

This means that specific adsorption (*i.e.* hybridization) should always yield a negative output voltage change if corresponding to a tensile stress while the sign of the output voltage change due to unspecific adsorption is very dependent on the relative number of unspecific sites on the bottom sides of cantilever A and C and the top side of cantilever C.

The adsorption of DNA at the specific and unspecific sites are also very different: at specific sites only complementary DNA can adsorb and this adsorption is irreversible (at a given temperature and salt concentration). While at unspecific sites, ssDNA of any sequence can adsorb. Moreover, it is probable that the adsorption is competitive, meaning that the occupancy of unspecific sites by

two different ssDNA sequences should represent the ratio of the two ssDNA in solution. This is consistent with the fact that at the first introduction of complementary DNA the signal remains stable after the end of the sample while for other injections, the voltage change represents the concentration of target and disappears when the flow is back to non-complementary DNA.

Never the less, it is not clear why the exchange of one ssDNA sequence for another of the same length at an unspecific site should yield a change of surface stress.

6.2.4 Outlook

Obviously, a better non-specific adsorption control experiment is needed in order to identify this signal. The introduction of a second non-complementary DNA before the introduction of the complementary DNA would definitely show if the signal obtained at the first introduction of the complementary DNA is specific. This non-complementary DNA sequence should not hybridize to any of the two other sequences. The signal is expected to be as the non-specific signal, meaning a slow voltage change that falls back to the initial level when the first non-complementary DNA is injected in the sensor.

Furthermore, according to the discussion above, immobilizing a second DNA sequence on the reference cantilever is the way of discriminating specific and non-specific responds of the sensor [13].

The measurements presented here can further be improved by using a different encapsulation that is optimized for creating a laminar flow inside the chamber and thus increasing the response time of the system.

6.3 Melting/hybridization by heat-cycling

6.3.1 Recapitulation of the experimental protocol

The typical procedure that was used in the numerous experiments on detecting melting and hybridization by heat cycling is as follows:

1. Encapsulation of a sensor according to 4.3.3.
2. Functionalization of one gold cantilever as described in 5.3.
3. Equilibration of the sensor in buffer or in target solution, at room temperature or at 4 °C.
4. Measurements during thermal cycling.

The thermal cycling is typically between 20 and 80 °C, at a rate of 0.2 °C/s, 1 minute 30 seconds at 80 °C and the time necessary for the sensor to stabilize at 20 °C.

6.3.2 What to expect

The results of the measurements are visualized as a diagram showing the slope of the voltage as a function of the temperature (see example in figure 6.7). The melting of the probe DNA immobilized on the cantilever and hybridized to target DNA is expected to produce a change of surface stress (ΔV_σ). It is possible to estimate the amplitude and the sign of this change of slope. Let us assume that ΔV_σ is proportional to the rate of the interaction. According to the measurements of the melting temperature by adsorbance measurements, the rate and thus ΔV_σ can be modelled as:

$$\frac{dV}{dT} = \frac{\alpha}{\pi}\frac{b}{(T-T_m)^2+b^2} \tag{6.3-1}$$

$$V = \frac{\alpha}{\pi}\left[\arctan\left(\frac{T-T_m}{b}\right)+\frac{\pi}{2}\right] \tag{6.3-2}$$

Here b is independent of the quantity measured (Adsorbance or the output voltage) because it characterizes the width in temperature of the melting process (*i.e.* the kinetics of the melting). α is characteristic of the change of output voltage and is equal to ΔV_σ. From the spectrophotometry measurement we know that b=3.24. The melting temperature can be calculated at the oligo concentration (1 μM) at T_m=56.8 ± 1.4 °C. Moreover, we calculate the slope of the voltage change in the time domain $\frac{dV}{dt}$ while the heating/cooling rate is maintained at 0.2 °C/s. Thus we can write

$$\frac{dV}{dt} = \frac{dV}{dT}\cdot\frac{dT}{dt} \; and \; \frac{dT}{dt} = 0.2 \tag{6.3-3}$$

The rate of the reaction and thus the voltage slope change is expected to be maximum at T=T_m and can be expressed as:

$$\left.\frac{dV}{dt}\right|_{T_m} = 0.2\,\frac{\Delta V_\sigma}{3.24\,\pi} \tag{6.3-4}$$

It is assumed that the melting of the DNA on the cantilever A would produce a compressive stress on this cantilever. According to the electrical scheme in figure 4.2 B, the compressive stress on A yields a positive change of V_{AC}. Assuming the voltage change (ΔV_σ) of +5 μV, corresponding to a compressive surface stress change (σ) of +16 mN/m, the change of $\frac{dV}{dt}$ is expected to be close to +0.1 μV/s at T=T_m [4].

[4] The surface stress change value is calculated using a sensitivity of +3252 $N.m^{-1}.V^{-1}$ under 1 V.

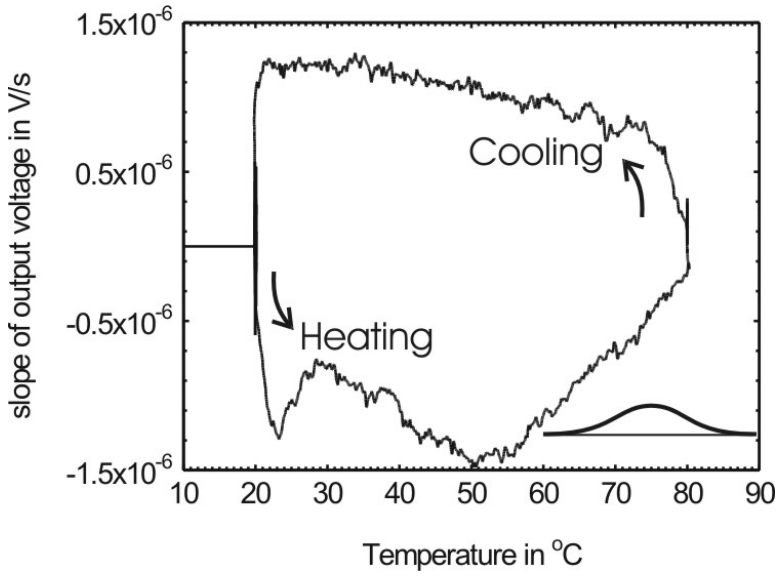

Figure 6.7: Typical output voltage slope vs. temperature during the heat cycling of a sensor with DNA-capture probes on the cantilever A and complementary DNA in a 1xTE + 0.1 M NaCl buffer. At the lower right corner, the curve shows how the signal expected on the heating branch of the diagram looks like.

6.3.3 Results

The experiment was attempted several times without success. The diagram showing the slope of the output voltage vs. the temperature was very variable for the sensors that were used. The figure 6.7 shows a typical diagram obtained during such an attempt. First of all, peaks larger than the signal expected (depicted in the lower right corner of figure 6.7) were observed at various temperatures. For some sensors, those peaks changed height and position (temperature) from one heat cycle to the other and, most often, symmetric peaks on the other branch of the diagram were not observed. Moreover, very often a large signal was observed on the heating branch of the diagram for temperatures in the range of 30 to 40 °C (but sometimes also at different temperatures). This signal was always very large for the first cycle and decreases and/or shift position for later heat cycles. Such signal is shown in the figure 6.8. Stress release process in the mechanical structure of the sensor can account for such signals.
On the other hand, the sensor used in the experiment depicted in figure 6.5A was stabilized in the complementary DNA solution (1 μM target DNA in 1xTE + 0.1 M NaCl at pH 7) and heat cycled. The diagram presented in figure 6.9 was obtained for the first three heat cycles. A change of output voltage slope occurred at the first heating of the sensor. The change of output voltage slope is positive, about 0.3 μV/s high and the width at half maximum is about 15 °C. The sign and width are as expected. The peak is positioned at 56 °C which is 1 degree

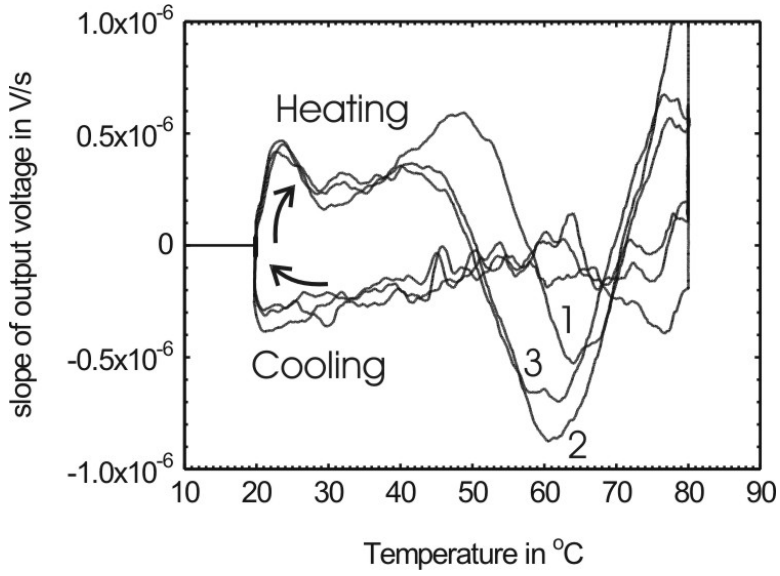

Figure 6.8: Output voltage slope vs. temperature during three heat cycles of a sensor with DNA-capture probes on the cantilever A and complementary DNA in a 1xTE + 0.1 M NaCl buffer. The order of the heat cycles are indicated. Large features are varying in size and temperature at successive heat cycles.

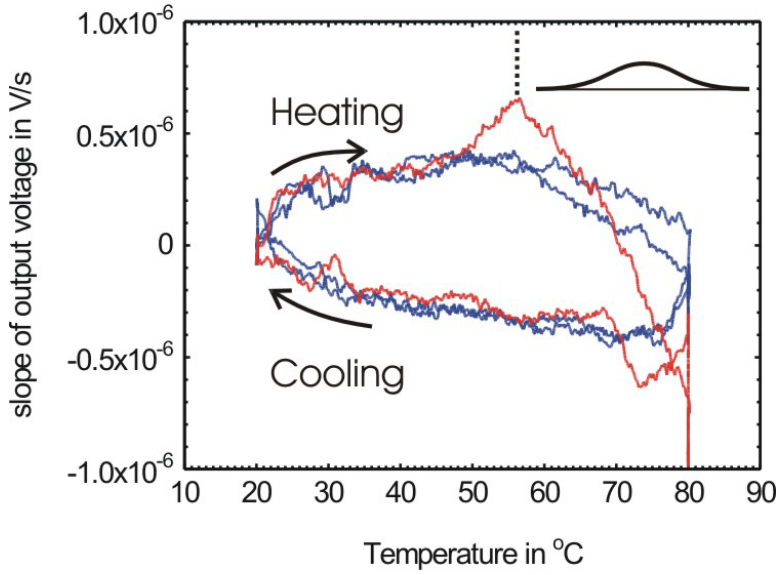

Figure 6.9: Output voltage slope vs. temperature during three heat cycles of a sensor with DNA-capture probes on the cantilever A and complementary DNA in a 1xTE + 0.1 M NaCl buffer. The feature on the first heating branch of the cycle is about 0.3 μV/s high, 15 °C wide and centered at 56 °C.

below the melting temperature of the DNA oligos. However, the amplitude of the peak would correspond to a 15 μV compressive stress signal which is three times larger than the output voltage change obtained at the isothermal hybridization on the same sensor (figure 6.5A). Moreover, no symmetrical peak on the cooling branch of the diagram was observed and this occurs only at the first cycle, which suggests that this can also be a signal that is not related to the melting of DNA. This result needs to be reproduced before concluding on the nature of the signal.

In conclusion, the signal due to the melting of the target DNA on the cantilever sensor might be observed during one attempt. However, the amplitude of the signal is three timer larger than expected and the signal corresponding to the re-hybridization was not obtained at the cooling of the sensor. Moreover, this has not been reproduced, which is partly due to the large and non-reproducible features obtained while making temperature cycling of the cantilever sensors. As mentioned earlier, reducing the TCR effect of the piezoresistors by choosing different materials or modifying the read-out system in order to minimize the effect of TCR mismatch between the piezoresistors in the Wheatstone bridge may be a way of reducing those undesired effects.

Chapter 7

Conclusion

The main goal of this project has been to detect the melting of DNA by cantilever-based surface stress sensing as this is the first step toward monitoring *in situ* a PCR process by this technique. The starting materials for this project were a generation of cantilever-based devices with integrated poly-silicon piezoresistive read-out. Remaining to achieve were

- To make and characterize a packaging of the chip that can stand temperatures and salt concentrations typical for performing nucleic acids reactions.
- To functionalize the cantilever-sensor locally with DNA-capture probes and to verify that the DNA-capture probes are functional during heat cycling.
- To show that the sensitivity of the sensor is high enough to detect DNA hybridization.
- To detect melting or non-isothermal hybridization of DNA.

During this project, cantilever chips with single crystalline piezoresisitve read-out were made available by Cantion A/S which improved greatly the noise level of the sensor. Never the less, availability and sensitivity of silicon chips were an issue through all this project.

In the introduction the cantilever-based surface stress sensing is presented. Several studies have reported the detection of DNA hybridization. Issues to the detection are the use of a proper reference and the unspecific adsorption of DNA. In that respect the detection of the melting of DNA is specific because the melting temperature is specific of the base sequence.

The cantilever chips were packaged in polymer. The final packaging uses PDMS as a sealant and a PMMA structure to encapsulate the electrical connections of the chip. This packaging method has been shown to sustain typical PCR heat cycling. The volume of the reaction chamber is about 3 μL.

A measurement set-up has been built and characterized. It comprises the sensor, a temperature controlled device, a Lock-in amplifier for reading out the output voltage of the sensor and a software for recording the voltage, the phase and the temperature of the sensor. Noise levels as low as 0.4 μV were obtained for chips with single crystalline silicon piezoresistors which is low enough to detect expected surface stress signals in the 1 to 10 μV range.

The sensor was functionalized with DNA using the adsorption of thiol-modified DNA on gold coated cantilevers. The method was first characterized by immobilizing DNA in a micro-array format and quantifying the coverage of capture probes by radio-labeling and the hybridization to the arrays by fluorescence scanning. The stability of such an immobilized layer of DNA capture probes during a full PCR-like heat cycling was investigated. It is shown that less than 10 % of the DNA-capture probes remains able to hybridize to the complementary DNA after 10 heat cycles. On one hand this is expected to reduce the sensitivity of the sensor during the PCR process. On the other hand the sensitivity remains constant after the 10^{th} cycle which may allow to detect an increase of the DNA concentration.

The immobilization method was then applied to the functionalization of the cantilever-based sensor. The method was characterized by fluorescence scanning and the selectivity of the adsorption with respect to the other surfaces on the chip was characterized, showing that the selectivity between the two sides of the measuring cantilever is at least four. Moreover, it was shown that almost no DNA was immobilized on the reference cantilever.

The detection of DNA hybridization in a flow was performed. In those experiments the sensor was stabilized in a flow of non-complementary DNA oligos before and after a sample of complementary DNA was injected. At the injection of complementary DNA, a negative voltage change of about 5 μV was obtained and the voltage was stable even after the injection of non-complementary DNA. Additionally characteristic voltage changes were identified at repeated sample injections and were interpreted as non-specific adsorption signals.

The detection of melting of DNA by the same sensor was attempted. According to the measurements of hybridization by cantilever-based sensor and of melting and rehybridization performed by spectrophotometry, the change of output voltage slope is expected to be 0.2 μV/s. In order to be able to detect such a signal, it is suggested to built a sensor specifically optimized for reducing either the mismatch of TCR between the piezoresistors of the sensor or to use piezoresistive materials with lower TCR.

Bibliography

[1] D.R. Baselt, B. Fruhberger, E. Klaasen, S. Cemalovic, C.L. Britton Jr, S.V. Patel, T.E. Mlsna, D. McCorkle, and B. Warmack. Design and performance of a microcantilever-based hydrogen sensor. *Sensors and Actuators*, 2003.

[2] J. Brugger, R.A. Buser, and N.F. de Rooj. Micromachined atomic force microprobe with integrated capacitive read-out. *J. Micromech. Microeng.*, 2:218–220, 1992.

[3] P.-F. Indermühle, G. Schürmann, G.-A. Racine, and N. F. de Rooj. Atomic force microscopy using cantilevers with integrated tips and piezoelectric layers for actuation and detection. *J. Micromech. Microeng.*, 7:218–220, 1997.

[4] A. Boisen, J. Thaysen, H. Jensenius, and O. Hansen. Environmental sensors based on micromachined cantilevers with integrated read-out. *Ultramicroscopy*, 82(1-4):11–16, 2000.

[5] A. Boisen. *Passive and active AFM probes: design, fabrication and characterisation*. PhD thesis, MIC, Technical University of Denmark, 1997.

[6] Jacob Thaysen. *Cantilever for bio-chemical sensing integrated in a microliquid handling system*. PhD thesis, MIC, Technical University of Denmark, 2001.

[7] Peter Andreas Rasmussen. *Cantilever-based sensors for surface stress measurements*. PhD thesis, MIC, Technical University of Denmark, 2003.

[8] P. Vettiger J. Thaysen, A.D. Yalinkaya and A. Menon. Polymer-based stress sensor with integrated readout. *Journal of Physics D: Applied Physics*, (35):2698–2703, 2002.

[9] M. Calleja, P. Rasmussen, A. Johansson, and A. Boisen. Polymeric mechanical sensor with piezoresistive read-out integrated in a microfluidic system. *Proceedings of the SPIE - The International Society for Optical Engineering*, 5116(Smart Sensors, Actuators, and MEMS):314–321, 2003.

[10] G. Wu, H. Ji, K. Hansen, T. Thundat, R. Datar, R. Cote, M.F. Hagan, A.K. Chakraborty, and A. Majumdar. Biological sciences - biophysics - origin of nanomechanical cantilever motion generated from biomolecular interactions. *Proceedings of the National Academy of Sciences of the USA*, 98(4):1560–1564, 2001.

[11] F. Liu, Y. Zhang, and Z.-C. Ou-Yang. Flexoelectric origin of nanomechanic deflection in DNA-microcantilever system. *Biosensors and Bioelectronics*, 18:655–660, 2003.

[12] J. Fritz, M.K. Baller, H.P. Lang, H. Rothuizen, P. Vettiger, E. Meyer, H.-J. Guntherodt, Ch. Gerber, and J.K. Gimzewski. Translating biomolecular recognition into nanomechanics. *Science*, 288(5464):316–18, 2000.

[13] R. McKendry, J. Zhang, Y. Arntz, T. Strunz, M. Hegner, H.P. Lang, M.K. Baller, U. Certa, E. Meyer, H.-J. Guntherodt, and C. Gerber. Multiple label-free biodetection and quantitative DNA-binding assays on a nanomechanical cantilever array. *Proceedings of the National Academy of Sciences of the USA*, 99(15):9783–9788, 2002.

[14] G. Wu, R. Datar, K. Hansen, T. Thundat, R. Cote, and A. Majumdar. Bioassay of prostate specific antigen (PSA) using microcantilevers. *Nature biotechnology*, 19:856–860, 2001.

[15] M. Alvarez, A. Calle, J. Tamayo, L.M. Lechuga, A. Abad, and A. Montoya. Development of nanomechanical biosensors for detection of the pesticide DDT. *Biosensors and Bioelectronics*, In Press, 2003.

[16] K. A. Stevenson, A. Mehta, P. Sachenko, K. M. Hansen, and T. Thundat. Nanomechanical effect of enzymatic manipulation of DNA on microcantilever surfaces. *Langmuir*, 18(23):8732–8736, 2002.

[17] J.D. Watson and F.H.C. Cricks. Molecular structure of nucleic acids. *Nature*, 171:737–738, 1953.

[18] V.A. Bloomfield. *Nucleic acids: structure, properties and function.* University Science books, 1999.

[19] *figure 2.11 in [18].*

[20] O. Resendis-Antonio, L.S. Garcia-Colin, and H. Larralde. A statistical model of DNA denaturation. *Physica A*, 318(3-4):435–446, 2003.

[21] P.M. Howley, M.F. Israel, M.-F. Law, and M.A. Martin. A rapid method for detecting and mapping homology between heterologous DNAs. Evaluation of polyomavirus genomes. *Journal of Biological Chemistry*, 254:4876–4883, 1979.

[22] http://www.promega.com/biomath/calc11.htm.

[23] R. Owczarzy, P.M. Vallone, F.J. Gallo, T.M. Paner, M.J. Lane, and A.S. Benight. Predicting sequence-dependent melting stability of short duplex DNA oligomers. *Biopolymers*, 44:217–239, 1997.

[24] S.O. Kelley and J.K. Barton. Electron transfer between bases in double helical DNA. *Science*, 283(4):375–381, 1999.

[25] N.J. Turro and J.K. Barton. Paradigms, supermolecules, electron transfer and chemistry at a distance. What's the problem? The science or the paradigm? *JBIC*, 3:201–209, 1998.

[26] *pp 284-287 in [18]: in Table 8.7 the free energy values per hydrogen bond was measured for different sequences and the values are comprised between -0.5 and - 2 kcal/mol of hydrogen bond.*

[27] W. Saenger. *Principles of nucleic acid structure.* Springer Verlag, New York, 1984.

[28] *p 308 in [18], the list of cosolvent/denaturant presented is not exhaustive but comprise methanol, ethanol, 1-propanol, 2-propanol, ethyleneglycol, glycerol, cyclohexyl alcohol, phenol, pyridine, 1,4-dioxane, formamide, N,N-dimethylformamide, urea, acetonitrile and TritonX-100.*

[29] A.J. Hartemink and D.K. Gifford. Thermodynamics simulation of deoxyoligonucleotide hybridization for DNA computation. *Proceedings of the 3rd DIMACS Workshop on DNA Based Computers*, 1997.

[30] *p 167 in [18].*

[31] K.A. Peterlinz, R.M. Georgiadis, T.M. Herne, and M.J. Tarlov. Observation of hybridization and dehybridization of thiol-tethered DNA using two-color surface plasmon resonance spectroscopy. *Journal of the American Chemical Society*, 119(14):3401–3402, 1997.

[32] K.B. Mullis, F. Faloona, S. Scharf, R.K. Saiki, G.T. Horn, and H.A. Erlich. Specific enzymatic amplification of DNA in vitro: the polymerase chain reaction. *Cold Spring Harbour Symp. Quant. Biol.*, 51(1):263–273, 1986.

[33] B. Schweitzer and S. Kingsmore. Combining nucleic acid amplification and detection. *Current Opinion in biotechnology*, 12:21–27, 2001.

[34] C.M. Nycz, C.H. Dean, P.D. Haaland, C.A. Spargo, and G.T. Walker. Quantitative reverse transcription strand displacement amplification: quantitation of nucleic acids using an isothermal amplification technique. *Nucleic Acids Research*, 20(7):1691–1696, 1992.

[35] L. Raeymaerkers. A commentary on the practical applications of competitive PCR. *Genome Research*, pages 91–94, 1995.

[36] A.R. Kopf-Sill. Successes and challenges of lab-on-a-chip. *Lab-on-a-chip*, 2:42N–47N, 2002.

[37] L.J. Bousse, C. Cohen, T. Nikiforov, A. Chow, A.R. Kopf-Sill, R. Dubrow, and J.W. Parce. Electrokinetically controlled microfluidic analysis systems. *Annual Review of Biophysics and Biomolecular Structure*, 29:155–181, 2000.

[38] R. Mei, P. C. Galipeau, C. Prass, A. Berno, G. Ghandour, N. Patil, R. K. Wolff, M. S. Chee, B. J. Reid, and D. J. Lockhart. Genome-wide detection of allelic imbalance using human SNPs and high-density DNA arrays. *Genome Research*, 10(8):1126–1137, 2000.

[39] S. Tombelli, M. Mascini, L. Braccini, M. Anichini, and A.P.F. Turner. Coupling of a DNA piezoelectric biosensor and polymerase chain reaction to detect apolipoprotein e polymorphisms. *Biosensors and Bioelectronics*, 15:363–370, 2000.

[40] K. Niikura, H. Matsuno, and Y. Okahata. Direct monitoring of DNA polymerase reactions on a quartz crystal microbalance. *J. Am. Chem. Soc.*, 120:8537–8538, 1998.

[41] D. Hao, M. Ohme-Takagi, and K. Yamasaki. A modified sensor chip for surface plasmon resonance enables a rapid determination of sequence specificity of DNA-binding proteins. *FEBS Letters*, 536(1-3):151–156, 2003.

[42] E. Kai, S. Sawata, K. Ikebukuro, T. Iida, T. Honda, and I. Karube. Detection of PCR products in solution using surface plasmon resonance. *Analytical Chemistry - Columbus*, 71(4):796–800, 1999.

[43] D. Klein. Quantification using real-time PCR technology: applications and limitations. *Trends in Molecular Medicine*, 8(6):257–260, 2002.

[44] C. Adessi, G. Matton, G. Ayala, G. Turcatti, J.J. Mermod, P. Mayer, and E. Kawashima. Solid phase DNA amplification, characterisation of primer attachment and amplification mechanisms. *Nucleic Acids Research*, 2000.

[45] Abraham Ulman. Formation and structure of self-assembled monolayers. *Chemical Reviews*, 96(4):1533, 1996.

[46] L. Henke, P.A.E. Piunno, A.C. McLure, and U.J. Krull. Covalent immobilization of single-stranded DNA onto optical fibers using various linkers. *Analytica Chimica Acta*, 344:201–213, 1997.

[47] J. D. Andreadis and L. A. Chrisey. Use of immobilized PCR primers to generate covalently immobilized DNAs for in vitro transcription/translation reactions. *Nucleic Acids Research*, 28(2):e5–, 2000.

[48] B. Joos, H. Kuster, and R. Cone. Covalent attachment of hybridizable oligonucleotides to glass supports. *Analytical Biochemistry*, 247(1):96–101, 1997.

[49] N. Zammatteo, L. Jeanmart, S. Hamels, S. Courtois, P. Louette, L. Hevesi, and J. Remacle. Comparison between different strategies of covalent attachment of DNA to glass surfaces to build DNA microarrays. *Analytical Biochemistry*, 280(1):143–150, 2000.

[50] M. Schena, D. Shalon, R. Heller, A. Chai, P. O. Brown, and R. W. Davis. Parallel human genome analysis: Microarray-based expression monitoring of 1000 genes. *Proceedings of the National Academy of Sciences of the USA - Paper Edition*, 93(20):10614–10619, 1996.

[51] Y.-H. Rogers, P. Jiang-Baucom, Z.-J. Huang, V. Bogdanov, S. Anderson, and M. T. Boyce-Jacino. Immobilization of oligonucleotides onto a glass support via disulfide bonds: A method for preparation of DNA microarrays. *Analytical Biochemistry*, 266(1):23–30, 1999.

[52] A. Kumar, O. Larsson, D. Parodi, and Z. Liang. *Nucleic Acids Research*, 28(142).

[53] V. G. Cheung, M. Morley, F. Aguilar, A. Massimi, R. Kucherlapti, and G. Childs. Reviews - making and reading microarrays. *Nature Genetics*, 21(1suppl):15–19, 1999.

[54] D. L. Allara, A. N. Parikh, and F. Rondelez. Evidence for a unique chain organization in long chain silane monolayers deposited on two widely different solid substrates. *Langmuir*, 11(7):2357–2360, 1995.

[55] F.R. Ortigao, F.M. Meklenburg, and M. Cieplik. XNA on gold^{TM} - universal platform for arraying biomolecules. *Proceedings. MICRO.tec 2000. VDE World Microtechnologies Congress*, pages 345–6 vol.2, 2000.

[56] S.O. Kelley, J.K. Barton, N.M. Jackson, L.D. McPherson, A.B. Potter, E.M. Spain, M.J. Allen, and M.G. Hill. Orienting DNA helices on gold using applied electric fields. *Langmuir*, 14(24):6781–6784, 1998.

[57] T.M. Herne and M.J. Tarlov. Characterization of DNA probes immobilized on gold surfaces. *Journal of the American Chemical Society*, 119(38):8916–8920, 1997.

[58] J. Zhang, Q. Chi, A.M. Kuznetsov, A.G. Hansen, H. Wackerbarth, H.E.M. Christensen, J.E.T. Andersen, and J. Ulstrup. Electronic properties of functional biomolecules at metal/aqueous solution interfaces. *Journal of Physical Chemistry B*, 106(6):1131–1152, 2002.

[59] R. Levicky, T. M. Herne, M. J. Tarlov, and S. K. Satija. Using self-assembly to control the structure of dna monolayers on gold: A neutron reflectivity study. *Journal of the American Chemical Society*, 120(38):9787–9792, 1998.

[60] S.O. Kelley, J.K. Barton, N.M. Jackson, and M.G. Hill. Electrochemistry of methylene blue bound to a dna-modified electrode. *Bioconjugate Chem.*, 8(1):31 – 37, 1997.

[61] J.C O'Brien, V.W Jones, M.D Porter, C.L Mosher, and E. Henderson. Immunosensing platforms using spontaneously adsorbed antibody fragments on gold. *Analytical Chemistry - Columbus*, 72(4):703–710, 2000.

[62] P. Facci, D. Alliata, and S. Cannistraro. Potential-induced resonant tunneling through a redox metalloprotein investigated by electrochemical scanning probe microscopy. *Ultramicroscopy*, 89(4):291–298, 2001.

[63] H. Wackerbarth, R. Marie, M. Grubb, J. Zhang, A. G. Hansen, I. Chorkendorff, C. B.V. Christensen, A. Boisen, and J. Ulstrup. Thiol- and disulfide-modified oligonucleotide monolayer structures on polycrystalline and single-crystal Au(111) surfaces. *Journal Of Solid State Electro-Chemistry*, Accepted for publication, 2003.

[64] P. Fenter, A. Eberhardt, and P. Eisenberger. Self-assembly of n-alkyl thiols as disulfides on Au(111). *Science - AAAS - Weekly Paper Edition*, 266(5188):1216–1217, 1994.

[65] Ch. Zubragel, C. Deuper, F. Schneider, M. Neumann, M. Grunze, A. Schertel, and Ch. Woll. The presence of two different sulfur species in self-assembled films of n-alkanethiols on Au and Ag surfaces. *Chemical Physics Letters*, 238(4-6):308–312, 1995.

[66] T. Ishida, S.'I. Yamamoto, W. Mizutani, M. Motomatsu, H. Tokumoto, H. Hokari, H. Azehara, and M. Fujihira. Evidence for cleavage of disulfides in the self-assembled monolayer on Au(111). *Langmuir*, 13(13):3261–3265, 1997.

[67] A. R. Badia, R.B. Lennox, and L. Reven. A dynamic view of self-assembled monolayers. *Acc. Chem. Res.*, 2000.

[68] F. Bensebaa, T. H. Ellis, A. R. Badia, and R.B. Lennox. Thermal treatment of n-alkanethiolate monolayers on gold, as observed by infrared spectroscopy. *Langmuir*, 1998.

[69] N. Garg, E. Carrasquillo-Molina, and T.R. Lee. Self-assembled monolayers composed of aromatic thiols on gold: Structural characterization and thermal stability in solution. *Langmuir*, 18(7):2717–2726, 2002.

[70] A. B. Steel, T. M. Herne, and M. J. Tarlov. Electrochemical quantitation of DNA immobilized on gold. *Analytical Chemistry - Columbus*, 70(22):4670–4677, 1998.

[71] T. Ishida, S. Tsuneda, N. Nishida, M. Hara, H. Sasabe, and W. Knoll. Surface-conditioning effect of gold substrates on octadecanethiol self-assembled monolayer growth. *Langmuir*, 13(17):4638–4643, 1997.

[72] S. Tsuneda, T. Ishida, N. Nishida, M. Hara, H. Sasabe, and W. Knoll. Tailoring of a smooth polycristalline gold surface as a suitable anchoring site for a self-assembled monolayer. *Thin Solid films*, 339:142–147, 1999.

[73] A.G. Hansen, M.W. Mortensen, J.E.T. Andersen, J. Ulstrup, A. Kühle, J. Garnæ s, and A. Boisen. Stress formation during self-assembly of alkanethiols. *Probe Microscopy*, 2(2):139–150, 2001.

[74] C.-J. Zhong, R. C. Brush, J. Anderegg, and M. D. Porter. Organosulfur monolayers at gold surfaces: Reexamination of the case for sulfide adsorption and implications to the formation of monolayers from thiols and disulfides. *Langmuir*, 15(2):518–525, 1999.

[75] R. Marie. DNA hybridisation investigated by microcantilever-based sensor. Master's thesis, MIC, Technical University of Denmark, 2000.

[76] M. Schena. *DNA microarrays: a practical approach*. Oxford University Press, 1999.

[77] D. D. L. Bowtell. Reviews - options available – from start to finish – for obtaining expression data by microarray. *Nature Genetics*, 21(1SUPPL):25–32, 1999.

[78] E. Southern, K. Mir, and M. Shchepinov. Reviews - molecular interactions on microarrays. *Nature Genetics*, 21(1SUPPL):5–9, 1999.

[79] A. Kumar and Z. Liang. Chemical nanoprinting: A novel method for fabricating DNA microchips. *Nucleic Acids Research*, 29(2):e2, 2001.

[80] F. Teran Arce and R.C. Salvarezza. Dynamic characteristics of adsorbed monolayers of 1-dodecanethiol on gold (111) terraces from in-situ scanning tunneling microscopy imaging. *Electrochimica Acta*, 44(6-7):1053–1067, 1998.

[81] A. Vainrub and B. M. Pettitt. Coulomb blockage of hybridisation in two-dimensional DNA arrays. *Physical Review*, e66:041905, 2002.

[82] Henriette Jensenius. *Microcantielver-based studies of bio/chemical systems.* PhD thesis, MIC, Technical University of Denmark, 2002.

[83] S.C. Eriksen. DNA detection on cantilever-based sensors. Master's thesis, MIC, Technical University of Denmark, 2002.

[84] J. Thaysen, A. Boisen, O. Hansen, and S. Bouwstra. Atomic force microscopy probe with piezoresistive read-out and a highly symmetrical wheatstone bridge arrangement. *Sensors and Actuators*, (83):47–53, 2000.

[85] S. Middelhoek and S.A. Audet. *Silicon sensors.* Academic press, 1989.

Appendix A

Solutions

10xTE solution pH 7.0

This is a solution of 100 mM of Tris·HCl (Sigma T-5941) and 10 mM EDTA·Na_2 (Sigma E-5134). Mix 1.576 g of Tris and 0.372 g of EDTA in 100 mL milli-Q water. Adjust pH to 7.0 by adding 1 M NaOH.

1 M NaCl

Dilution of a 5 M NaCl solution (Promega, V422A).

0.17 M potassium phosphate pH 8.0

Prepare a 0.17 M potassium phosphate monobasic (Sigma, P-5379) solution and a 0.17 M potassium phosphate dibasic (Sigma, P-3786) solution in milli-Q water. Adjust the pH to 8.0 of the first solution by addition of the second one.

53 mM DTT in 0.17 M potassium phosphate pH 8.0

Dilute 16.46 mg of DTT (Sigma, D-9779) in 2 mL of 0.17 M potassium phosphate pH 8.0.

PBS pH 7.4

Phosphate Buffered Saline solution contains typically 0.1 M Sodium phosphate.

PCR II buffer

Commercially available (Perkin-Elmer) contains 10 mM tris·HCl and 50 mM of potassium chloride at pH 8.3.

Appendix B

Deprotection protocol for thiol-modified oligos

The protocol used in the thesis for preparing freshly deprotected thiol-modified oligos was established by Cantion A/S. It is based on the reduction of the disulfide bridge by an incubation overnight with DTT.

1. Prepare 2 mL of 0.053 M DTT in 0.17 M potassium phosphate pH 8.0.
2. Mix 25 μL of 200 μM disulfide-modified oligos with 75 μL of DTT, both in 0.17 M potassium phosphate pH 8.0.
3. Let react overnight at room temperature.
4. Open the top cap of the NAP-5 column. Poor the excess liquid. Open the bottom cap.
5. Equilibrate the column with 10 mL of 0.17 M potassium phosphate pH 8.0. Let the solution enter the gel.
6. Introduce 100 μL of the oligo solution. Let the solution enter the gel.
7. Introduce 400 μL of buffer. Let the solution enter the gel.
8. Elute the oligos in a tube by introducing 500 μL of buffer.
9. Eventually mix with 20 mg of KH_2PO_4 (Sigma, P-5379) and 46.5 mg of K_2HPO_4 (Sigma, P-3786) in order to adjust the salt concentration to 1 M and the pH to 7.0.

Alternatively to 9, evaporate 10 μL of solution in vacuum and re-dissolve in 2 μL of 0.17 M potassium phosphate. The concentration of thiol-oligos is then about 50 μM in 1 M Potassium phosphate at pH 8.0.

Published by:
MIC, Department of Micro and Nanotechnology
DTU, Technical University of Denmark
Building 345 east
DK-2800 Kgs. Lyngby
Denmark

ISBN: 87-89935-78-0

Printed in Denmark by Synergi